



Strål
säkerhets
myndigheten

Swedish Radiation Safety Authority

Authors:

Richard Kłos
Laura Limer
George Shaw
Anders Wörman

Technical Note

2014:35

Modelling comparison of alternative
biosphere models with LDF models and
evaluation of selected parameter values
used in the biosphere dose assessment

Main Review Phase

SSM perspektiv

Bakgrund

Strålsäkerhetsmyndigheten (SSM) granskar Svensk Kärnbränslehantering AB:s (SKB) ansökningar enligt lagen (1984:3) om kärnteknisk verksamhet om uppförande, innehav och drift av ett slutförvar för använt kärnbränsle och av en inkapslingsanläggning. Som en del i granskningen ger SSM konsulter uppdrag för att inhämta information och göra expertbedömningar i avgränsade frågor. I SSM:s Technical note-serie rapporteras resultaten från dessa konsultuppdrag.

Projektets syfte

Det övergripande syftet med projektet är att ta fram synpunkter på SKB:s säkerhetsanalys SR-Site för den långsiktiga strålsäkerheten hos det planerade slutförvaret i Forsmark. Det specifika syftet med detta uppdrag är att utföra modelleringsjämförelser mellan alternativa biosfärmodeller och SKB:s LDF modellering för att undersöka osäkerheter i nyckelparametrar. En annan aspekt uppdraget är att genomföra en fördjupad granskning av viktiga parametrar som valda Kd-värden och överföringsfaktorer som används av SKB i modelleringen.

Författarnas sammanfattning

Denna rapport har upprättats som en del av SSM:s huvudgranskning av SKB:s långsiktiga säkerhetsanalys (SR-Site) för ett geologiskt slutförvar enligt KBS-3 metoden som föreslås för byggnation i Forsmark. Granskningen tar upp den metodik som används för dosberäkningarna i SR-Site, särskilt frågor om transport, ackumulering och överföring av radioaktiva ämnen i ytnära miljö och hur doser till framtida människor, växter och djur kan uppkomma. De frågor som tas upp här är: representationen av hydrologi i SR-Site, jämförelse av SKB:s radionuklidtransportmodell för biosfären med en oberoende alternativ biosfärmodell, samt en utvärdering av nyckelparametrar som används i SKB:s biosfärmodell, inklusive om överföringshastigheter och valda Kd-värden och koncentrationfaktorer är lämpliga.

Vattenflöden i den ytnära miljön är de viktigaste drivkrafterna för förorenings-spridning. I granskningen av den yhydrologiska modelleringen i SKB:s transportmodellering för biosfären finner vi en brist på motivering av den hydrologi som antas för flodområden i ett framtida Forsmarks landskap. Dessutom är det en brist att informationen som härleds från en detaljerad hydrologisk modellering av det framtida landskapet inte används för att få hydrologiskt stöd för biosfärtransportmodellen, vilket kan betyda att hänsyn inte tas till potentiellt viktiga parametrar och processer. Tolkningen av yhydrologin som användas i radionuklidtransportmodelleringen av biosfären lämpar sig därför endast för en viss klass av landskapsobjekt som en ögonblicksbild av förhållandena vid en viss tidpunkt. Följaktligen är det svårt att med säkerhet hävda att de hydrologiska representationerna i radionuklidtransportmodelleringen av biosfären är ändamålsenliga.

En alternativ modell för radionuklidtransport i biosfären har utvecklats som ger en ram för genomförandet av alternativa tolkningar av hydrologi. Syftet är att skapa en modell med flexibiliteten att representera förhållanden inom en rad olika flodområden i framtida landskap, inklusive representation av utveckling och succession i hela flodområdet. Initiala känslighetsanalyser tyder på att SR-Site LDF-värden i vissa fall kan vara lägre än vad som erhålls med den alternativa tolkningen.

Radionuklidtransportmodellen kan ge en bild av hur föroreningar sprids i landskapet. Radionuklidernas hydrogeokemi avgör graden av ackumulation. En detaljerad granskning av nuklidspecifika data som används i dosberäkningarna i SR-Site har därför genomförts. Radionuklid distributionskoefficienter (K_d) har granskats genom att spåra dokumentationen till sitt ursprung i SKB:s primära databas (SICADA). Vi har inte kunnat återfinna samma antal parvisaprover från platsspecifika data som SKB redovisar, så vissa oklarheter återstår. Databasen för ^{226}Ra är dock väl dokumenterad och beskriven och hanteringen utgör ett riktmärke för härledning av platsspecifika data.

Vissa numeriska problem har upptäckts vid härledningen av vissa värden för växtupptag. Källan till dessa verkar ligga i SKB:s användning av koncentrationer uttryckta som Bq kg^{-1} kol, i stället för det i litteraturen mer vanliga Bq kg^{-1} torrsvikt eller färsksvikt. Det finns också tveksamheter kring SKB:s förenklade hantering av radionuklidackumulering i naturlig vegetation. Överföringsfaktorer för terrester och akvatisk fauna är hämtade främst från befintliga generiska databaser. Det har inte varit möjligt att verifiera att de värden som används för vilda växtätare är lämpliga för bedömningen i SR-Site.

Projektinformation

Kontaktperson på SSM: Shulan Xu

Diarienummer ramavtal: SSM2011-4268

Diarienummer avrop: SSM2013-2539

Aktivitetsnummer: 3030012-4048

SSM perspective

Background

The Swedish Radiation Safety Authority (SSM) reviews the Swedish Nuclear Fuel Company's (SKB) applications under the Act on Nuclear Activities (SFS 1984:3) for the construction and operation of a repository for spent nuclear fuel and for an encapsulation facility. As part of the review, SSM commissions consultants to carry out work in order to obtain information and provide expert opinion on specific issues. The results from the consultants' tasks are reported in SSM's Technical Note series.

Objectives of the project

The general objective of the project is to provide review comments on SKB's postclosure safety analysis, SR-Site, for the proposed repository at Forsmark. The objective of this assignment is to perform modelling comparison between alternative biosphere models and SKB's LDF modelling approach to explore uncertainties in key parameters. Another aspect of this assignment is to carry out in-depth reviews of key parameters such as selected Kd values and transfer rates used by SKB in modelling.

Summary by the authors

This report has been prepared as part of the SSM's Main Review Phase of SKB's SR-Site performance assessment of the long-term safety of the KBS-3 geological disposal facility (GDF) proposed for construction at Forsmark. The review addresses the methodology employed in the dose assessment calculations of SR-Site; specifically issues of transport, accumulation and transfers of radionuclides in the near surface environment and the way in which doses to future human and non-human populations can arise.

The issues addressed here are: representation of hydrology within the SR-Site assessment; comparison of SKB's dose assessment modelling with an independent alternative biosphere modelling approach; and an evaluation of key parameters used in the SKB biosphere model, including whether transfer rates and selected Kd values and concentration ratios are appropriate.

Water flows in the near surface environment are the main drivers of contaminant transport. The review of the surface hydrological modelling in the SKB dose assessment model finds that there is a lack of justification of the hydrology assumed for basins in the future Forsmark landscape, and that the information derived from a detailed hydrological model of the future landscape is not used to best advantage in deriving the hydrological underpinning of the dose assessment model, with potentially significant parameters and processes discarded. The interpretation of the surface hydrology used in the dose assessment modelling is thus suitable only for a certain class of landscape object as a snapshot of conditions at a particular time. Consequently, it is hard to state with confidence that the hydrological representations in the dose assessment model are fit for purpose.

An alternative modelling approach has been developed which provides a framework for implementing alternative interpretations of hydrology. The aim is to provide a dose assessment model with the flexibility to represent conditions in a range of different basins in the future landscape, including evolution and succession to be represented in the whole basin. Initial sensitivity studies suggest the SR-Site LDF values can be, in some cases, lower than obtained with the alternative interpretation. The radionuclide transport model determines patterns of contaminants migration in the landscape. The hydrogeochemistry of the radionuclides determines how much accumulation there will be. A detailed review of nuclide specific data used in the SR-Site dose calculations has therefore been carried out.

Radionuclide distributions coefficients (Kds) have been traced through the documentation to their origins in the SKB primary database (SI-CADA). The reviewers have been unable to achieve the same number of paired samples from the site specific data as claimed by SKB and so there remain some inconsistencies. The database for ^{226}Ra , however, is well documented and described and the treatment sets a benchmark for the derivation of site specific data.

Some numerical problems have been discovered in the derivation of some values for plant uptake. The source of these appears to lie in SKB's use of concentrations expressed in Bq kg⁻¹ of carbon, rather than the more usual literature measurements using Bq kg⁻¹ dry weight or fresh weight. There is also concern about the simplistic treatment of radionuclide accumulation in natural vegetation. Transfer factors for terrestrial and aquatic fauna are taken primarily from existing generic databases. In particular it has not been possible to verify that the values used for wild herbivores are appropriate for the assessment.

Project information

Contact person at SSM: Shulan Xu



Strålsäkerhetsmyndigheten

Swedish Radiation Safety Authority

Authors: Richard Kłos¹, Laura Limer², George Shaw³, Anders Wörman⁴

¹Aleksandria Science Ltd, Sheffield, United Kingdom.

²Limer Scientific Consulting, Shanghai, China.

³University of Nottingham, Nottingham, United Kingdom.

⁴KTH, Stockholm, Sweden.

Technical Note 59

2014:35

Modelling comparison of alternative biosphere models with LDF models and evaluation of selected parameter values used in the biosphere dose assessment

Main Review Phase

Date: January, 2014

Report number: 2014:35 ISSN: 2000-0456

Available at www.stralsakerhetsmyndigheten.se

This report was commissioned by the Swedish Radiation Safety Authority (SSM). The conclusions and viewpoints presented in the report are those of the author(s) and do not necessarily coincide with those of SSM.

Contents

1. Introduction	3
2. Review of SKB's interpretation of hydrology	5
2.1. Introduction	5
2.2. SKB's presentation	5
2.2.1. MIKE-SHE modelling	5
2.2.2. Basis for the hydrological parameters in SR-Site	7
2.2.3. Radionuclide transport in the dose assessment model	7
2.3. The Consultants' assessment	7
2.3.1. Motivation of the assessment	7
2.3.2. MIKE-SHE and the "average object"	9
2.3.3. Radionuclide transport model	10
2.3.4. Average object and implementation	11
2.3.5. Derivation of parameters in the landscape model	12
2.3.6. Numerical results for the radionuclide transport model: Object 116 at 5000 CE	18
2.3.7. The "average object" as a snapshot	22
2.4. Conclusion of the review of SKB interpretation of hydrology	24
2.4.1. Suitability	24
2.4.2. Requests for data	26
3. Independent landscape modelling	28
3.1. SKB's presentation	28
3.2. Motivation of the assessment	28
3.3. The Consultants' assessment	29
3.3.1. System Identification and justification	29
3.3.2. Module structure and radionuclide transport	31
3.3.3. Evolution and hydrology in the three module basin	33
3.3.4. Radionuclide release and evaluation of dose	35
3.3.5. Numerical characterisation of the GEMA-Site basin	35
3.3.6. Illustrative results for LDF using GEMA-Site	38
3.3.7. Sensitivity of dose to time of agricultural conversion	41
3.3.8. Sensitivity of dose to object dimensions	43
3.3.9. Conclusions	44
4. Review of SKB's derivation of nuclide specific data	47
4.1. SKB's presentation	47
4.1.1. Distribution coefficients	47
4.1.2. Plant uptake	49
4.1.3. Transfer factors for terrestrial biota associated with human exposure calculations	50
4.1.4. Concentration ratios used for aquatic biota	51
4.2. Motivation of the assessment	52
4.3. The Consultants' assessment	53
4.3.1. Distribution coefficients (K_d)	54
4.3.2. Plant uptake	60
4.3.3. Transfer factors for terrestrial biota associated with human exposure calculations	63
4.3.4. Concentration ratios used for aquatic biota	65
4.4. Conclusion of review of derivation of element specific data	66
5. Review of SKB's ¹⁴C modelling	69
5.1. SKB's presentation	69
5.1.1. Conceptual model	69
5.1.2. Data	70

5.2. Motivation of the assessment	73
5.3. The Consultants' assessment	73
5.3.1. Conceptual model	74
5.3.2. Data	75
5.3.3. Derivation of peak LDF value (biosphere object 118)	76
5.4. Conclusion of review of ¹⁴ C modelling	80
6. Review of SKB's interpretation of human exposure routes	81
6.1. SKB's presentation	81
6.1.1. Total exposure rates and dietary composition	81
6.1.2. Data relating to the peak LDF values for ⁷⁹ Se, ⁹⁴ Nb, ¹²⁹ I and ²²⁶ Ra used in the SR-Site assessment	83
6.2. Motivation of the assessment	83
6.3. The Consultants' assessment	83
6.3.1. Dietary composition	85
6.3.2. Timing of the peaks	86
6.3.3. Radionuclide specific LDF	86
6.4. Conclusion of review of SKB's interpretation of human exposure routes	88
7. The Consultants' overall assessment	89
7.1. SKB's interpretation of hydrological modelling	89
7.2. Independent landscape modelling	89
7.3. Derivation of nuclide specific data	90
7.3.1. Distribution coefficients	90
7.3.2. Plant uptake	90
7.3.3. Terrestrial and aquatic animal uptake parameters	91
7.4. ¹⁴ C modelling and assessment	91
7.5. Human exposure	91
8. References	92
APPENDIX 1	96
APPENDIX 2	97
APPENDIX 3	99
APPENDIX 4	106

1. Introduction

In 2011 the Swedish Nuclear Fuel and Waste Management Company (SKB) submitted an assessment of the long-term safety of a KBS-3 geological disposal facility (GDF) for the disposal of spent nuclear fuel and high level radioactive waste in Forsmark, Sweden. This assessment, the SR-Site project, supports the licence application of SKB to build such a final disposal facility. The SKB documents which comprise and support the licence application will be reviewed by SSM in a stepwise and iterative fashion. The first step, called the Initial Review Phase, was undertaken in 2012, with the overall goal to achieve a broad coverage of SR-Site and supporting references and in particular to identify the need for complementary information and clarifications to be delivered by SKB.

With respect to the biosphere aspect of the assessment and consequence analysis, the Initial Review Phase raised a number of issues for more detailed consideration in the Main Review Phase (Egan et al., 2012; Klos et al., 2012; Klos and Wörman, 2013). These issues included:

- Representation of hydrology within the SR-Site assessment
- Comparison of SKB's dose assessment model with alternative biosphere modelling approaches, considering both
 - Alternative biosphere models
 - Reference biosphere models
- An evaluation of key parameters in the SKB biosphere model, including whether transfer rates and selected K_d values used are appropriate.
- A review of the assessment of impacts to non-human biota

This report forms part of the Main Review phase, with a particular focus on the following specific issues relating to the SR-Site biosphere assessment and consequence analysis. The first objective of this report is to present the results of a modelling comparison between alternative biosphere models and SKB's LDF modelling approach to explore uncertainties in key parameters. Here consideration has been given both to the representation of hydrology (Section 2) and the option for an independent dose assessment model (Section 3).

Another aspect of this report is an in-depth review of key parameters such as selected K_d values and transfer rates used by SKB in modelling. Focus here is upon the five radionuclides which contributed most to the calculated annual effective human dose presented by SR-Site for the shear failure scenario (SKB, 2011), and the data used to support the assessment model parameterisation for these radionuclides: ^{14}C , ^{79}Se , ^{94}Nb , ^{129}I and ^{226}Ra . The nuclide specific transfer parameters relating to the four trace elements (Se, Nb, I and Ra) are reviewed in Section 4. The ^{14}C assessment is considered separately in Section 5. Consideration is also given to the parameterisation of human exposure in Section 6.

Overall conclusions of this main phase of the review are given in Section 7.

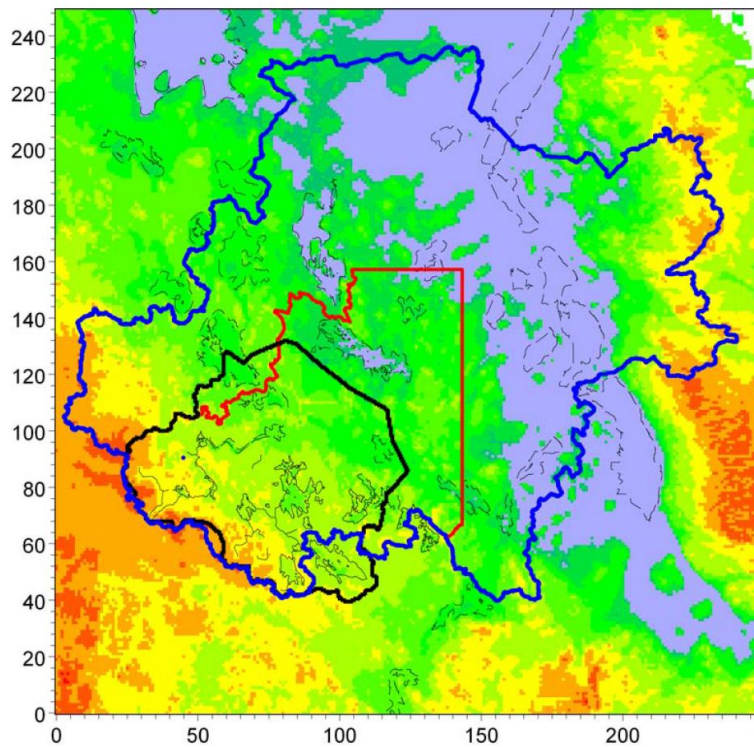


Figure 8-1. MIKE SHE model area in the “pre-modelling” (red line) shown together with the SDM-Site MIKE SHE model area (black line) and the final SR-Site regional model area (blue line) considered in the modelling presented in Chapters 5 and 6 of this report.

Figure 1: Areas used at different stages in the development of the MIKE-SHE hydrological model. Taken from Bosson et al. (2010).

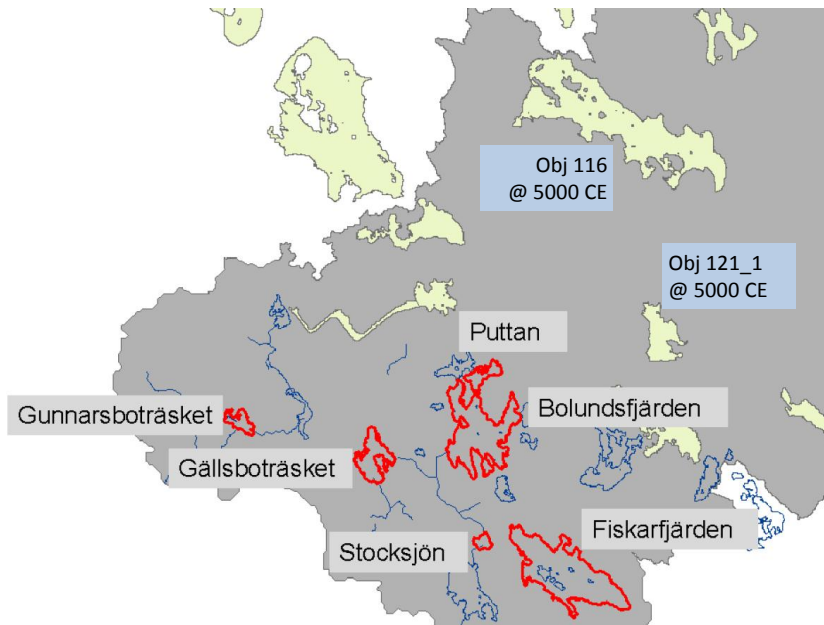


Figure 2: Lake/mire areas used to define the “average object” in Bosson et al. (2010). The lighter areas are lakes in the future landscape. Two objects featured in dose modelling are labelled: Object 116 and Object 121_1.

2. Review of SKB's interpretation of hydrology

2.1. Introduction

The near surface hydrology is the main driver of the radionuclide transport model. In this section consideration is given as to how SKB has utilised detailed hydrological modelling to inform the water flows used in the SR-Site dose assessment model.

During this review a number of issues requiring clarification were identified. A joint SSM/SKB/Consultants meeting (Klos, 2013) to resolve these. Discussions at this meeting are therefore included as part of the SKB presentation.

2.2. SKB's presentation

Given the importance of the hydrological representation within the biosphere dose assessment, SKB have a hierarchical approach to defining the parameters used in the dose assessment model. There are three elements to the hydrological model used in the dose assessment calculations:

- i. the use of MIKE-SHE to characterise the hydrology of the objects in the evolving landscape at Forsmark;
- ii. the characterisation of the “average object” from the MIKE-SHE modelling of the Forsmark area and its use in parameterising the hydrological fluxes in the evolving landscape models; and
- iii. the water flow velocities as implemented in the dose assessment model.

2.2.1. MIKE-SHE modelling

Results presented in Section 5 of Bosson et al. (2010) indicate that the model captures the important features of the present day system giving confidence that it could adequately describe the hydrology of emerging objects in the future landscape.

MIKE-SHE modelling was applied to five areas (Figure 1); the regional model (blue border) and two local models (essentially Object 116 and Object 121; not identified in Figure 1) are part of the SR-Site assessment. A smaller area was used at the SDM-Site stage (black) and an extended area used as the “pre-modelling” area (red) was set up before the final runs were started (pp. 303 – 304 or Bosson et al., 2010).

The “pre-model” area was used to generate the hydrological model details for use in the radionuclide transport model. The reason that the SDM-site results were used is that the timescales for the MIKE-SHE and assessment modelling conflicted so that the earlier (available) dataset was used. The impact of modelling using different areas was not discussed by Bosson et al., (2010) however, at the joint meeting between SSM, SKB and respective consultants, it was stated there is no difference in the results that would affect the hydrological modelling described below (Klos, 2013).

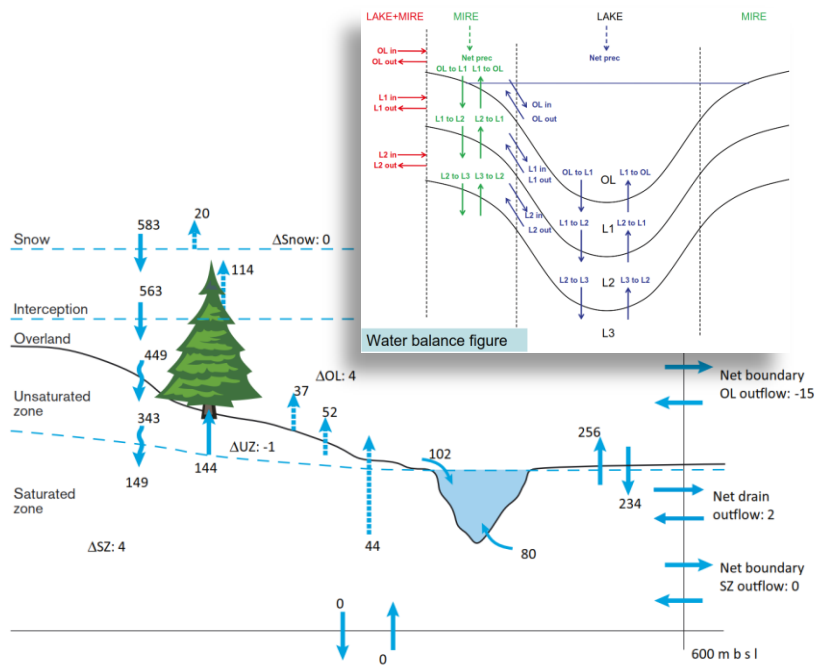


Figure 5-20. Water balance from the 2000AD_2000QD model for the catchment area of Lake Bolundsfjärden.

Figure 3. Conceptualisation of the water fluxes from the MIKE-SHE mass balance output (inset) and numerical mass balance for Lake Bolundsfjärden at 2000 CE, taken from Bosson et al. (2010). It is understood that a combination of similarly derived numerical details for the six lakes at 5000 CE is used to generate the mass balance scheme for the “average object” shown in Figure 4 (Kios, 2013).

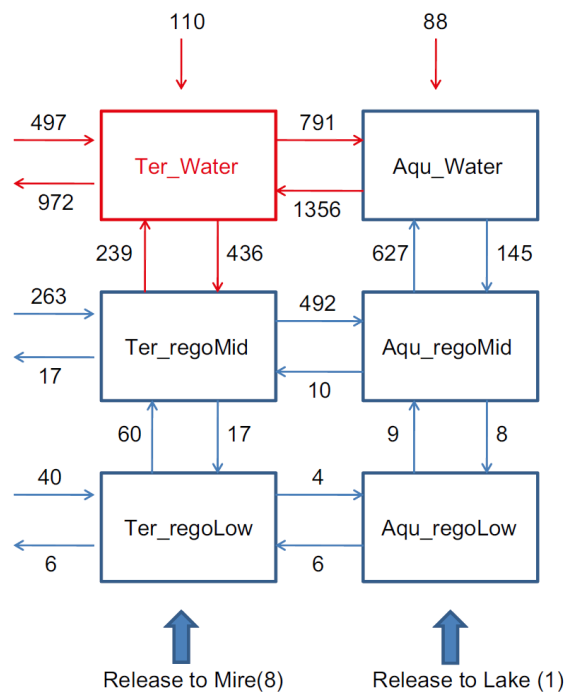


Figure 8-5. Advective fluxes (units in mm y^{-1}) for an average lake-mire object obtained from the MIKE SHE simulations and transformed to a box model.

Figure 4: Water balance for the “average object” as derived in Bosson et al. (2010)

2.2.2. Basis for the hydrological parameters in SR-Site

The “pre-model” area contains six lakes of various sizes (Figure 2). These constitute the typical “lake-centred catchment” believed to be representative of the typical basins in the modelled region. However, the expected distribution of lakes in the future landscape includes objects with a greater range of sizes, as indicated in Figure 2, where future lakes are shown as lighter coloured areas on the map.

The hydrology of the six objects was evaluated using MIKE-SHE at 2000, 3000 and 5000 CE using the 2000 CE model for the distribution of the QD in the modelled area. Temperate climate data were used for application to temperate periods. Periglacial conditions were treated separately and are not addressed here. Only the data from 5000 CE were carried forward to the definition of the radionuclide transport model used in the dose assessment.

Figure 4 shows the formulation of the numerical values obtained from MIKE-SHE, with the numerical example of Lake Bolundsfjärden at 2000 CE. Carried forward into the radionuclide transport model used in the dose assessment, this type of information - from the six lake/mire objects at 5000 CE - was treated as a statistical sample of the lakes in the landscape and so was used to generate water balance for the “average object” on the basis that these six objects are somehow representative of the all lake-centred catchments in the past, present and future Forsmark landscape (Figure 4). Essentially, detailed outputs from MIKE-SHE are sublimated into a single mass balance scheme (Figure 4) that is the “average” for the six objects in the “pre-modelling” area.

2.2.3. Radionuclide transport in the dose assessment model

Fig A-1 from Appendix 1 of Avila et al. (2010) shows the scheme of exchanges in the radionuclide transport model used in the dose assessment calculations, and is produced here as Figure 5.

There are many processes and the relative importance of these changes in time as the object evolves. In Figure 5, below, those with advective transfers are circled. From the description in Appendix 1 of Avila et al. (2010) it is possible to extract expressions for how the advective processes are modelled, i.e. a parametric description of the hydrological model in the radionuclide transport model. Working from the parametric description given in Avila et al. (2010) Figure 6 illustrates the advective fluxes for a “typical lake-mire object” with associated “mathematised” expressions for the fluxes. This interpretation of the hydrological fluxes has subsequently been confirmed by SKB (Kłos 2013).

2.3. The Consultants’ assessment

2.3.1. Motivation of the assessment

Looking at the numerical values of the parameters in the transport model (landscape model compartments) we see (Table 1) that advective transfer processes dominate the accumulation of radionuclides in the regolith and surface water compartments.

Table 1: Numerical values of inter-compartmental transfer rate coefficients (y^{-1}) in the SSM implementation of SKB's model for Object 121_3. Results for ^{129}I and ^{226}Ra . (Derived from the model implemented in Kłos & Wörman, 2012, as produced by Xu et al., 2013).

Source	Receptor	type	^{129}I	advective/ diffusive ratio	^{226}Ra	advective/ diffusive ratio
lower regolith	terrestrial mid-regolith	Advective	5.22E+00	12.9	5.90E-03	12.0
		Diffusive	4.04E-01		4.91E-04	
terrestrial mid-regolith	terrestrial upper regolith	Advective	4.66E-01	15.8	1.40E-04	14.7
		Diffusive	2.95E-02		9.57E-06	

This part of the review deals with the assumptions and simplifications made when converting the detailed MIKE-SHE hydrology into the model used in the evolving landscape model which determines SKB's landscape dose factors (LDFs). There are many simplifying assumptions in the process and it will be shown that:

- a. the hydrology in the dose assessment model is substantially different to that represented by the "average object";
- b. the "average object" is neither representative of the range of lake-mire objects to be expected in the future Forsmark landscape nor is it representative of other key object classes, most notably the stream object (from which the highest LDFs are obtained in SR-Site) and the hydrological model of agricultural land;
- c. the hydrology as modelled is suitable only for a snapshot of the lake-mire objects during the evolution of the Forsmark site.

Consequently, it is hard to state with confidence that the hydrological representations in the dose assessment model are fit for purpose.

2.3.2. MIKE-SHE and the "average object"

As noted in Section 2.2, the "pre-model" area was used to generate the hydrological model details for use in the radionuclide transport model. The reason the SDM-site results were used is that the timescales for the MIKE-SHE and assessment modelling conflicted, so the earlier (available) dataset was used. No attempt seems to have been made to reconcile the two sets of results.

From the documentation it is not clear what difference this makes to the numerical values carried forward to the dose modelling. At the joint SSM/SKB/consultants meeting it was confirmed that the results do not change with different overall modelled areas in MIKE-SHE (Kłos, 2013). This confirms that the individual landscape objects can be treated individually and the hydrology of the various basins in the landscape is independent of the others. This was anticipated given the low relief of the region it is likely that the regional scale has a limited influence at the local level.

The procedure for the generation is not described in R-10-02. At the November joint SSM/SKB/consultants meeting (Klos, 2013, meeting protocol) it was agreed that SKB would make available details for each of the six lakes at each of the three times so that the sensitivity of the dose factors to these parameters can be investigated by SSM (see Section 3, below). It is anticipated that this information will be in the form of the figures shown in Figure 3.

One potentially important feature of this model of the hydrology is that advective velocities (mm a^{-1}) are quoted rather than advective fluxes ($\text{m}^3 \text{a}^{-1}$). The implications of this can be seen when the conversion to the radionuclide transport model in the dose assessment model is carried out. Further details of the numerical aspects of this scheme are discussed below. There are, therefore, a couple of issues here. The “average object” is bigger than the smaller radiologically more sensitive objects and the hydrology it exhibits is not necessarily representative of the larger objects. Questions can be raised as to the relevance of the hydrology of the “average object” in the context of the landscape.

By use of the “average object” as the basis for *each basin in their landscape model* SKB cannot be said to utilise the details in the presented landscape model for deriving parameters exported to the dose assessment. The abstractions of the “average object” (with larger or smaller object and sub-catchment areas) fails to capture any of the unique features of the landscape’s hydrological properties. Rather than a true landscape model, the resulting model for dose assessment reduces to a linked array of reference objects. It is also potentially significant that the most important object in terms of the magnitude of the Landscape Dose Factors is not a lake-centred catchment but a sub-area within a lake-centred catchment. Details of the hydrology of this type of object are not discussed.

2.3.3. Radionuclide transport model

There is a difference between the MIKE-SHE hydrological balance model (Figure 4) and the hydrological interpretation implemented in the radionuclide transport model (Figure 6) in that the compartments are different and the fluxes between the compartments differ. Additionally the output from MIKE-SHE in the “average-object” hydrology is written in terms of numerical values that are a snapshot of advective *velocities* averaged for the six lake/mires at 5000 CE whereas the model employed in the radionuclide transport model is a fully parameterised implementation of the fluxes. The reason for this is that the model needs to be able to evolve the hydrological fluxes in the object as the landscape evolves. In order to generate the transfer rate coefficients in the radionuclide transport model, the hydrological model uses advective fluxes ($\text{m}^3 \text{a}^{-1}$) rather than the advective velocities (mm a^{-1}) of the MIKE-SHE output.

The final form of the hydrological model parameterisation in the LDF radionuclide transport model is not discussed in detail by Avila et al. (2010). Instead other reports (Andersson, 2010; Aquilonius, 2010; Lindborg, 2010; Löfgren, 2010) are all referenced in Appendix 1 of Avila et al. (2010) as the source material for the description of the parameterisation in the radionuclide transport model. This section of the report further investigates the numerical interpretation of the “average object” with respect to the hydrological model implemented in the dose assessment model. A complicating feature of the radionuclide transport model description is how the transfer rates between compartments are handled. The parameterisation discussed is generic and is so coded as to be applicable to all of the transfer rates at all times.

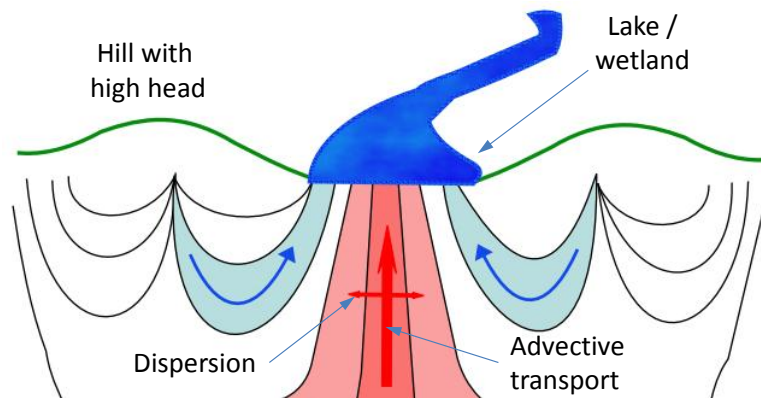


Figure 7: Schematic of groundwater discharge from large depths to surface water systems. Because the surface water system is generally located in local topographical minima the relative symmetry in the groundwater flow implies that local groundwater flow cells discharge from each side into the near-shore bottoms of the surface water, whereas deeper and more large-scale groundwater flows discharge more or less vertically into central parts of the bottom following a converging stream tube. (Taken from Kłos & Wörman 2012).

There are therefore a great number of numerical switches with associated internal logic that governs which processes are active at different times. This makes traceability a long and drawn-out process. SKB have confirmed that the parameterisation given in Appendix 1 of Avila et al. (2010) is a full description, taken directly from the coding used in the models (Kłos, 2013).

2.3.4. Average object and implementation

As discussed, the “average object” is a construct averaged from six not particularly representative objects in the 5000 CE landscape. It is a lake-centred catchment with a surrounding wetland. The resulting average water balance (Figure 4) therefore presupposes a number of spatial and physical relationships, most importantly the size of the contaminated object relative to the entirety of the basin. This aspect is discussed further below but there are other concerns related to the applicability of this “average object” to the general characterisation of objects in the landscape over the temporal domain of the model.

From Kłos & Wörman (2012), the topography-driven groundwater circulation is as shown in Figure 7; a qualitative sketch of the interactions depicted in Figure 4. A key role for the hydrological modelling with, in this case, MIKE-SHE is to identify the boundaries between the contaminated system and the uncontaminated catchment representing the rest of the basin. MIKE-SHE codes the flow vectors in the basins at different times, it would be theoretically possible to extract the flows system in Figure 7. In practice this would be difficult, however and Section 3 of this report looks at alternative ways of coding this kind of information in dose assessment models.

Highest Landscape Dose Factors (LDFs) arise from terrestrial ecosystems (specifically agricultural systems) for which the lake/mire system is broadly appropriate. In SKB’s dose modelling, however, other states – sea, bay and stream -

are interpreted from the system described in TR-10-06 Fig A-1 (Figure 5 here) using this water flux scheme. The sea and bay states are relatively straightforward to interpret since the terrestrial components of Fig A-1 are not present and the water flux is greatly simplified as a vertical movement through the regolith driven by the input from below. Water exchanges are also modelled via turnover time parameters relevant to the parcels of water in each object. Modelling of sea and bay objects is not pursued here because the resulting concentrations of radionuclides (and therefore doses) are not significant compared to the accumulation in the terrestrial components of the system.

There are therefore two types of objects for which the SKB water flux scheme in Figure 4 and the corresponding water fluxes as modelled are of interest, namely stream objects and the agricultural systems (from which the highest doses arise). In SR-Site, the highest LDFs come from object 121_3. Object 121 is a lake-centred catchment that is split into three sub-objects. Object 121_3 is located on the slope of the large basin and at no point during the future evolution of Object 121 is Object 121_3 a lake. Nevertheless, according to the distribution of release points in the landscape (see Klös et al., 2012) there is a potential radionuclide discharge point that makes this area important. It is not clear that the LDF radionuclide transport model coding of the hydrology presented in Avila et al. (2010) adequately represents this object. The treatment of stream (as opposed to lake-centred catchment objects) is not discussed in sufficient detail.

Klös & Wörman (2012) discuss the total separation of the transport and accumulation model in LDF radionuclide transport model for natural ecosystems as presented in Avila et al. (2010). Hydrology in the agricultural land model is therefore not related to that shown in Figure 4. The hydrology model shown in Figure 6, here, is therefore only used to model transport and accumulation during the evolution of natural ecosystems. The hydrology of the agricultural systems is much simpler in conception and is seemingly designed to leach accumulated activity as quickly as possible. Given the importance of agriculture it is surprising that a more robustly justified description of agricultural land hydrology is not implemented. SKB have stated that it is possible to use MIKE-SHE to characterise agricultural systems (Klös, 2013).

2.3.5. Derivation of parameters in the landscape model

So far two hydrological models have been considered – the MIKE-SHE-based “average object” and the hydrological model embedded in the LDF radionuclide transport model used in the evaluation of doses. This section looks at the process by which Fig 8-5 of Bosson et al. (2010) - Figure 4 here – is turned into the hydrological model as used in the dose evaluation.

Average Object – implications of mass balance

As a check of the implications of the “average object”, Figure 8 shows the water balance matrix implied by Bosson et al. (2010) flow velocity scheme (Figure 4). It also illustrates the lack of clarity in working with the “average object” since there is some ambiguity in the sources and sinks. Figure 4 is a map of the advective velocities in the contaminated object. It does not explicitly account for the water balance of the whole basin. In this interpretation it is assumed that lateral inflows to the terrestrial compartments come from the uncontaminated area (i.e. the sub-catchment in the language of Avila et al., 2010) and that lateral outflows represent drainage of the landscape object, downstream to other landscape objects. Ideally

	geosphere	sub-catchment	Ter_regoLow	Ter_regoMid	Ter_Water	Aqu_regoLow	Aqu_regoMid	Aqu_Water	Atm	Down-stream
geosphere										
sub-catchment			40	263	497					
Ter_regoLow				60		4				6
Ter_regoMid			17		239		492			17
Ter_Water				436				791		972
Aqu_regoLow			6				9			
Aqu_regoMid				10		8		627		
Aqu_Water					1356		145			
Atm					110			88		
Upstream										
Inflow	0	0	63	769	2202	12	646	1506	0	995
Outflow	0	800	70	765	2199	15	645	1501	198	0
Balance	0	-800	-7	4	3	-3	1	5	-198	995
% difference		100.0%	10.0%	0.5%	0.1%	20.0%	0.2%	0.3%	100.0%	100.0%

Figure 8: Mass balance for the “average object”. Numerical values for advective velocities (mm a^{-1}) are taken from Fig 8-5 or R-10-02. Inflows and outflows are evaluated and the balance (inflow – outflow) calculated. For the six compartments of the model shown explicitly in Fig. 8-5 there is a slight imbalance. The yellow shaded elements of the matrix suggest that there is a net 10 mm a^{-1} flow from the “geosphere” to this “average object”.

there should be balance for each of the six compartments explicit to the model but the percentage difference between the in- and out-flows is small. However, as written there is an implied net inflow to the model from the geosphere, amounting to 10 mm a^{-1} , of which 7 mm a^{-1} of this goes to the mire and 3 mm a^{-1} to the aquatic sub-system. According to Figure 4 these values are, respectively, 8 and 1 mm a^{-1} ; consistent with p308 of Bosson et al. (2010), discussing net input from the bedrock to a range of objects

Radionuclide transport model – derivation of parameters

Appendix 1 provides a detailed review of the relationship between the parameterisation of the object in the radionuclide transport model and the numerical values for the “average object”. This is the basis for the link between the two hydrological models. The key parameters are listed in Table 2. These ten parameters are used to define all of the fluxes shown in Figure 6 and the parametric relationships are given in Table 3.

Tables 3 and 4 can then be used to determine water balance for each of the lake-mire objects in the model as a function of time using data taken from SKB’s Sicada database (Xu, 2013). This is performed in the section (below) on the numerical implications of the radionuclide transport model implementation. First, however, the relation between the 11 parameters identified in Table 2 and the water-balance of the “average object” is considered, via the discussions in the ecosystem reports, primarily Löfgren (2010) and Andersson (2010).

Table 2: Parameters in the radionuclide transport model. The parameterisation is illustrated in the compartment structure shown in Figure 8. All areas are object-specific whereas all other parameters are fixed with respect to the advective velocities in the Fig 8-5 in Bosson et al. (2010).

Parameter name (Avila et al., 2010)	Symbol	Description	Reference
Ter_area_object	A_{ter}	Area of terrestrial part of object (mire). Object specific.	TR-10-05
Aqu_area_object	A_{aqu}	Area of aquatic part of object (lake). Object specific	TR-10-05
Area_Obj	A_{obj}	Total area of biosphere object $A_{obj} = A_{ter} + A_{Obj}$	TR-10-06
area_subcatch	$A_{subCatch}$	Area of the sub-catchment. Object specific	TR-10-05
Area_wshed	$A_{watershed}$	Watershed area. Object specific	TR-10-05
fract_mire	f_{mire}	Fraction of upward flux from regoLow (till) directed to the terrestrial part of the biosphere object. Fixed value	TR-10-01, TR-10-02, TR-10-03
Adv_low_mid	v_{Low}^{Mid}	Total advective flux from regoLow (till) to regoMid (glacial and post glacial deposits) for the lake/terrestrial stage	TR-10-01
runoff	$P - E$	Total annual runoff (ie, difference between precipitation and ETP)	TR-10-01, TR-10-02, TR-10-03
Ter_adv_midup_norm	f_{terMid}^{terUp}	Advective flux from glacial and post glacial deposits to peat in the terrestrial ecosystem. Normalised by net lateral flux from sub-catchment. Object specific	TR-10-01, TR-10-02
Aqu_adv_mid_up_norm	f_{aquMid}^{aquUp}	Advective flux between sediment and water during lake stage, normalised by net lateral advective flux from wetland to lake/stream. Object specific	TR-10-01, TR-10-02
flooding_coef	f_{flood}	Gross lateral flux of water from lake/stream to wetland, normalised by the net lateral flux from wetland to lake/stream.	TR-10-01, TR-10-02

Table 3: Water fluxes between compartments in the radionuclide transport model using the parameters in Table 3. Water fluxes are as illustrated in Figure 8. The parametric expressions are “mathematised” to facilitate a better understanding of the numerical characteristics of the model.

Flux	From	To	Expression
F_{terMid}^{Low}	Low	terMid	$A_{obj} f_{mire} v_{LowMid}$
F_{aquMid}^{Low}	Low	aquMid	$A_{obj} (1 - f_{mire}) v_{LowMid}$
F_{terUp}^{terMid}	terMid	terUp	$A_{subCatch} f_{terMidUp} (P - E)$
F_{Water}^{terUp}	terUp	Water	$A_{subCatch} (1 + f_{flood}) (P - E)$
F_{terUp}^{Water}	Water	terUp	$A_{subCatch} f_{flood} (P - E)$
F_{aquUp}^{aquMid}	aquMid	aquUp	$A_{subCatch} f_{aquMidUp} (P - E) + (1 - f_{mire}) A_{obj} v_{LowMid}$
F_{aquMid}^{aquUp}	aquUp	aquMid	$A_{subCatch} f_{aquMidUp} (P - E)$
F_{Water}^{aquUp}	aquUp	Water	$A_{subCatch} f_{aquMidUp} (P - E) + (1 - f_{mire}) A_{obj} v_{LowMid}$
F_{aquUp}^{Water}	Water	aquUp	$A_{subCatch} f_{aquMidUp} (P - E)$
F_{loss}^{Water}	Water	Downstream	$A_{waterShed} (P - E)$

Central to the interpretation of the MIKE-SHE “average object” is Fig 13-2 of Löfgren (2010), which is reproduced here as the inset to Figure 6 here. This is a composite figure showing two equivalent forms of the “average object” mass balance, emphasising the model compartments arising from the MIKE-SHE interpretation. The third element shows the compartment structure of the radionuclide transport model with what is referred to as a “conceptual representation of the water fluxes”. Whilst there are clear links to the model in Avila et al. (2010) there is obviously some additional interpretation.

In the mass balance scheme for the “average object” there are 22 advective velocities. In the radionuclide transport model implementation there are 10 advective fluxes. These are conditioned by five object (basin) specific areas and six parameters expressing the movement of water between the components of the system, including two advective velocities and four fractional parameters related to the flow system described in Figure 4. The areas are derived for each object as a function of time in relation to the landscape model (e.g. the quaternary deposit description for 2000 CE is cited in the discussion of the data transferred to the radionuclide transport model from the MIKE-SHE modelling in Chapter 8 of Bosson et al., 2010) linked to the land-rise / sea-level retreat model.

Table 4: Numerical parameters for the hydrological model of landscape object 116 at three times. Numerical values taken from SKB data file Parameters_TS_all_basin_stream_Converted.xlsx.

Parameter	Units	Date CE		
		4500	5000	6500
A_{ter}	m ²	0	807600	1137600
A_{aqu}	m ²	4379850	753600	423600
$A_{obj} = A_{ter} + A_{aqu}$	m ²	4379850	1561200	1561200
$A_{subCatch}$	m ²	14103000	14103000	14103000
$A_{watershed}$	m ²	10392300	14103000	14103000
v_{Mid}^{Low}	m a ⁻¹	0.044		
f_{terMid}^{terUp}	-	0.31		
f_{aquMid}^{aquUp}	-	0.64		
$P - E$	m a ⁻¹	0.186		
f_{mire}	-	0.98		
f_{flood}	-	1.3		

Constant hydrological parameters in the radionuclide transport model

The six constant parameters listed in Table 4 express the snapshot of the hydrology in the average object and these are used to generate the water fluxes used in the SR-Site radionuclide transport model. The evolution of the objects is represented through changes to the areas in the model domain whereas these six parameters remains constant irrespective of the area of the object.

Understanding the process by which they are derived from the mass balance assumed for the “average object” in Figure 4 is detailed and the results are given in Appendix 3. The implications of the re-parameterisation of the *fluxes* from the *velocities* in Figure 4 are discussed for a specific object at a specified time in the following section.

lobj116.ta at 5000	geosphere	subCatch	Low	terMid	terUp	aquMid	aquUp	Water	Downstream
geosphere									
subCatch									
Low				67318.9		1373.9			
terMid					813179.0				
terUp								6033263.4	0.0
aquMid							1680195.0		
aquUp						1678821.1		1680195.0	
Water					3410105.4		1678821.1		2623158.0
Inflow	0	0	0.0E+00	6.7E+04	4.2E+06	1.7E+06	3.4E+06	7.7E+06	2.6E+06
Outflow	0.00E+00	0.00E+00	6.9E+04	8.1E+05	6.0E+06	1.7E+06	3.4E+06	7.7E+06	0.0E+00
Balance	0	0.0E+00	-6.9E+04	-7.5E+05	-1.8E+06	0.0E+00	0.0E+00	1.4E+03	2.6E+06
% difference			100.0%	91.7%	30.0%	0.0%	0.0%	0.0%	

(a) No account of inflows from sub- catchment and geosphere

lobj116.ta at 5000	geosphere	subCatch	Low	terMid	terUp	aquMid	aquUp	Water	Downstream
geosphere			15612.0						
subCatch			53080.8	736952.0	1819074.4	0.0	0.0	0.0	
Low				67318.9		1373.9			
terMid					813179.0				
terUp								6033263.4	0.0
aquMid							1680195.0		
aquUp						1678821.1		1680195.0	
Water					3410105.4		1678821.1		2623158.0
Inflow	0.00E+00	0.00E+00	6.87E+04	8.04E+05	6.04E+06	1.68E+06	3.36E+06	7.71E+06	2.62E+06
Outflow	1.56E+04	2.61E+06	6.87E+04	8.13E+05	6.03E+06	1.68E+06	3.36E+06	7.71E+06	0.00E+00
Balance	-1.56E+04	-2.61E+06	0.00E+00	-8.91E+03	9.10E+03	0.00E+00	0.00E+00	1.37E+03	2.62E+06
% difference			0.0%	1.1%	0.2%	0.0%	0.0%	0.0%	

(b) Including implicit fluxes from the sub-catchment and geosphere

Figure 9: Mass balance for Object 116 at 5000 CE using the details given in Tables 2 and 3. These water flux matrices work with fluxes in m3 a 1. Two schemes are presented, one without the implied inputs from the sub-catchment and bedrock and the second with these fluxes evaluated as described in the text. The second of these matrices allows the definition of the fraction of the total flux in the basin that flows through into each of Low, terMid and terUp to be identified.

2.3.6. Numerical results for the radionuclide transport model: Object 116 at 5000 CE

Tables 2 and 3 can be used to give the numerical balance for objects in the radionuclide transport model the results are shown in Figure 9. Object 116 is chosen to illustrate mass balance since it is, at this time, a classic lake/mire object.

Figure 9(a) shows that there balance is not achieved as written in the radionuclide transport model and that it is the terrestrial sub-model that is affected. Looking at each compartment in the model in turn allows the fluxes implied to be determined. It also allows a review of how the compartments in the “average object” are interpreted in the radionuclide transport model, where there is a different structure. The approach here interprets the outputs of Figure 4 as losses to drainage (the downstream landscape object) and all inputs from the sub-catchment, the atmosphere or the bedrock.

Mass balance on regolith Low¹

On the basis of the full mass balance scheme as reconstructed from the model, balance in the combined lower regolith means

$$F_{in, Low} = F_{subCatch, Low} + F_{geo, Low} \equiv \left(\frac{40-6}{40-6+10} + \frac{10}{40-6+10} \right) v_{Low, Mid} A_{Obj}$$

$$F_{subCatch, Low} = \frac{34}{44} v_{Low, Mid} A_{Obj} \quad F_{geo, Low} = \frac{10}{44} v_{Low, Mid} A_{Obj}$$

The important thing here is that this quantifies the total flow from the sub-catchment to the lower regolith. The total flow into the sub-catchment is

$$F_{in, subCatch} = (P - E) A_{subCatch}.$$

Thus, the fraction of the total flux into the sub-catchment that flows to the lower regolith is, in fact,

$$f_{subCatch, Low} = \frac{F_{subCatch, Low}}{F_{in, subCatch}} = \frac{34}{44} \frac{v_{Low, Mid} A_{Obj}}{(P - E) A_{subCatch}},$$

$$F_{subCatch, Low} = \frac{34}{44} v_{Low, Mid} A_{Obj} = \frac{v_{subCatch, Low}}{v_{subCatch, Low} + v_{geo, Low}} v_{Low, Mid} A_{Obj}.$$

Mass balance on terMid

Looking at the balance for **terMid** we have an implied excess inflow which is the difference between the flux upwards from terMid to terUp

$$F_{SubCatch, terMid} = f_{terMid, terUp} (P - E) A_{subCatch} - f_{mire} A_{Obj} v_{Low, Mid}$$

From the numerical definition of $f_{terMid, terUp}$ in Figure 4, above:

¹ NB, the usage of A_{Obj} here is confirmed by the derivation of the transfer coefficient on page 101 of TR-10-06. SKB have also confirmed that this is the appropriate normalising factor (Klos 2013).

$$f_{\text{terMid}}^{\text{terUp}} = \frac{\left(\begin{matrix} v_{\text{terMid}} \\ \text{terWater} \end{matrix} + v_{\text{terMid}}^{\text{aquMid}} + v_{\text{terMid}}^{\text{terLow}} \right) - \left(\begin{matrix} v_{\text{terWater}} \\ \text{terMid} \end{matrix} + v_{\text{aquMid}}^{\text{terMid}} \right)}{v_{\text{terWater}}^{\text{Loss}} + v_{\text{terMid}}^{\text{Loss}} + v_{\text{Low}}^{\text{Loss}}}$$

$$= \frac{(239 + 492 + 17) - (436 + 10)}{972 + 17 + 6} = \frac{305}{995}$$

Furthermore, the definition of f_{mire} ,

$$f_{\text{mire}} = \frac{\text{net flux from Low to terMid}}{\text{total upward flux from Low}} = \frac{v_{\text{terLow}}^{\text{terMid}} - v_{\text{terMid}}^{\text{terLow}}}{v_{\text{terLow}}^{\text{terMid}} - v_{\text{terMid}}^{\text{terLow}} + v_{\text{aquLow}}^{\text{aquMid}} - v_{\text{aquMid}}^{\text{aquLow}}}$$

$$= \frac{60 - 17}{60 - 17 + 9 - 8} = \frac{43}{44}$$

gives the inflow from the sub-catchment as

$$F_{\text{SubCatch}}^{\text{terMid}} = \frac{305}{995} (P - E) A_{\text{subCatch}} - \frac{43}{44} A_{\text{Obj}} v_{\text{Low}}^{\text{Mid}}$$

Mass balance on terUp

Balance in gives

$$F_{\text{in}}^{\text{terUp}} = F_{\text{terUp}}^{\text{out}} = F_{\text{subCatch}}^{\text{terUp}} + F_{\text{terMid}}^{\text{terUp}} + F_{\text{Water}}^{\text{terUp}} = (1 + f_{\text{flood}}) (P - E) A_{\text{subCatch}}$$

So that

$$F_{\text{subCatch}}^{\text{terUp}} = (1 + f_{\text{flood}}) (P - E) A_{\text{subCatch}} - f_{\text{terMid}}^{\text{terUp}} (P - E) A_{\text{subCatch}} - f_{\text{flood}} (P - E) A_{\text{subCatch}}$$

$$= \left(1 - f_{\text{terMid}}^{\text{terUp}} \right) (P - E) A_{\text{subCatch}}$$

So

$$F_{\text{subCatch}}^{\text{terUp}} = \frac{690}{995} (P - E) A_{\text{subCatch}}$$

Mass balance on aquMid

$$F_{\text{aquMid}}^{\text{out}} = F_{\text{aquMid}}^{\text{aquUp}}$$

$$= (1 - f_{\text{mire}}) v_{\text{Low}}^{\text{Mid}} A_{\text{Obj}} + f_{\text{aquMid}}^{\text{aquUp}} (P - E) A_{\text{subCatch}}$$

$$F_{SubCatch_{terMid}} = \frac{305}{995}(P - E)A_{subCatch} - \frac{43}{44}A_{Obj}v_{Low_{Mid}}$$

$$F_{SubCatch_{terUp}} = \frac{690}{995}(P - E)A_{subCatch}$$

$$F_{SubCatch_{aquMid}} = 0, F_{SubCatch_{aquUp}} = 0, F_{SubCatch_{aquUp}} = 0.$$

Total inflow to the system from the catchment is therefore

$$F_{SubCatch_{Model}} = F_{SubCatch_{Low}} + F_{SubCatch_{terMid}} + F_{SubCatch_{terUp}} + F_{SubCatch_{aquMid}} + F_{SubCatch_{aquUp}} + F_{SubCatch_{Water}}$$

$$= \frac{34}{44}v_{Low_{Mid}}A_{Obj} + \frac{305}{995}(P - E)A_{subCatch}$$

$$- \frac{43}{44}A_{Obj}v_{Low_{Mid}} + \frac{690}{995}(P - E)A_{subCatch}$$

$$= \frac{305}{995}(P - E)A_{subCatch} + \frac{690}{995}(P - E)A_{subCatch}$$

$$+ \frac{34}{44}v_{Low_{Mid}}A_{Obj} - \frac{43}{44}A_{Obj}v_{Low_{Mid}}$$

$$= (P - E)A_{subCatch} - \frac{43 - 34}{44}v_{Low_{Mid}}A_{Obj}$$

$$= (P - E)A_{subCatch} - \frac{9}{44}v_{Low_{Mid}}A_{Obj}$$

On this basis there is a slight discrepancy at the base of the lower regolith in that the input from the geosphere is not accounted for properly. Interestingly the implied flux from the geosphere amounts to 9 mm a^{-1} rather than the 10 mm a^{-1} from Figure 4.

With this implementation there is a much closer balance for Object 116 at 5000 CE. The terrestrial compartments are a per cent or so out which is not much to be on any concern. However, the balance scheme looks nothing like Figure 4, there is no justification for many of the assumptions in the definition of the model. In fact the MIKE-SHE balance scheme (Bosson et al., 2010) is not like the radionuclide transport model scheme (Löfgren, 2010), and the radionuclide transport model scheme is not like the LDF model scheme (Avila et al., 2010). There are no documented explanations for this. So, although there is a reasonable mass balance scheme in the model its provenance is uncertain. Some of the individual parameters are discussed (though some of the normalised fluxes are questionable – e.g. $ter_adv_mid_up_norm$) and related to Figure 4, many of the fluxes are interactions in Figure 4 are discounted in the radionuclide transport model.

A significant discrepancy here is the translation from the MIKE-SHE balance to the radionuclide transport model structure. In the MIKE-SHE balance for the “average object” at 5000 CE the fractions of the input to the sub-catchment entering respectively TerLow, TerMid and TerWater are,

5%, 32.875% and 62.125%.

the fractions Low, terMid and terUp compartments in the radionuclide transport model are

2.03%, 28.25% and 69.72%

These are significantly different in terms of the potential for migration and dilution. It is not easy to reconcile them because there are different structures to the models with compartments of different character. Some clarification is therefore needed.

To summarise the results of this part of the review:

- A reasonable mass balance is achieved in the model as implemented. This implies a different mix of inflows to the terrestrial compartments that is accounted for in the MIKE-SHE derived “average object”.
- Mass balance as modelled in the SR-Site assessment is not the same as Figure 4 (structure & interactions)
- Main role for Figure 4 is to define the inputs relative to the net precipitation on the sub-catchment.
 - SKB have confirmed that it would be possible to implement the Figure 4 fluxes directly. The choice of the parameterisation was enable a consistent formulation for all objects in the landscape modelling (as reported in Kłos, 2013).
- There is no discussion in any of the reports for the justification of hydrology in the model. There is limited discussion of the origin of parameter values but no justification of the structure. Decisions and assumptions have been made but they are not discussed.
- Mass is not conserved in the model as applied.
- The reviewers have not been able to follow the derivation of the two normalising fluxes in the radionuclide transport model; $Ter_adv_midup_norm$ and $Aqu_adv_midup_norm$ and so are not able to confirm that suitability of their usage. There are also difficulties in understanding the derivation of the flooding coefficient.

2.3.7. The “average object” as a snapshot

The above analysis expresses the mass balance as depicted in the model. That it differs from the MIKE-SHE derived “average object” is clear. There is the issue of the normalising area for Figure 4 that would allow the volumetric fluxes to be evaluated. Although SKB have confirmed the use of the total area of the object in this role (Kłos 2013), here remains some ambiguity in the implications of the approach taken in the dose assessment modelling.

Looking at the one direct usage of an advective velocity from Figure 4 in the radionuclide transport model, it appears that the normalising flux is the area of the object. The flux from Low to the two mid-regolith is

$$F_{Low} = v_{Low} A_{Obj}$$

In the derivation of the normalising factors representing the inflow from the sub-catchment to the terrestrial regolith, the total input to the sub-catchment is

$(P - E) A_{subcatch}$. The upwards flow from terMid is therefore

$$F_{terMid} = f_{terMid} (P - E) A_{subcatch}$$

(neglecting the input from the lower regolith, of course).

Table 5. Normalisation factors for two objects as a function of time.

object	Time CE	A_{Obj} [m ²]	$A_{subCatch}$ [m ²]	f_{norm} [-]
“Average object”	5000	-	-	0.187
lobj121_03.ta	2500	410675	637500	0.644
	3000	179425	637500	0.281
	3500	81876.0001	637500	0.128
	3600	81876.0001	637500	0.128
lobj116.ta	4000	6869600	14103000	0.487
	4500	4379850	14103000	0.311
	5000	1561200	14103000	0.111
	6500	1561200	14103000	0.111
	7000	1561200	14103000	0.111
	7500	1556800	14103000	0.110
	8000	1556800	14103000	0.110
	8400	1556800	14103000	0.110

According to the definition of $f_{terMid, terUp}$, it is based on an incomplete water balance for the terMid compartment:

$$f_{terMid, terUp} = \frac{\left(v_{terMid, terWater} + v_{terMid, aquMid} + v_{terMid, terLow} \right) - \left(v_{terWater, terMid} + v_{aquMid, terMid} \right)}{v_{terWater, Loss} + v_{terMid, Loss} + v_{Low, Loss}}$$

The denominator is the total mass of water entering the model, so

$$\left(v_{terWater, Loss} + v_{terMid, Loss} + v_{Low, Loss} \right) A_{norm} = (P - E) A_{subcatch}$$

is the volume of water leaving the system. The normalising area – as far as the total drainage is concerned is

$$A_{norm} = \frac{P - E}{\frac{v_{terWater}}{Loss} + \frac{v_{terMid}}{Loss} + \frac{v_{Low}}{Loss}} A_{subcatch}$$

$$= \frac{186}{972 + 17 + 6} A_{subcatch} = \frac{186}{995} A_{subcatch}$$

In the radionuclide transport model used in the LDF calculations (Avila et al., 2010), therefore, the advective velocity balance in Figure 4 can be converted to volumetric fluxes by multiplying each flux by the common normalising area

$$A_{norm} = 0.187 A_{subCatch}$$

From the flux from Low to Mid, above the normalising area is $A'_{norm} = A_{Obj}$. **This mass balance scheme is therefore only consistent for landscape objects for which**

$$A_{Obj} = 0.187 A_{subCatch}$$

$$f_{norm} = \frac{A_{Obj}}{A_{subCatch}} = 0.187$$

For the numerical parameters used in the SR-Site dose assessment model to be valid therefore requires that the relationship between the area of the subcatchment and the area of the object to be a constant ratio of $A_{Obj} = 0.187 A_{subCatch}$.

As shown in Table 5 for two objects at different times, this is not the case. The mass balance schemes *as implemented*, are lacking in this respect. The normalisation factors must change in time. Similarly, for different basins in the landscape it is unlikely that the 0.187 ratio is an accurate reflection of the relative sizes of the basin and lake/mire. There is potentially a large uncertainty in the results for LDF associated with this approximation.

2.4. Conclusion of the review of SKB interpretation of hydrology

2.4.1. Suitability

This review of the derivation and implementation of the hydrological conditions relevant to the future of the Forsmark site during over the timescale of the dose assessment using the radionuclide transport model described in Avila et al. (2010) finds that:

- The hydrology in the dose assessment model is substantially different to that represent by the “average object”. This can be seen in a comparison of the structures in Figure 4 and Figure 6 or, equivalently, Figure 8 and Figure 9.
- Many of the interaction shown in the hydrology of the “average object” are not reproduced in the radionuclide transport model and there is no justification or discussion in either Löfgren (2010) or Avila et al. (2010) to support the change in structure of the hydrology. Similarly there are other assumptions in the radionuclide transport model that pass without comment; for example the separation of the terrestrial and aquatic flow systems in the lake/mire object.
- The “average object” is neither representative of the range of lake-mire objects to be expected in the future Forsmark landscape nor is it representative of other

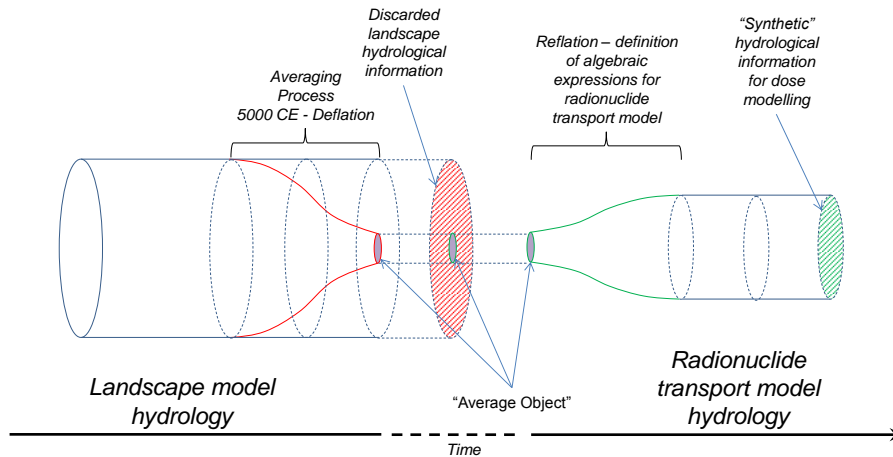


Figure 10: Hydrology information available to SKB and the use and interpretation in the radionuclide transport model. Only a small fraction of the available information in the MIKE-SHE modelling is conveyed to the radionuclide transport model via the “average object”. In order to render the “average object” suitable to characterise the future objects the details are “reflated” by means of the parameterisation listed in Table 3.

key object classes, most notably the stream object (from which the highest LDFs are obtained in SR-Site) and the hydrological model of agricultural land. In generating the “average object” SKB treat the six objects (Figure 2) as representative sample from the landscape. This is done without justification and it is clear that the morphology of lakes in the future landscape differs considerably.

- The hydrology as modelled is suitable only for a snapshot of the lake-mire objects during the evolution of the Forsmark site. Many of the flows in the radionuclide transport model are scaled according to the total water flow through the basin – these are the so-called normalised fluxes. These are shown here to only be applicable for a given balance between the terrestrial area and the area of the contaminated object and the wider sub-catchment. In part the problem of interpretation here arises because the water balance scheme from MIKE-SHE (Figure 4) is written in terms of advective velocities (mm a^{-1}) when what is required are the volumetric water fluxes ($\text{m}^3 \text{a}^{-1}$) – as used in the radionuclide transport model. To convert between the two an area factor is required. At the joint SSM-SKB meeting of 18.11.2013, SKB verified that it is the basin sub-catchment area that is used.

Furthermore, the forensic analysis suggest that the much detailed and relevant hydrological understanding achieved by use of a well calibrated MIKE-SHE is discarded and a much – possibly overly – simplified model is used in its place. This is illustrated by the sketch in Figure 10.

In cosmology, it is believed that the smoothness of our local space-time results from the inflationary period that followed the big bang, effectively ironing out irregularities that are effectively over the horizon to observers in our part of the universe. The approach taken by SKB produces something similar. The reflation of the description of the average object results in a similarly configured “clones” of a (reduced) “average object” that populate the landscape. They differ only in that they have larger or smaller sub-catchment areas.

Although the hydrology of the “average object” is based on water-balance this is not carried over to the radionuclide transport model. Future modelling should be based on a more thorough analysis of sources and sinks for all compartments. The bedrock, uncontaminated sub-catchment, atmosphere and downstream sink should all be included.

A further alternative for SKB to consider is that the water balances provided by MIKE-SHE should be translated directly into the hydrology of the landscape objects. This would lead to a genuine “landscape model”.

Following the review carried out here, it is not a quick and easy task to estimate what the effects of a more coherent hydrological basis would be on the LDFs. Alternative approaches are set out below in a consideration of future work.

2.4.2. Requests for data

The joint meeting between SSM/SKB and consultants on 2013.11.19 clarified a number of issues that had arisen during the review (Klös 2013). As noted, there remain two issues for which SKB should provide additional information:

Request 1 – Results for the mass balance of six lakes at six times

As discussed, Chapter 8 of SKB Report R-10-02 presents a balance scheme for an “average object” based on the combination of water fluxes derived from six lakes close to the Forsmark NPP in the present day (Gunnarsboträsket, Gällboträsket, Stocksjön, Puttan, Bolundsfjärden and Fiskarfjärden).

Please supply the following details from the MIKE-SHE modelling:

For the times 2000 CE, 3000 CE and 5000 CE **and** for each of the six lakes provide

1. The areas of
 - a. catchment (basin)
 - b. lake
 - c. mire
 - d. lake + mire
2. Water fluxes between the compartments used in the MIKE-SHE tool for defining mass balance in compartment models
 - a. Fluxes in $\text{m}^3 \text{ year}^{-1}$
 - b. Fluxes expressed as mm year^{-1} (as for the “average object” mass balance scheme shown in R-10-02, Fig 8-5.)

In total, then, there should be mass balance schemes for six lakes at each of three times, making 18 sets of results in total.

Results in the form of Fig 8.5 of R-10-02 would be preferable. It is understood, however, that results in the form of Fig 8-4 of R-10-02 (with numerical values attached) would show the same details.

Request 2 – Detailed derivation of parameters in the TR-10-06 radionuclide transport model

Of the six parameters

- i) Upwards velocity out of lower regolith: *adv_low_mid*;
- ii) Fraction of flow from lower regolith directed to mire: *fract_mire*;
- iii) Net precipitation: runoff;

- iv) Fraction of infiltration to catchment moving laterally in terrestrial subsystem: *Ter_adv_midup_norm*
- v) Fraction of infiltration to catchment moving laterally in aquatic subsystem: *Aqu_adv_midup_norm*
- vi) Fractional lateral flux from subcatchment to wetland: *flooding_coef*

Please provide detailed step-by-step description of the procedure used to *justify*, *define* and *calculate* the numerical values used in the model.

Please note that the description in TR-10-01 does not provide sufficient information. At the meeting an extract from the developer's log relating to these parameters was made available.

Please provide the extract for the developer's log but note, again, that the details therein were insufficient to enable us to understand the justification of the procedure.

Request3 – Justification of the suitability of the normalising factors used in the radionuclide transport model

SKB uses a balance scheme for an “average object” based on the combination of water fluxes derived from six lakes close to the Forsmark NPP in the present day at 5000 CE to derive scaling factors of advective flow velocities between compartments used in Radionuclide Model. Further these factors are used to scale advective flow parameters for the modelled biosphere objects as they evolve in time. A justification of the suitability of these scaling factors as applied to all biosphere objects at times over the period of the assessment is required.

3. Independent landscape modelling

3.1. SKB's presentation

The model used by SKB to evaluate the radiological impact of radionuclides releases to the biosphere is described in detail in Avila et al. (2010). Xu et al. (2013) were able to reproduce – to close agreement – most features of the results from Avila et al. using the documented description therein. As discussed in the previous section, the hydrology encoded in the model is the principal driving force for radionuclide transport. The hydrological description outlined in the previous section is therefore key to understanding radionuclide transport and accumulation. Bosson et al. (2010), Löfgren (2010) and Avila et al. (2010) provide important background information that allow the construction of dose assessment models.

3.2. Motivation of the assessment

Over the last decade SSM has developed and maintained an independent dose assessment modelling capability (eg. Klos et al., 2011; Klos & Wörman 2013b). This allows SSM to investigate uncertainties in dose assessments in a systematic and quantitative manner.

In this project, the requirement was to provide:

[an] implementation of an alternative biosphere model including the most plausible transport processes. For a comparison with the Landscape Dose Factors (LDFs) calculated by SKB, the alternative biosphere model should include two or three biosphere objects and some elements of succession within biosphere objects.

Given the findings of the review of the hydrological description in the SKB dose assessment modelling discussed in the preceding section of this report, the model described below takes care to provide a framework in which the hydrological represent at on biosphere objects can be varied and, therefore, from which a range of LDF values, contingent on the hydrological representation, can be derived.

The model described below relies on the documentation provided by SKB for many parameter values and, in some instances, for the parameterisations themselves (particularly in the evaluation of exposure pathways). Nevertheless the model is fully independent of the SKB description and is a stand-alone assessment model. It is implemented in Ecolego and is named GEMA-Site 1.0. A complete description of the model is given in Klos (2014).

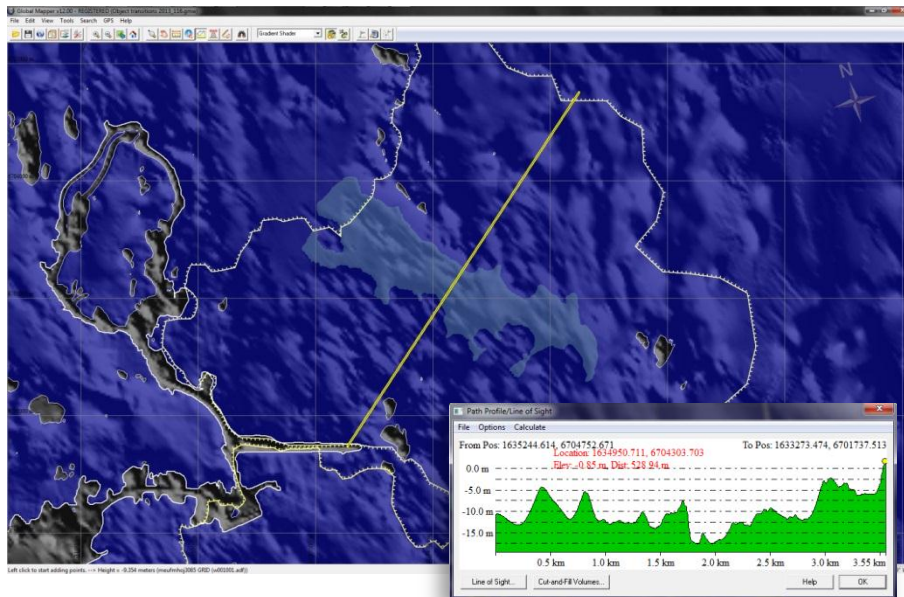


Figure 11: A typical lake-centred catchment - Object 116 in the future Forsmark landscape. Map drawn and objects identified using [Global Mapper 12](#) with the topographic data set provided by SKB (file \\meufmhoj3085\w001001.adf). The depth profile shown runs from NE to SW. The basin boundary is indicated and the area of the future lake/wetland is shaded at the deeper part of the basin. Depths are representative of the situation at 2000 CE.

3.3. The Consultants' assessment

3.3.1. System Identification and justification

Walke (2013) has carried out an analysis of the future Forsmark system using standard Reference Biosphere Models. The SKB landscape modelling approach is rather more complex in that it includes a representation of the entire future landscape. The intention with GEMA-Site is to derive a simple model in the manner of the Reference Biospheres Methodology (IAEA, 2003) but one that is specifically configured to the conditions in the future landscape.

With the focus on hydrology as the main transport driver in Section 2 of this report the model needs to take into account changes in the system as a result of land rise and thereby how the hydrological regime changes in time. Figure 11 illustrates the key features of a “typical lake centred catchment”, taking basin 116 as an example.

As basin hydrology is practically independent of the neighbouring basins, being determined by net precipitation and any discharges from the bedrock, modelling need consider water fluxes only within a single basin. Three areas can be distinguished, using the SKB terminology from Avila et al. (2010):

- The water body area – “the lake” - A_{aqu}
- The terrestrial area surrounding the lake - A_{ter}
- Subcatchment area, ie the area outside the lake/wetland system- $A_{SubCatch}$.

Figure 12 illustrates the conceptual model for this system, with water fluxes.

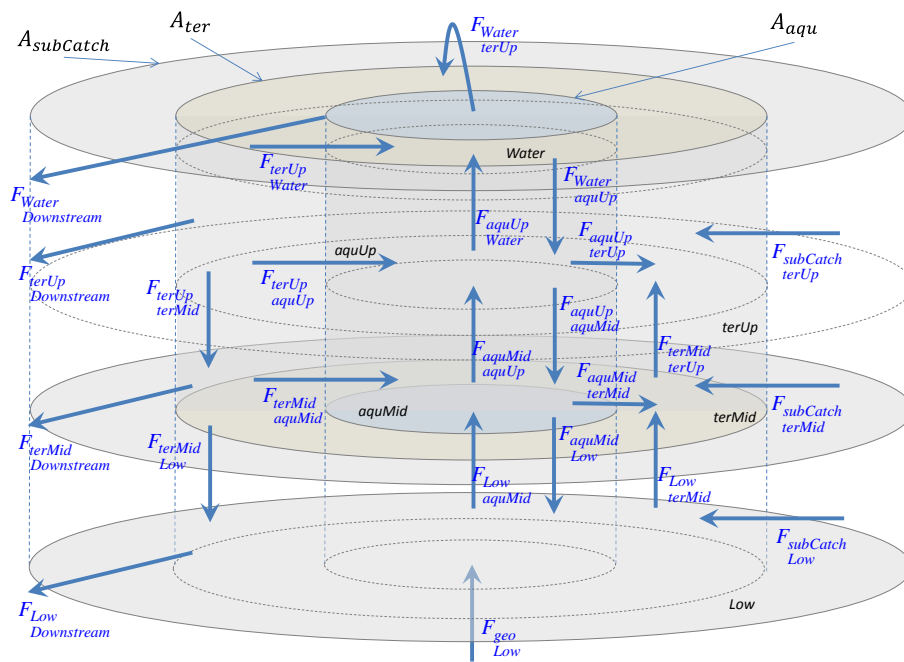


Figure 12: Alternative interpretation of areas and boundaries for a lake-centred catchment. Arrows indicated water fluxes ($\text{m}^3 \text{a}^{-1}$) required to characterise transport and accumulation. The three domains of aquatic, terrestrial and uncontaminated sub-catchment are indicated.

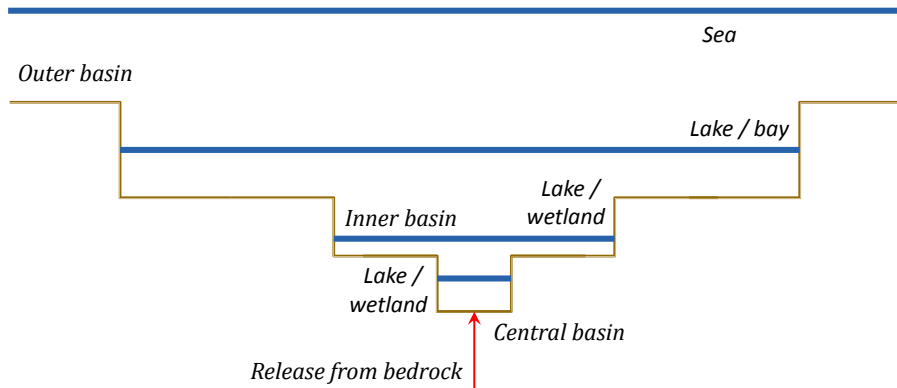


Figure 13: Topography and spatial discretisation of the basin in GEMA-Site. At early times there is complete water cover for the basin – this is the sea stage. As land rises the outer basin emerges (bay/lake stage). Further land rise (and sedimentation) causes the water columns to be confined to the inner basin (lake/wetland stage) and subsequently the inner basin is a wetland and the lake in the central basin. Ultimately the basin drains through a small water body situated in the centre of the basin. Agriculture is possible at any stage in any module where there is a land surface.

In contrast to the generic reference biosphere models this site specific model needs to be able to quantify spatio-temporal changes. Different spatial locations within the basin have ecological and hydrological characteristics as a function of time. The SKB approach has been to focus on the “contaminated area” as a function of time. This is the water column and sediments during the sea stage. As the land emerges from the sea the contaminated region shrinks and the spatial boundary for total contamination moves with it. This rather unphysical interpretation at least maximises the activity concentration available for dose. In part it arises from the treatment of the sub-catchment area (after emergence of the terrestrial areas) as outside the system. There is then a complex treatment of the relative areas of the aquatic and terrestrial subsystems that has the benefit of producing smooth transitions.

In GEMA-Site a more physical approach is taken to defining spatial boundaries and the whole basin is modelled. The cross-section in Figure 11 suggests that a spatial discretisation based on the depth profile can be used. In this way a series of nested modules can be identified as required. A coarse representation would have a single object (the whole basin). At a higher spatial resolution, two modules can represent the outer and inner parts (equivalent to SKB’s subcatchment + object); with three modules the outer, inner and central basin are distinguished (subcatchment + terrestrial and aquatic objects) and so on. A fourth module – at the deepest part of the basin could represent the associated drainage channel.

The model developed here includes three modules: i) Outer basin, ii) Inner basin, and iii) Central basin. The way these evolve with land rise is illustrated in Figure 13.

3.3.2. Module structure and radionuclide transport

GEMA-Site is implemented in [Ecolego](#) as a network of interconnected compartments. Interactions between compartments use first order linear dynamics. The transfer coefficient λ_{ij} between the i^{th} and j^{th} compartments are written as

$$\lambda_{ij} = \frac{1}{l_i A_i} \frac{F_{ij} + k_i M_{ij}}{\theta_i + (1 - \varepsilon_i) \rho_i k_i} + \frac{\dot{l}_{ij}}{l_i} + \frac{\dot{A}_{ij}}{A_i} \quad (1)$$

where

l_i	m	thickness of the compartment,
A_i	m ²	surface area of compartment,
\dot{l}_{ij}	m a ⁻¹	thickness of i transferred to j in unit time
\dot{A}_{ij}	m ² a ⁻¹	portion of surface are of i transferred to j in unit time
ε_i	-	porosity of solid material in the compartment,
θ_i	-	volumetric moisture content,
ρ_i	kg m ⁻³	Density of solid material in the compartment,
k_i	m ³ kg ⁻¹ dw	solid – liquid distribution coefficient,
F_{ij}	m ³ a ⁻¹	water flux between compartments i and j , and
M_{ij}	kg dw a ⁻¹	Solid material flux between compartments i and j .

To account for changes in time of the compartment size there are two additional terms to the inter-compartment transfer, depending on the change in compartment size that can be described as moving from i to j (compartment thicknesses and areas,

respectively \dot{l} m year⁻¹ and \dot{A} m² year⁻¹). In principal, each of the quantities defined in Equation 1 can be defined as an instantaneous value and its rate of change. In practice this Lagrangian formalism can be somewhat mitigated by the use of logical statements to control transitions (as in Avila et al., 2010). Some parameters, such as the compartment thickness are smoothly varying functions (eg water depth as a function of isostatic uplift and sedimentation).

Other processes of lesser importance (see Table 1), eg, diffusion can also be represented. In the present form of the model these processes are not yet accounted for since the focus is on hydrology.

The matrices of water and solid fluxes (**F** and **M** with elements F_{ij} and M_{ij} , respectively) are approximated in the model as shown inset. The model therefore considers, for each compartment each set of fluxes four pairs (each in the in and out directions):

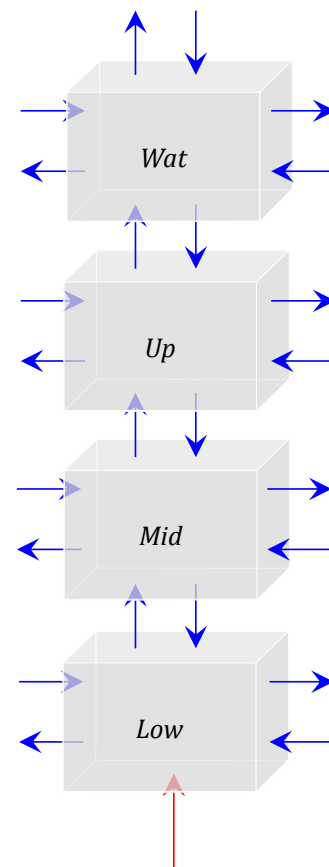
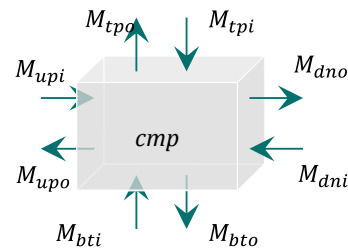
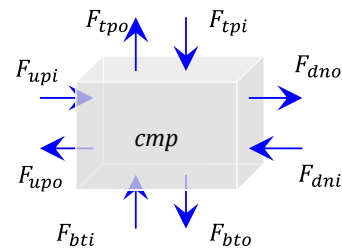
- upstream – *upi*, *upo*
- downstream - *dni*, *dno*
- top – *tpi*, *tpo*; and
- bottom – *bti*, *bto*.

The benefits of this formalism are that the exchange between modules (eg sea state) can be managed as a combination of upstream and downstream flows in and out. By combining inputs and outputs the modelled fluxes can be readily used to verify mass balance during the construction of the model for a specific application. Each specific implementation of hydrology (and solid material fluxes) is a specific and planned representation of the object to be modelled.

Each module comprises a stack of four modules with the internal parameters of each compartment selected to represent the physical nature of the media:

- *Wat* – surface water compartment
- *Up* – upper regolith
- *Mid* – mid-regolith
- *Low* – lower regolith

This follows the standard formulation in the SKB model. Because of the focus on the role of hydrology in determining dose in the landscape and it is reasoned that the higher resolution models recently investigated (Kłós et al., 2011, Kłós et al., 2013) were not necessary at this stage.



3.3.3. Evolution and hydrology in the three module basin

There are spatial and temporal considerations to the representation of hydrology in the basin. Peak dose may arise in the agricultural system but it is the accumulated activity concentrations that are responsible for the dose at this time (Kłos et al., 2011; Kłos & Wörman, 2013). As the system evolves the hydrology changes. The model must capture this.

The aim is to codify the near surface circulation represented in Figure 8. Figure 14 illustrates this for the example considered here. Three time parameters are used to control the changes in hydrology in each of the modules.

$$\text{End of the sea stage - } t_{sea} = \left| \frac{l_0 - l_{bay}}{\dot{l}_{uplift} - (M_{tpi} - M_{tpo}) / A_{obj} \rho_{gl}} \right|$$

Where the assumed depth of the bay is used as well as the net sedimentation (assumed to be glacial clay). The land uplift rate is the $\dot{l}_{uplift} = 0.006 \text{ m a}^{-1}$ at Forsmark.;

$$\text{End of the aquatic stage - } t_{aqu} = t_{sea} + \left| \frac{l_{bay}}{\dot{l}_{uplift} - (M_{tpi} - M_{tpo}) / A_{obj} \rho_{peat}} \right|$$

Where the deposited material is assumed to be peat from senescent vegetation. The solid transfers relate to the upper regolith compartment. The sedimentation rates are evaluated at the top of surface of the upper regolith compartment during the different phases. During the lake phase peat production becomes important.

Start of the agricultural period - t_{agri} . In practice t_{agri} is a user defined value and transition can occur at any time after the end of the aquatic period in the module. As written in Figure 14 the central basin is the focus of attention. This is because the highest radionuclide accumulations are likely to arise here.

Details of the implementation are quite complex. Central to the interpretation is the input from the net precipitation. As implied in the review of hydrology above, particularly Figure 4, there is a lateral flux from the outer basin for $t \geq t_{aqu}^{Outer}$. In GEMA-Site there are two parameters used to code this. The net flux at the surface of the outer basin is $(P - E) A_{Outer}$. A fraction of this moves laterally through each of the upper, mid and lower regolith layers, respectively, $F_{dno}^{upp} = \phi_{upp} (P - E) A_{Outer}$, $F_{dno}^{mid} = \phi_{mid} (P - E) A_{Outer}$ and $F_{dno}^{low} = (1 - \phi_{upp} - \phi_{mid}) (P - E) A_{Outer}$. These fractional fluxes ϕ_i , $i = \text{upper and mid regolith compartments}$ are therefore key parameters. Details for the specific application are discussed in (Kłos, 2014).

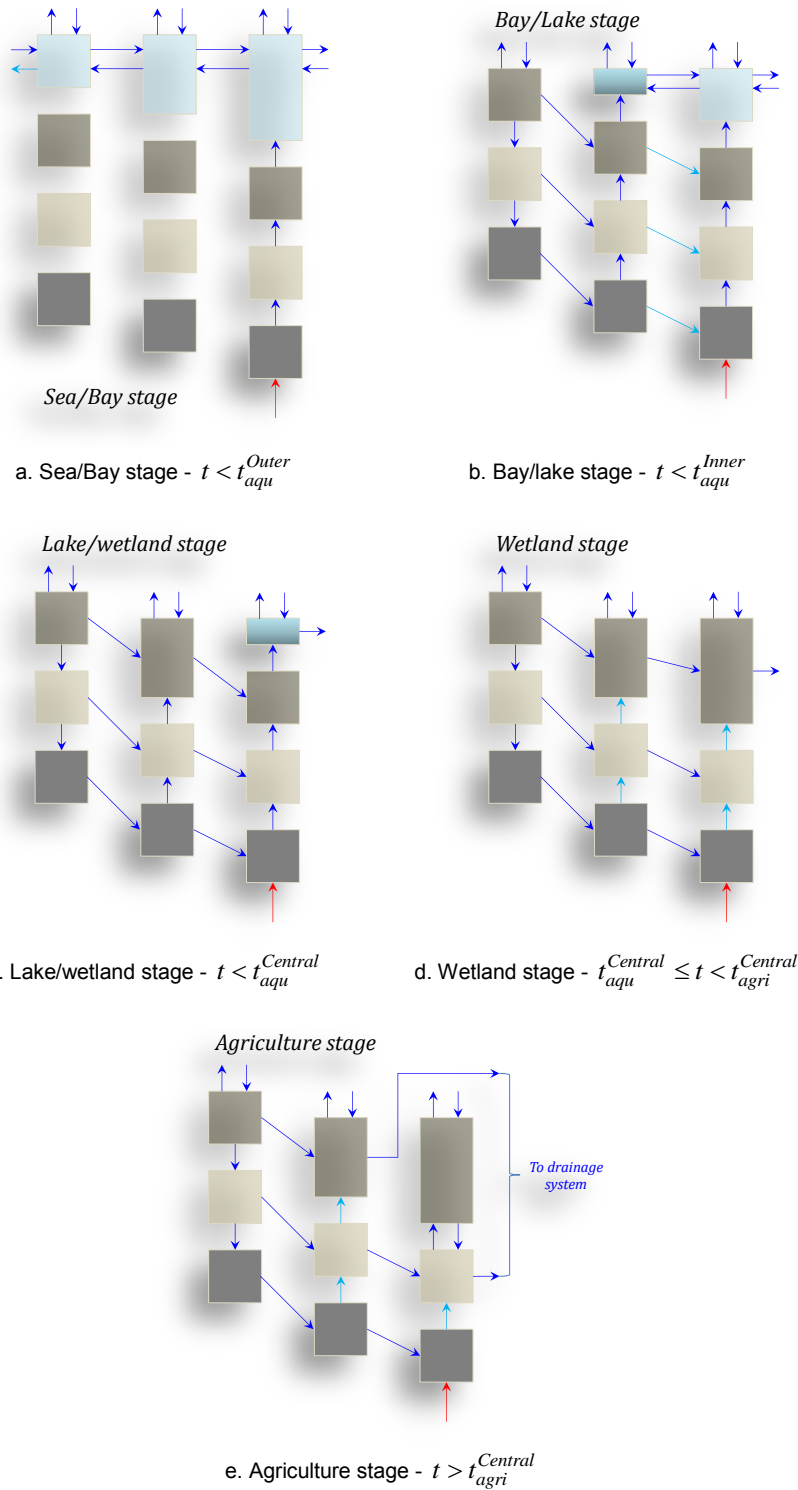


Figure 14: Evolution of hydrology during land uplift. The time domains relevant to each of the stages are indicated. The outer, inner and central basins are shown from left to right. With uplift and sedimentation the water level drops in each module. Release is to the lowest part of the basin. It is assumed that this produces a small upward flux at all times. As water levels form the flow from the outer, then inner basin is directed sub-horizontally towards the central basin where it contributes to an increase upward flux. The change to agricultural conditions necessitates the diversion of relatively large water fluxes in a maintained drainage system.

3.3.4. Radionuclide release and evaluation of dose

The model calculates the distribution of radionuclides in the compartments of the modules on the basis of input to any of the compartments in the ensemble. Typically release would be expected to occur to the lowest point of the topography. In this case release is therefore assumed to be to the lower regolith of the central basin (as shown in Figure 14). An input of 1 Bq a^{-1} is therefore assumed, enabling results to be evaluated in comparison to the LDF values derived by SKB (Avila et al., 2010).

Doses are evaluated for each module. To facilitate the comparison with the SR-Site LDFs the exact formulations used in Avila et al. are used. Consumption is reformulated to avoid the unnecessary reliance on carbon consumption that features in the SKB modelling. The exposure pathways calculated are listed below, including the ecosystems at which they are applicable.

Sea/bay stage	natural ecosystems (lake/wetland)	agricultural ecosystem
Fish (marine)	Fish (freshwater)	berries
Crustacea (marine)	Crustacea (freshwater)	mushrooms
	water	game
	berries	external irradiation
	mushrooms	inhalation
	game	meat
	external irradiation	dairy products
	inhalation	green vegetables
		root vegetables
		cereals

The amount of consumption takes into account an autarky factor – the degree to which the area of land can support the required level of consumption. Plant concentrations are derived from both root uptake and interception of contaminated irrigation water. This latter option is not used in these initial calculations.

3.3.5. Numerical characterisation of the GEMA-Site basin

A complete description of the large dataset required to characterise the set of three modules is outside the scope of this report. Klos (2014) shows how the numerical values compiled for radionuclide specific and many site specific but element independent values are derived from the SKB database used for SR-Site.

The model used here is configured to describe a representative basin. In this way the numerical values for the areas of the modules and the lateral fluxes are the key distinguishing features for the modules in the basis employed here are shown in Table 6.

The main distinguishing characteristics for three modules are the area of the outer, inner and central basin and their water depth, respectively 10^7 m^2 , 10^6 m^2 and 10^5 m^2 and 80 m, 75 m and 70 m. This basin is therefore based on typical values for the objects described in the database for the SR-Site basins in Löfgren (2010). The values therefore represent a mid-sized object with a central part of the basin 10 m deeper than the outer basin.

Table 6: Basin specific details for the implementation of GEMA-Site described here.

Parameter	Value	Module	Description	
P	m year^{-1}	0.56	all basin	Precipitation
E	m year^{-1}	0.4	all basin	Evapotranspiration
$v_{geo,sea}$	m year^{-1}	0.01	all basin	Bedrock adv. velocity sea stage
$v_{geo,ter}$	m year^{-1}	0.01	all basin	Bedrock adv. velocity non-sea stage
\dot{l}_{uplift}	m year^{-1}	-0.006	all basin	Isostatic uplift rate
A_0	m^2	10^5	Central Basin	Initial object area
l_{bay}	m	5	Central Basin	Depth on isolation from sea
t_{agri}	year	19000	Central Basin	Time of conversion to agriculture
l_{min}	m	0.01	lower regolith	Minimum allowed thickness
l_0	m	1	lower regolith	Initial thickness
l_{min}	m	0.01	mid regolith	Minimum allowed thickness
l_0	m	0.9	mid regolith	Initial thickness
l_{min}	m	0.01	upper regolith	Minimum allowed thickness
l_0	m	0.1	upper regolith	Initial thickness
$l_{agri,root}$	m	0.3	upper regolith	Agricultural rooting zone
l_{min}	m	0.2	water	Depth at end of aquatic state
l_0	m	80	water	Initial water depth
A_0	m^2	10^6	Inner Basin	Initial object area
l_{bay}	m	5	Inner Basin	Depth on isolation from sea
t_{agri}	year	25000	Inner Basin	Time of conversion to agriculture
l_{min}	m	0.01	lower regolith	Minimum allowed thickness
l_0	m	1	lower regolith	Initial thickness
l_{min}	m	0.01	mid regolith	Minimum allowed thickness
l_0	m	0.9	mid regolith	Initial thickness
l_{min}	m	0.01	upper regolith	Minimum allowed thickness
l_0	m	0.1	upper regolith	Initial thickness
$l_{agri,root}$	m	0.3	upper regolith	Agricultural rooting zone
l_{min}	m	0.2	water	Depth at end of aquatic state
l_0	m	75	water	Initial water depth
A_0	m^2	10^7	Outer Basin	Initial object area
l_{bay}	m	5	Outer Basin	Depth on isolation from sea
t_{agri}	year	25000	Outer Basin	Time of conversion to agriculture
l_{min}	m	0.01	lower regolith	Minimum allowed thickness
l_0	m	1	lower regolith	Initial thickness
l_{min}	m	0.01	mid regolith	Minimum allowed thickness
l_0	m	0.9	mid regolith	Initial thickness
l_{min}	m	0.01	upper regolith	Minimum allowed thickness
l_0	m	0.1	upper regolith	Initial thickness
$l_{agri,root}$	m	0.3	upper regolith	Agricultural rooting zone
l_{min}	m	0.2	water	Depth at end of aquatic state
l_0	m	70	water	Initial water depth

The thickness of the upper regolith is typically around 0.1 m. It is assumed that the lower regolith (comprising till layers) is 1 m thick and the mid-regolith 0.9 m in thickness. These values are consistent with the values described in Löfgren (2010) but are more generic in nature in the context of the Forsmark context; not representing any basin in particular. Of course, with more specific detail of release location in the landscape a more specific basin can be modelled.

The same is true for the hydrological model here. For this initial implementation the aim is to set a generic model in the context of the site that is not so dependent on the numerical values used in the SR-Site modelling. The way the hydrology evolves is rather different to that described by Avila et al. (2010) and neither is the network of fluxes equivalent to that of the “average object” described by Bosson et al. (2010).

The two drivers for the hydrology are the net precipitation and the input from the bedrock. These are listed in Table 6, as are the other important parameters - the areas of the modules in the basin. Input from the geosphere is determined by the advective velocity v_{geo} m year⁻¹. As shown in Table 6 this can vary between marine and terrestrial conditions but the interpretation of the fluxes in the “average object” in Table 4, above, suggest that the constant value of 0.01 m year⁻¹ is appropriate. During the joint SSM/SKB/consultants meeting (Klos, 2013) it was confirmed that the correct normalising area used to derive volumetric fluxes in the object is the combined area of the terrestrial and aquatic objects. In terms of the GEMA-Site model this corresponds to the area of the inner basin.

The interpretation of the hydrology of the model is as follows. During the sea stage (Figure 14a) there is little movement in the regolith due to the flat hydraulic gradient imposed at the surface. Exchanges within the water column take place. Discharge from the fracture at the lowest part of the basin implies a vertical flux through the regolith of the central basin (lateral diffusion neglected here as a simplifying assumption). Discharge to the water column results in rapid mixing in the water column of all three modules with loss to other sea areas.

On emergence of the outer basin the net precipitation is down through the regolith (Figure 14b and c). Alternative methods exist for estimating the fractional fluxes in the three regolith layers. From the model of Object 116 interpreted from the Avila et al. (2010) hydrology (see Figure 9), fractional lateral fluxes are given by

$$f_i = \frac{F_{subCatch,i}}{\sum_{i=Low, Mid, Upp} F_{subCatch,i}} \quad (2)$$

yielding:

$$\begin{aligned} \phi_{upp} &= 0.697 \\ \phi_{mid} &= 0.282 \\ \phi_{low} &= 1 - \phi_{upp} - \phi_{mid} = 0.021 \end{aligned}$$

These values differ from the those implied by the “average object” scheme in Figure 4, which gives, $\phi_{upp} = 0.621$, $\phi_{mid} = 0.329$ and $\phi_{low} = 0.050$. Clearly they are important parameters that need to be refined with a more basin specific approach.

Emergence of the inner basin then adds this volume to the overall circulation and the fluxes though the inner basin’s regolith are largely influenced by the outer basin. In

the final stage of natural evolution the basin (Figure 14d) all the water from the sides migrates through the central basin to the wetland area from where the drainage is assumed via the upper regolith layer (which by now has grown by the deposition of a sizeable peat layer). This corresponds to the drainage assumption in the Avila *et al.* model.

The agricultural stage is more complex than that the agricultural land in Avila *et al.* In the SKB formulation the hydrology is configured to leach accumulated radionuclides from the top soil of the agricultural land. In this model there remains the possibility of cycling between upper regolith and the deeper layers, wherein there may remain significant accumulations of activity.

During the agricultural phase emplaced drainage is used to divert lateral inflow from the outer catchment. This is represented (Figure 14e) as a diversion of the major flow from the inner basin upper regolith. Similarly the deeper circulation in the lower and mid-regolith of the outer and inner basins discharge downstream (and out of the basin) via the emplaced drainage system in the mid-regolith. There is a net down flow from the upper regolith of the agricultural soil (set to an overall depth of $l_{agri,root} = 0.3$ m) but there remains the possibility of evapotranspiration from the rooting zone soil acting to produce some upwards mixing through the mid-regolith.

This interpretation is a simple reference-biospheres level of description based on a logical deduction about the direction of fluxes as a function of time. It is not intended to provide a definitive value for the calculated LDFs. Its purpose is to show how a simple interpretation of local conditions can be used to inform a simple biosphere model configured for those local conditions. Because the hydrology of the basin can be rapidly reconfigured it is therefore possible to investigate alternative hydrology schemes in the framework of the same dose assessment model and so to provide estimates of the sensitivity of LDF to model parameters – not just hydrology but the full set of parameters characterising near-surface geology, hydrogeochemistry as well as the biotic components of the system. The results in the following section illustrate the application of the model for a single interpretation of the hydrology, using the nuclides specific parameter values from Avila *et al.* (2010).

3.3.6. Illustrative results for LDF using GEMA-Site

To illustrate the functioning of GEMA-Site and to derive representative LDF values for the basin as described, four radionuclides are released to the base of the regolith in the central basin. The release rate is 1 Bq year⁻¹ of each of ⁷⁹Se, ⁹⁴Nb, ¹²⁹I and ²²⁶Ra. The daughters of ²²⁶Ra, ²¹⁰Pb and ²¹⁰Po grow in in the model.

The release is assumed to begin at the end of the last glaciation with the basin part of the Baltic sea. The overall period of the simulation is 20 000 years.

Results for the concentration of ¹²⁹I in the compartments of the basin are shown in Figure 15. With the hydrology as implemented and in the absence of diffusive processes that would spread the activity concentration across the basin, the results indicate that, for this relatively weakly sorbing radionuclide, the central basin is predominantly affected by the release. This is consistent with the results from Bosson *et al.* (2010) where the spreading of the plume is restricted to areas not greater than the central basin module here. Mixing in the sea stage means that there is a rapid equilibration of concentrations in the water column. Differences are seen as a consequence of the progressive shallowing of each module in turn.

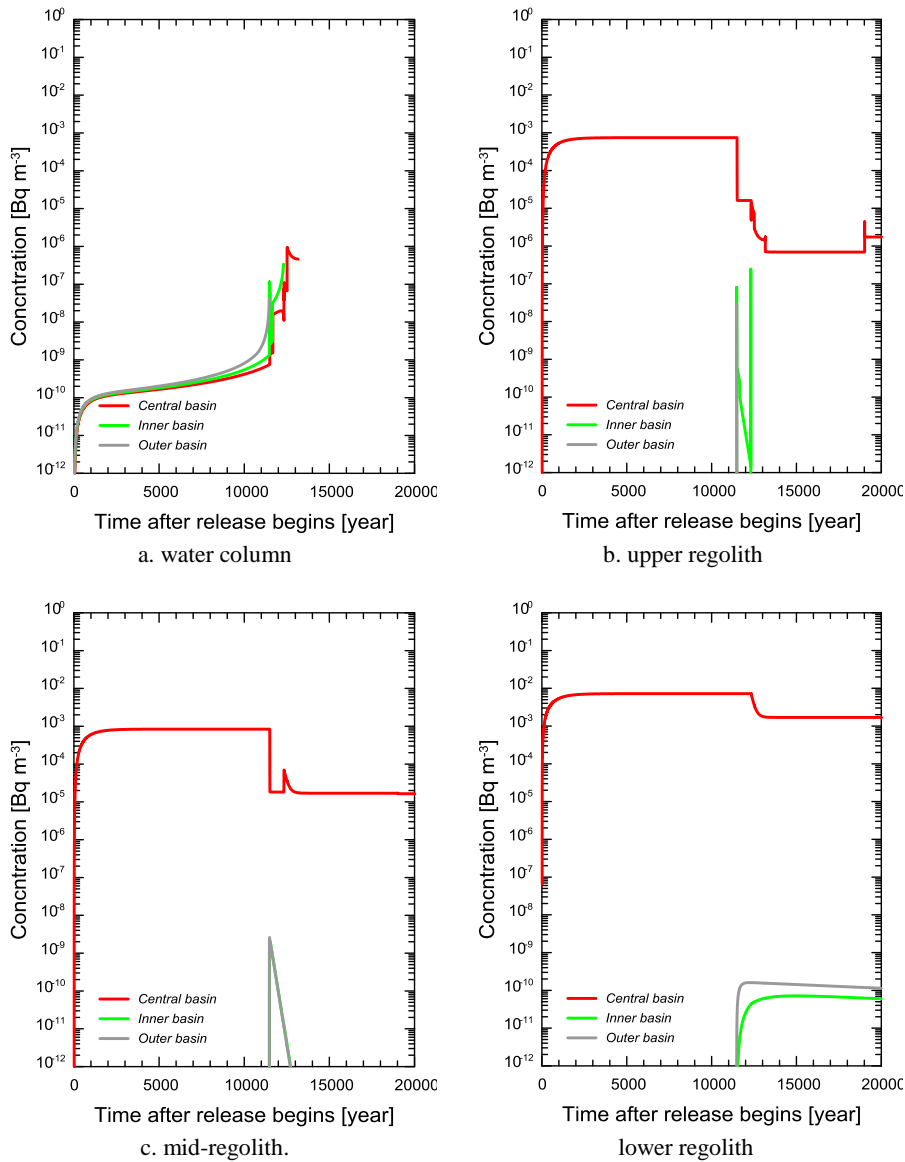


Figure 15: Concentrations of ^{129}I in the water, upper, mid and lower regolith of the Outer, inner and Central Basins.

The sharp edges seen in the results from this model arise from the interpretation of sudden changes at the different times described in Section 3.3.3. A more gradual implementation of change would be possible. This could take the form of higher spatial resolution (more modules) or a more sophisticated interpretation in the evolution of the flow system. An example is seen in the evolution of the concentration in the inner and outer basin regolith layers. At the end of the aquatic period there is a sudden transition in the flow system. The water column now does not drain downstream but rather recirculates through the regolith towards the central basin.

There is one genuine step-change – that at the conversion to agricultural conditions in the central basin at 19,000 years. Such a transition is possible but, again, the dynamics of the conversion to agricultural land needs further review.

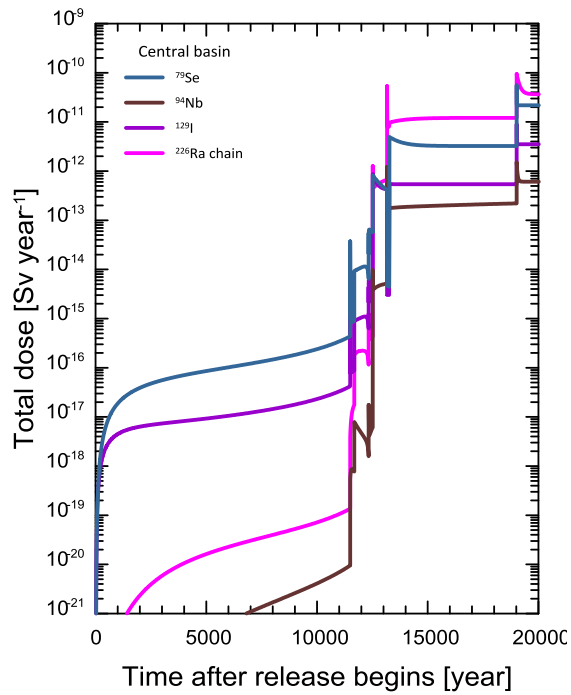


Figure 16: Dose as a function of time for the GEMA-Site implementation. Doses for ^{226}Ra are summed over the chain (^{210}Pb and ^{210}Po).

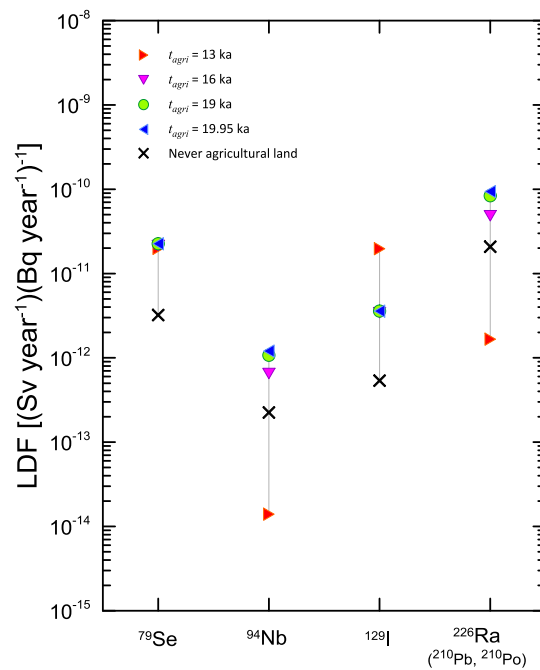


Figure 17: Peak dose from the central basin with conversion to agriculture at different times after the end of the bay period (at 13.15 ka). Doses calculated for a fifty year average after time of conversion.

The spike at 19000 years carries through into the results for dose shown in Figure 16, where there is a gradual leaching of the ^{226}Ra chain members from the agricultural land. This is the situation that the 50 year integration time in the dose model was designed to avoid. This was implemented in the SKB model and reviewed by Kłos & Wörman (2013a).

This simple presentation of results from the GEMA-Site model shows to important features of the implementation. The first is that the doses from agricultural land dominate the exposure scenarios. Accumulation in natural ecosystems followed by exposure in agricultural system (cf Kłos & Wörman, 2013b) is again seen to be important.

The second result is that the ecosystem around the release location is the most important spatial domain in the model. This may change with alternative interpretations of hydrology and with additional (eg. diffusive) processes explicitly modelled. The spreading of the plume around the discharge point should be considered.

3.3.7. Sensitivity of dose to time of agricultural conversion

In the preceding model development (for which the dose evolution in the three basins is shown in Figure 16) the time of conversion of the central basin to agricultural land was arbitrarily set to 19000 years on the basis that this allows time for the radionuclides to accumulate. It also allows for a period in which the radionuclides released to the basin can redistribute. Doses in the Avila *et al.* modelling are averaged over a fifty year period:

$$\langle D_{50} \rangle = \frac{1}{50} \int_{t_{agri}}^{t_{agri}+50} D_{tot}(t) dt . \quad (3)$$

Conversion of the central basin could occur at any time. after the isolation of the central basin. To investigate the influence of the time of conversion of the central basin on total dose the transition to agriculture is assumed to take place at 13 ka (allowing for the infilling and draining of the lake), 16 ka, 19 ka and 19.95 ka. The case where natural ecosystems are left undisturbed is also considered. Figure 17 shows the results.

That the natural ecosystems dose is relatively low is to be expected since agriculture allows for a greater range of foods to be produced with higher efficiency than natural ecosystems. The difference between the strongly and weakly sorbing species (^{226}Ra chain and ^{94}Nb vs ^{79}Se and ^{129}I) is informative and can be linked to the hydrological model of this example system. The change to the drainage system on the development of the wetland in the central basin allows for a remobilisation of the higher k_d elements in the deeper parts of the system. At the earlier conversion time there is little of the ^{94}Nb and ^{226}Ra chain in the upper parts of the central basin. The change in the groundwater circulation after this time and with the conversion to agriculture means that the highest doses for these radionuclides occur at the later times of conversion. For ^{94}Nb the later the conversion the higher the dose (though the effect is relatively small). For the ^{226}Ra chain the highest dose is seen to arise at 16 ka. It is likely that there is progressive leaching of radionuclides in the upper soil horizons after this time.

For ^{79}Se , the results indicate that doses are relatively insensitive to the timing of conversion and therefore to the changes in groundwater circulation patterns as the basin evolves. Agricultural doses are around an order of magnitude higher than the natural ecosystem doses calculated here. Conversion before the end of the aquatic period allows soils with a relatively high ^{129}I concentration to come into production.

Table 7. Object areas used in the sensitivity analysis on the effect of module size on dose. A range of module areas is considered linked to the sizes of Object 116 and Object 121_03 in the Avila *et al.* (2010) model. The reference model has been configured to approximate the overall dimensions of Object 116. The variant cases consider alternative configurations based on the smaller Object 121_03 from which the highest LDFs arise. These results are a preliminary investigation of the behaviour of the GEMA-Site modelling approach and should not be taken as a critique of the SR-Site results.

	A_{outer}	A_{inner}	$A_{central}$	$\frac{A_{inner} + A_{central}}{A_{outer}}$
reference model	1.0×10^7	1.0×10^6	1.0×10^5	11%
large catchment	1.0×10^7	7.0×10^4	1.0×10^4	1%
small catchment	6.0×10^5	7.0×10^4	1.0×10^4	13%
equal small catchment	8.0×10^4	7.0×10^4	1.0×10^4	100%
extreme small catchment	1.0×10^4	7.0×10^4	1.0×10^4	800%

	$A_{subCatch}$	$A_{subCatch} = A_{terr} + A_{aqu}$	$A_{obj} / A_{subCatch}$
SR-Site LDF Obj. 121_03	6.4×10^5		13%
Object 116	1.4×10^7		11%

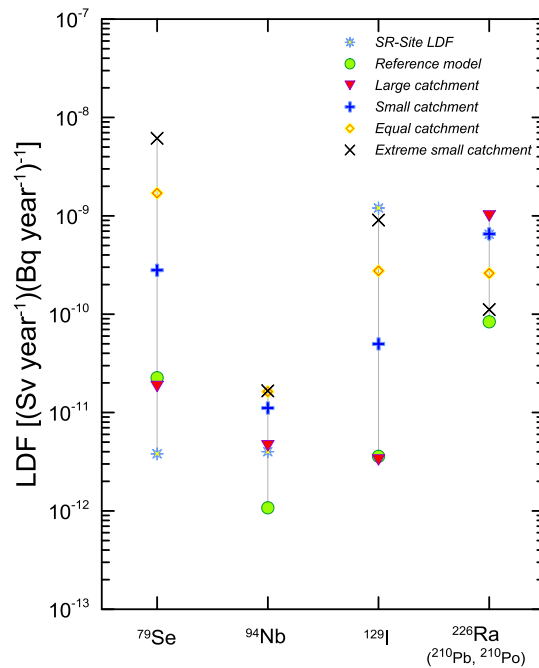


Figure 18: Sensitivity of maximum 50-year averaged dose to assumptions about areas in the model. Doses calculated over the 50 year period after conversion to agricultural land at 19 ka.

As suggested by Figure 16, leaching of the ^{129}I in the nascent soils is rapid and, thereafter, there is little sensitivity to the timing of the conversion. Agricultural doses are a factor of almost ten higher than the natural ecosystem doses. Similarly drainage of the mature lake can lead to doses almost an order of magnitude higher than is the case with conversion to agriculture after to formation of the central wetland.

The effect of the time of conversion is a feature of the GEMA-Site model to investigate when more detailed of the drainage systems in the basins used to define the “average object” are available.

3.3.8. Sensitivity of dose to object dimensions

The relative size of the different modules in GEMA-Site allows a brief sensitivity study to be carried out. The default case for the model set up here is with order of magnitude change between each module. The time series describing the geometry of the objects and subcatchments described in Nordén *et al.* (2010) shows that the subcatchment areas range from $6.4 \times 10^5 \text{ m}^2$ (Object 121_03) to over 10^9 m^2 . The object with the highest LDF is Object 121_03 and this has the smallest combined terrestrial and aquatic area ($8.2 \times 10^4 \text{ m}^2$). Of interest are the relative sizes of the outer basin compared with the inner and central basins (ie, watershed area compared to the object size in the SKB terminology).

To investigate the effect of different of module sizes within the basins a range of values are considered, as set out in Table 7². This includes the reference case and four variants on an object similar in size to Object 121_03. Here the size of the outer basin is also varied so that the amount of water flushing through the system changes. The ratio of object size to subcatchment area in the Avila *et al.* modelling ranges from less than 1% to 18%. For the “large catchment” variant here the ratio is 1% and the ratio of 13% for the “small catchment” case here is similar to that in the case of SKB’s Object 121_03. The “equal small catchment” has an outer basin equal to the size of the combined inner and central basins, and, for illustrative purposes only, an extreme case is also considered where the catchment is small compared to the inner basin with a ratio of 800%.

Results are shown in Figure 18, wherein doses are calculated for agriculture in the Central basin, averaged over the 50 years after conversion at 19000 years. They show that for a larger area from which the agricultural produce is derived, the doses are lower as a result of spatial dilution. The reference model gives lowest doses in all cases, except that the SR-Site LDF from ^{79}Se is around a factor of 5 lower. The reason for this is not understood and needs clarification. Conversely, the smaller the area from which the produce is derived, the higher the dose and this is as expected. However, the relationship is complex reflecting the changes in the groundwater circulation implemented in the GEMA-Site model.

² With its clear evolutionary trajectory Object 116 has been the basis of the definition of the GEMA-Site model development. In Avila *et al.* (2010) it is assumed that there is always an aquatic body at the centre of Basin 116. However, by the end of the object’s evolution at year 8400 CE in the SKB simulations the area of the “water body” is $1.3 \times 10^3 \text{ m}^2$. The longest dimension of the wetland area in the basin is around 2.6 km (see Figure 11) so the width of this aquatic object is typically 0.5 m; ie, a stream. This emphasises the need for i) at least a stream/aquatic module in all representations of the basins in GEMA-Site, ii) a clear distinction between water bodies and the surface drainage system and iii) the need to clearly identify the areas of the catchment where the local farms might be located, in this case close to the (implemented drainage) stream but with a relatively small area.

There is a difference in response between weakly and strongly sorbing radionuclides. The potential variation is lower for the high k_d -species (^{226}Ra chain and ^{94}Nb here), covering a range of around one order of magnitude. For the weakly sorbing radionuclides the range in the analysis here is a little over two order of magnitudes. Only in the case of ^{129}I is the SR-Site LDF greater than the values calculated here. The reason for the high LDF value for ^{129}I is not clear at present and should be clarified.

The model's response is clearly dependent on k_d . The k_d s for ^{226}Ra (and ^{210}Pb) in the inorganic material of the lower regolith are $7.3 \text{ m}^3 \text{ kg}^{-1}$. For ^{94}Nb , $1.9 \text{ m}^3 \text{ kg}^{-1}$ and for ^{79}Se and ^{129}I , 0.022 and $0.0071 \text{ m}^3 \text{ kg}^{-1}$ respectively. For ^{79}Se , ^{94}Nb and ^{129}I the highest calculated doses in the sensitivity analysis arise for the "extreme small catchment" (outer basin much smaller than combined inner and central basins). This is understandable since there is overall less water moving through the system and correspondingly lower dilution. This is further demonstrated by the "equal catchment" (outer basin = inner + central areas), where the results for ^{79}Se and ^{129}I are the second highest. For ^{94}Nb the "extreme" and "equal" catchments give a similar result. The "small catchment" result is similarly lower and the "large catchment" result lower still.

In contrast the highest dose for the strongly sorbing ^{226}Ra chain is seen in the case of the "large catchment" and the lowest for the reference model. The "extreme small catchment" is close to this value however. This suggests that there is an important dilution factor related to the inner and central catchment modules and this is illustrated in the results for three more weakly sorbing radionuclides.

The counterintuitive results for the ^{226}Ra chain arises because of the modelled groundwater circulation. The high k_d of the ^{226}Ra in the inorganic material of the lower regolith acts to retain it there. (Similar considerations apply to ^{210}Pb though ^{210}Po is more mobile.) In the case of the "extreme small" catchment there is little circulation captured outside the release area and so only a small driving flux. In the case of the "large" catchment there is a substantial circulation remobilising sorbed radionuclides in a flux of contaminated water upwards in the central basin. Interestingly, the SKB LDF for ^{226}Ra is close to that of the "small" catchment case here.

These results clearly shows the importance of understanding the groundwater circulation as a function of time. However, it should be remembered that the sensitivity analysis carried out here is preliminary in nature and is used to primarily illustrate characteristics of the GEMA-site model only. It should not be seen as a statement on the uncertainty in the estimates of LDF calculated by Avila *et al.*

3.3.9. Conclusions

Summary

The objective of this part of the SR-Site review project was to provide an "implementation of an alternative biosphere model including the most plausible transport processes. For a comparison with the Landscape Dose Factors (LDFs) calculated by SKB, the alternative biosphere model should include two or three biosphere objects and some elements of succession within biosphere objects". This has been fulfilled.

The model developed for the purpose – GEMA-Site – features:

- A representation of a whole basin representative of and customisable for, basins in the future Forsmark landscape,

- A system of near surface hydrology based on a modular spatial discretisation of regolith and surface water in the basin. The current discretisation uses $n = 3$ modules to represent the outer basin, inner basin and central basin. Alternative discretisations with $n > 3$ are possible if necessary.
- Evolution of the system: with isostatic uplift the coverage of the initial depth of water decreases in time. Peat formation is included during lake and wetland conditions and this leads to a more rapid filling of water filled parts of the basin.
- In contrast to the fixed hydrology assumed in the SR-Site evaluation of LDFs, the hydrology can be treated as part of the model realisation. Mass balance for the whole basin is computed at each stage of the evolution.
- On transition to agricultural land (in any or all of the modules) the hydrology can be configured to match assumptions about local conditions.

The modularisation of the system implies that the different levels of modularisation in the basin have different meanings. For $n = 1$ the basin is treated as a whole and the large size of the basin does not give a good indication of the distribution of radionuclides introduced into the system. With an outer and inner basin model ($n = 2$) there is a better description of the localised accumulations of radionuclides.

The $n = 3$ representation here is a further sophistication. Depending on the hydrological model implemented there will be a greater or lesser spreading of contaminants from central to inner basin. As it is understood that there is a relatively small contaminant plume to be expected it would be possible to add this as a smaller module located around the assumed release location. Kłos et al. (2012) commented that the areas of the biosphere objects were too large and this is also a finding of the parallel numerical review carried out by Walke (2013) using simple reference biosphere models.

A further refinement including a smaller release location module and a dedicated drainage system object would provide a more complete description of the contaminant – hydrology interaction. Development of the modelling approach could also add diffusive transfers between contiguous compartments.

A role for GEMA-Site

SR-Site's radionuclide transport model is a complex model. It embodies many object specific details (at least in terms of the change in ecosystem and – to some extent – land areas). It also evolves.

At the other end of the complexity spectrum, Reference Biosphere models (Walke, 2013) do not fully capture the accumulation scenarios necessary for the highest dose. The use of such obviously non-site-linked models is of questionable utility since they fail to capture the essence of the landscape features and the interaction of the future human population with the local hydrology. They are too stylised.

GEMA-Site therefore lies between the two at an intermediate level of complexity; it uses a more generalised set of site characteristics to get a better fit to local conditions without using all the details from the Avila et al. (2010) representation.

Based on the review of hydrology in Section 2 above and the model development reported in this section the following options are recommended for sensitivity studies using GEMA-Site to investigate the uncertainty in LDFs in a series of sensitivity studies

- Hydrology and basin size

- In addition to the “logical” hydrology add the hydrology of:
 - i. the “average object”
 - ii. the specific details for the six lakes used to define the “average object” using the water balance schemes at the times 2000 CE, 3000 CE and 5000 CE.
 - Irrigation
- Discretisation of basins
 - Release area and drainage stream
 - additional discretisation to better represent the identifiable areas within a basin, doubling the number of modules to better approximate the basin to the spatial scales identified by Avila et al.
- Alternative data values for k_d s and CRs (as discussed in the following sections)

4. Review of SKB's derivation of nuclide specific data

In this section, the values assumed for trace element or radionuclide specific transfer rates in SR-Site are reviewed. Rather than consider all elements, focus is given to iodine, niobium, radium and selenium as it these elements which were reported by SKB to contribute most to the estimated dose associated with the shear failure scenario (see Figure S-11 of SKB, 2011). There are three key radionuclide-specific transfer parameters used in the assessment modelling:

- Distribution coefficients for soil, sediments and suspended matter
- Plant uptake concentration ratios
- Transfers to milk, meat and game

4.1. SKB's presentation

4.1.1. Distribution coefficients

The site-specific K_d values used in the SR-Site assessment were derived by measuring concentrations of elements in paired samples of pore water and solid phase of the regolith for terrestrial locations and filtered water and suspended matter for aquatic locations (Nordén et al., 2010). Site-specific K_d values are reported in Sheppard et al. (2009), though not the raw data used to derive them.

For Se, I and Nb, Table 2-1 in Tröjboom and Nordén (2010) contains references to where the site specific data used to derive terrestrial K_d s is reported. This report points to Hannu and Karlsson (2006) and Engdahl et al. (2006) for measurements of element concentrations in the solid phase of regolith (mg kg^{-1} dw) at the Forsmark and Oskarshamn sites, respectively. The associated soil pore water analysis method is reported in Sheppard et al. (2009). However, the soil pore water data could not be found in any of the available reports. Thus, the problem in evaluating the site specific K_d distributions used as input the SR-Site assessment is that the paired data are not presented in full or separately in the aforementioned reports, or in one single location.

However, for Ra-226 the opposite is true. The concentrations in paired solid phase and pore water samples are given in Table B-1 of Appendix B of Nordén et al. (2010), so the consultants have been readily able to verify the site specific terrestrial K_d distributions derived for Ra-226.

Measured elemental concentrations in both the filtered water and suspended particles of lakes and seas, in both the Forsmark and Oskarshamn areas, are reported in the appendices of Engdahl et al. (2008), such that it should be possible to re-derive the site-specific K_d values for Se, I and Nb. However, the number of samples does not coincide with the number of site specific data used (according to Tables D-3 and D-4 of Nordén et al., 2010).

The best estimates and log-normal distributions of K_d s used in SR-Site calculations were typically derived from a combination of site-specific and literature data, using Bayesian techniques. For any given element-parameter combination a single literature source was used only; these sources were themselves often reviews and compilations of literature (Beresford et al., 2007; IAEA, 2004, 2010; Karlsson and Bergström, 2002; Sheppard et al., 2009). The particular literature source used in any instance was that with the greatest number of samples (Nordén et al., 2010). The data sources used are summarised in Table 8 below.

Table 8: Source of data used to derive distribution of K_d values used in SR-Site

Media	Source of data used to derive distributions of K_d values		
	Se	I	Ra ^a
Soil	Site specific	Site specific	Site specific only
	IAEA (2010) – all	IAEA (2010) – mineral	
Organic soil	Site specific	Site specific	Site specific only
	IAEA (2010) – organic	IAEA (2010) – organic	
Suspended matter in lakes	Site specific	Site specific	No site data
	Karlsson and Bergström (2002)	IAEA (2010) – all	IAEA (2010)
Suspended matter in brackish water	Site specific	Site specific	No site data
	Sheppard et al. (2009)	Karlsson and Bergström (2002)	IAEA (2004) ^b

^a No Bayesian updating undertaken for Ra K_d distributions.

^b Open water for GM. Not clear where GSD comes from.

The number of data points used by SKB to derive the distributions is given in Appendix D of Nordén et al. (2010), but are summarised here for convenience (Table 9).

Table 9: Number of data points used derive distribution of K_d values

Media	Source of data used to derive distribution of K_d values		
	Se	I	Ra
Soil	Site: 4	Site: 2	Site: 18
	Literature: 172	Literature: 196	Literature: N/A
Organic soil	Site: 27	Site: 20	Site: 30
	Literature: 172	Literature: 11	Literature: N/A
Suspended matter in lakes	Site: 7	Site: 6	Site: N/A
	Literature: N/A ^a	Literature: 124	Literature: 75
Suspended matter in brackish water	Site: 5	Site: 5	Site: N/A
	Literature: 3	Literature: 10	Literature: not given

^a Note that Table D-4 of Nordén et al. (2010) says that the literature provided 10 K_d values, yet Section 3.5 of the same report says that "the number of observations in literature data was not known" and so only the site-specific data were used in the end.

In addition, radioisotope concentrations of ^{129}I and ^{226}Ra in a small number of regolith samples are contained in Appendix 1 of Roos et al. (2007). For each of the

two sites that were investigated there is one value each of a soil, limnic sediment and marine sediment radionuclide concentration; it is noted in Roos et al. (2007) that many of these values are based upon a pooled sample. Further measurements of ^{226}Ra in soil, vegetation and water (stream, lake, sea) were reported by Grolander and Roos (2009).

4.1.2. Plant uptake

Whereas in previous assessments (SR-97 and SR-Can) concentration ratios were given on a dry weight (for pasture) or wet weight (for all other vegetation) basis, in SR-Site the concentrations of elements within a specific vegetation type were normalised to the carbon content of that vegetation type. They were derived using the following equation, where the element concentrations in the plant and soil (X_y) are both expressed in $\text{Bq kg}^{-1} \text{ dw}$, and the carbon content of the plant is expressed as $\text{kg C kg}^{-1} \text{ dw}$, giving a concentration ratio expressed in $\text{kg dw kg}^{-1} \text{ C}$.

$$CR_{plant}^X = \frac{X_{plant}}{C_{plant}} X_{soil}$$

The carbon content and dry weight estimates of vegetation are given in Table 4-1 of Nordén et al. (2010).

The site-specific CR values were derived by measuring concentration of elements in unpaired samples of vegetation and solid phase of the regolith (Nordén et al., 2010). The concentrations of elements in various tree, shrub and field layer vegetation samples are reported in Hannu and Karlsson (2006) and Engdahl et al. (2006) for the Forsmark and Laxemar-Simpevarp sites, respectively. The data in these reports were used to calculate the primary producer CR values. The concentration of iodine in mushrooms was reported separately (Johansson et al., 2004). The numbers of data points used to derive the distributions are given in Appendix D of Nordén et al. (2010), but are summarised here for convenience (Table 9).

Table 10: Number of data points used to derive distributions of vegetation CR values

Vegetation type	Source of data used to derive distribution of vegetation CR values		
	Se	I	Ra
Primary producers	Site: N/A	Site: 19	Site: 5
	Literature: not stated	Literature: 25	Literature: 42
Pasturage	N/A ^a	N/A ^a	N/A ^a
Cereals	Literature: not stated	Literature: -	Literature: 24
Root crops	Literature: not stated	Literature: -	Literature: 45
Vegetables	Literature: not stated	Literature: -	Literature: 77
Berries	N/A ^a	N/A ^a	N/A ^a
Mushrooms	Site: N/A	Site: 9	Site: N/A
	Literature: not stated	Literature: N/A	Literature: -

^a Values assumed in SR-Site were the same as for primary producers, so no plant specific data used.

However, in most instances literature data were used, the sources of which are summarised below. For Se the same data have been used in SR-Site as for the preceding SR-97 and SR-Can assessments (Karlsson and Bergström, 2002). Due to the limited availability of site-specific data, the Bayesian methodology used to

derive many of the K_d distributions used in the SR-Site assessment was only applied to a limited number of plant CR: $CR_{PrimProd}^I$ and $CR_{PrimProd}^{Ra}$.

Table 11: Sources of data used to determine the distribution of vegetation CR

Plant type	Source of data used to derive distribution of vegetation CR values		
	Se	I	Ra
Primary producers	Karlsson and Bergström (2002)	Limited site data combined with other sources	Site combined with IAEA (2010) pasture
Pasturage	<i>As primary producers</i>	<i>As primary producers</i>	<i>As primary producers</i>
Cereals	Karlsson and Bergström (2002)	Robens et al. (1988)	IAEA (2010) - grain
Root crops	Karlsson and Bergström (2002)	IAEA (2010) – tubers ^a	IAEA (2010) - tubers
Vegetables	Karlsson and Bergström (2002)	Robens et al. (1988) ^a	IAEA (2010) - leaves of leafy vegetables
Berries	<i>As primary producers</i>	<i>As primary producers</i>	<i>As primary producers</i>
Mushrooms	Pasturage data from Karlsson and Bergström (2002)	Site specific data only	Literature data from Avila (2006a). GSD for primary producers.

^a GSD was the maximum GSD of all crops (cereal, tuber, vegetable) in IAEA (2010). Robens et al. (1988) data presented in Karlsson and Bergström (2002).

Including, and beyond the three elements focussed upon here, the general lack of mushroom specific data leads to either understorey plants or pasture CR values being used as a proxy. Note that although the iodine values in mushrooms are based on site-specific data, there is not a clear relationship between the value reported in Table 4-6 of Nordén et al. (2010) and Table 3-10 of Johansson et al. (2004), even when taking into account the conversion to $Bq\ kg^{-1}\ C$ in mushrooms / $Bq\ kg^{-1}\ dw$ soil, using the C content given in Table 4-1 of Nordén et al. (2010).

4.1.3. Transfer factors for terrestrial biota associated with human exposure calculations

No site-specific data were available for transfers of radionuclides to milk and meat. In the case of Se, Nb, I and Ra transfers to milk, data presented in IAEA (2010) were used (Nordén et al., 2010). For transfers to meat, the data presented in IAEA (2010) were again used, except for the uptake of Se, which was taken from Karlsson and Bergström (2002).

The transfers of elements to wild herbivores are based upon either site-specific data or have been estimated using a kinetic-allometric model, originally developed for the SR-Can assessment (Avila et al., 2006a); the data are presented in Section 4.2.3 of Tröjbom and Nordén (2010) and the model is described in Section 2.4 of Nordén et al. (2010). The allometric model has been modified for SR-Site to consider the concentration ratio as being relevant to the soft tissues of the animal only; the model used in SR-Can took the whole body mass into account. According to Table 4-10 of Nordén et al. (2010), the CRs for I, Ra and Se for herbivores were all derived using the model. The concentration ratio associated with Nb was based on site-specific vegetation data.

4.1.4. Concentration ratios used for aquatic biota

As with the concentration ratios and transfer factors used for terrestrial plants and animals, the concentration ratios for aquatic biota used in the SR-Site assessment were based on a per kg C basis ($\text{m}^3 \text{kg}^{-1} \text{C}$). The carbon content of the biota, used to convert concentrations from $\text{m}^3 \text{kg}^{-1} \text{dw}$ to $\text{m}^3 \text{kg}^{-1} \text{C}$, are based on site data as there are limited reported carbon contents of aquatic biota in the literature (Nordén et al., 2010).

For the radionuclides being considered in this review, the vast majority of the concentration ratio values used for phytoplankton and microphytobenthos in the SR-Site assessment are based upon site specific data. For the other biota (macrophytes, crustaceans, fish) literature data were more readily available (Beresford et al., 2007; IAEA, 2010) and so the Bayesian updating of parameters has been used in most of these cases. The source of the data used to parameterise these transfers is given in Table 12 and Table 13.

Note that although literature data was available for the uptake of iodine in fish this was not used to inform the parameter distribution used in SR-Site (Nordén et al., 2010), as the literature source did not indicate the number of data points upon which the distribution cited was based upon.

Table 12: Source of concentration ratios for freshwater biota used in SR-Site (adapted from information in Section 5.1 of Nordén et al., 2010)

Biota	Element	Comments
Phytoplankton	Se, Nb, I, Ra	Site-specific data for macrophytes
Microphytobenthos	Se, Ra	Site-specific data for macrophytes
	Nb	Site-specific data (only one observation). GSD for Lake_cR_pp_macro (Nb)
	I	Site-specific data (only one observation). GSD for Lake_cR_pp_macro (I)
Macrophytes	Se	Prior from population
	Nb	Site-specific data
	I, Ra	Prior from subpopulation
Crustaceans	Se, I	Site-specific data for filter feeder (prior from population)
	Nb	Site-specific data for filter feeder (prior from subpopulation)
	Ra	Site-specific value for filter feeder (BE prior from subpopulation, GM and GSD prior from population)
Fish	Se, Nb, I	Prior from subpopulation
	Ra	Prior from subpopulation. Prior from population used for probabilistic calculations.

Table 13: Source of concentration ratios for marine biota used in SR-Site (adapted from information in Section 5.2 of Nordén et al., 2010)

Biota	Element	Comments
Phytoplankton	Se	Prior from subpopulation
	Nb	Site-specific data for macrophytes
	I	Site-specific data
	Ra	Literature data (Beresford et al., 2007)
Microphytobenthos	Se, I	Site-specific data
	Nb	Site-specific data for macrophytes
	Ra	Literature data for phytoplankton (Beresford et al., 2007)
Macrophytes	Se, I	Prior from population
	Nb	Prior from subpopulation
	Ra	Literature data (Beresford et al., 2007)
Fish	Se	Prior from subpopulation
	Nb	Prior from population
	I	Site-specific data
	Ra	Literature data (Beresford et al., 2007)

4.2. Motivation of the assessment

As clearly stated by Nordén et al. (2010, p. 14) “The choice of appropriate CR and K_d values is a difficult task, taking into account that values reported in the literature often vary by several orders of magnitude. The most appropriate solution would be to derive the values used in the assessments from representative site-specific data (US EPA, 1999; Xu et al., 2008)”. SKB’s use of site-specific data obtained from the SR-Site studies is something we strongly support and which we have previously recommended (Xu et al., 2008).

Nordén et al. (2010, p. 14) go on to say that “As a result of the site investigations conducted by SKB at Forsmark and Laxemar quite a large set of site-specific data has been made available and has been used in the selection of CR and K_d values.” The site specific parameter values used either directly in SR-Site, or to derive the distributions used in SR-Site when combined with literature data, are listed in several tables in Chapters 3 and 4, and in Appendix D, of Nordén et al. (2010). This report refers to Tröjbom and Nordén (2010), in which Chapter 2 provides a 'Description of site specific data', together with references to the underlying P-reports in which measurement data from individual sites are reported. However, searching back to these underlying reports we have found that the links between the ratio parameters (CR and K_d) in the higher level document (Nordén et al., 2010) and the actual site measurements are not always clear.

For this reason, the consultants requested access to relevant data from the Sicada database, to enable an evaluation of data from the SR-Site programme, from measurement of samples from study sites at the lowest level (the Sicada database), through the relevant ratio calculations (K_d and CR) to the final selected parameter

values presented in Nordén et al. (2010). Specifically, data from the Sicada database relating to measured concentrations of Se, I, Nb and Ra in soils, sediment, porewaters, filtered waters, vegetation and mushroom fruiting bodies were requested. In the request it was highlighted that Tröjbom & Nordén (2010) included the following tables which provide a summary of information it was considered was needed to find the relevant data sets within the Sicada database:

- Table 2-1 (Regolith and porewater)
- Table 2-5 (Vegetation)
- Table 2-9 (Mushrooms)
- Table 2-11 (Limnic sediments and porewater)
- Table 2-12 (Limnic suspended matter and filtered water)
- Table 2-16 (Marine sediments and porewater)
- Table 2-17 (Marine suspended matter and filtered water)
- Table 2-18 (Marine primary producers)

It was requested that all data for Se, I, Nb and Ra were provided for the activity types identified in each of these tables.

4.3. The Consultants' assessment

Figure 19 shows the primary SR-Site documentation used in the review of the derivation of element specific data. In addition, data from the SICADA database were used for the raw measurements taken at the site as part of SKB's SDM-Site project. Comparison of the best estimate values used in the SR-Site assessment are compared to those used in the preceding SR-97 and SR-Can assessments in [Appendix 4](#).

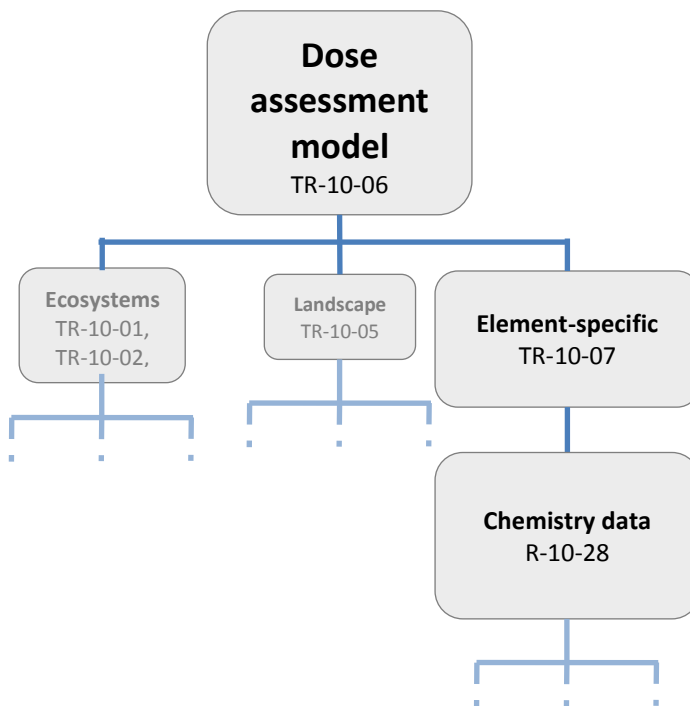


Figure 19: SR-Site documents used in the review of the derivation of element specific data

4.3.1. Distribution coefficients (K_d)

On p. 15 of Nordén et al. (2010) (Section 2.2 – Calculation of CR and K_d values from site-specific data) it is stated that “The only ‘true sample pairs’ in the site-specific data set were ‘pore water/ solid phase of regolith’ and ‘filtered water/suspended matter’ belonging to the same sample. These were used to calculate K_d values, by matching the samples according to an identification code (unique for each locality) and sediment layer, where relevant.”

We have scrutinised these statements by examining the Excel data sheets extracted from the Sicada database by SKB following our data request outlined in Section 4.2. Data sheets were provided separately for the Forsmark and Laxemar (Simpevarp) sites. The analysis of the data provided in these data sheets from which K_d values can be calculated is presented below. It focuses first on data on ‘pore water/ solid phase of regolith’ from which terrestrial K_d values can be calculated, then considers ‘filtered water/suspended matter’ from which aquatic K_d values can be calculated. Filtered sediment / sediment pore water analyses are also available for the Forsmark site only, from which *in situ* K_d values can be calculated for submerged marine and lake sediments. A point of possible confusion is the extent to which these aquatic K_d s have been treated in SKB’s analysis as being equivalent to terrestrial K_d s. In the data sheet ‘p_filtered_sediment.xls’ samples of limnic and marine origin are clearly identified as belonging to the ‘SAMPLE_TYPE Regolith’ and the ‘SAMPLE_SUB_TYPE Organic’, which implies that this aquatic material is considered to be equivalent to terrestrial organic regolith (i.e. organic soil). This is a highly dubious assumption since the physico-chemical conditions in saturated aquatic sediments and organic terrestrial soils are likely to be very different, reflecting their very different origins and modes of formation.

Request to SKB: *Is this assumption based on the notion that organic terrestrial sediment has been formed primarily by the drying out of marine and / or lake sediment?*

Analysis of Sicada data on “pore water/ solid phase of regolith”

Excel sheets extracted from the SICADA data base were as follows:

- *p_soil_pore_water.xls*
(separate sheets with the same name for Forsmark and Simpevarp)
- *p_centrifugated_soil.xls*
(separate sheets with the same name for Forsmark and Simpevarp)

The Activity Type (WC501) and Activity IDs (13207393, 13207394 and 13207395) indicated on both data sheets were first cross-checked against the entries in the *activity_comments.doc* (pages 17 – 18, page 629 and page 652, respectively) and found to correspond to ‘Soil sampling - pore water analys’, which is consistent with the types of data reported. In summary, measurements of soil pore water concentrations were carried out from August to December 2007 by ALS Analytica AB, on behalf of ECOMatters who evaluated the data.

As we requested, results are reported for iodine, niobium and selenium in soil pore water (in $\mu\text{g L}^{-1}$) and soil solid matter (in mg kg^{-1} dry solids).

From a total of 11 analyses of soil pore water from 3 soils at Forsmark (sites A, B and G) only 4 positive data for iodine and selenium, and one positive datum for niobium, are reported. Similarly, from a total of 11 analyses of soil solids from 3

soils at Forsmark (sites A, B and G) only 3 positive data for iodine, 5 positive data for selenium and 6 positive data for niobium are reported.

From a total of 17 analyses of soil pore water from five soils at Laxemar (sites C, D, E, F and H) only eight positive data for iodine, six positive data for niobium and nine positive data for selenium are reported. Similarly, from a total of 17 analyses of soil solids from the same five soils at Laxemar only seven positive data for iodine, and nine positive data for each of niobium and selenium are reported.

After checking the availability of relevant data within the data sheets extracted from Sicada, the individual data sets for solid and pore water phases of soils for Forsmark and Laxemar were combined to identify ‘true sample pairs’ which could be used to calculate solid-liquid K_d values. To identify ‘true sample pairs’ we matched solid and pore water samples according their identification codes, as described by Nordén et al. (2010, p. 15 Section 2.2), with the following results.

Forsmark samples

For iodine none of the samples have valid data for both solid and liquid phases, therefore no ‘true sample pairs’ exist within the data base and no K_d values can be calculated for these samples.

For selenium 4 samples (A dup, B dup, G dup and G) have valid data for both solid and liquid phases, therefore 4 ‘true sample pairs’ exist within the data base for selenium (see Table 14; IN or OR indicates inorganic or organic soil).

Table 14: Reviewer derived site specific K_d for selenium at Forsmark

Sample	Regolith concentration (mg kg ⁻¹ dw)	Soil pore water concentration (µg L ⁻¹)	K_d (L kg ⁻¹)	Soil type IN / OR
A dup	0.400	38.500	10.39	IN
B dup	0.200	10.700	18.69	OR
G dup	0.400	27.100	14.76	IN
G	0.400	28.700	13.94	IN

For niobium, only one of the samples (G dup) has valid data for both solid and liquid phases, therefore one ‘true sample pair’ exists within the data base for niobium (Table 15).

Table 15: Reviewer derived site specific K_d for niobium at Forsmark

Sample	Regolith concentration (mg kg ⁻¹ dw)	Soil pore water concentration (µg L ⁻¹)	K_d (L kg ⁻¹)	Soil type IN / OR
G dup	1.900	0.053	35849	IN

Simpevarp samples

For iodine, three samples (C INA, D INA and D) have valid data for both solid and liquid phases, therefore three ‘true sample pairs’ exist within the data base for iodine (Table 16).

Table 16: Reviewer derived site specific K_d for iodine at Simpevarp

Sample	Regolith concentration (mg kg ⁻¹ dw)	Soil pore water concentration (µg L ⁻¹)	K_d (L kg ⁻¹)	Soil type IN / OR
C INA	1.20	20.0	60	IN
D INA	34.70	10.0	3470	OR
D	43.50	10.0	4350	OR

For selenium, nine samples (C, C same pore, D dup, D, E dup, E, F dup, F, H) have valid data for both solid and liquid phases, therefore nine ‘true sample pairs’ exist within the data base for selenium (Table 17).

Table 17: Reviewer derived site specific K_d for selenium at Simpevarp

Sample	Regolith concentration (mg kg ⁻¹ dw)	Soil pore water concentration (µg L ⁻¹)	K_d (L kg ⁻¹)	Soil type IN / OR
C	0.200	4.90	40.82	IN
C same pore	0.200	4.90	40.82	IN
D dup	1.300	57.20	22.73	OR
D	1.600	9.80	163.3	OR
E dup	2.00	15.50	129.0	OR
E	2.20	8.00	275	OR
F dup	4.20	40.80	102.9	OR
F	4.20	22.10	190	OR
H	2.20	34.60	63.58	OR

For niobium 6 samples (C, C same pore, D, E dup, E, H) have valid data for both solid and liquid phases, therefore 6 ‘true sample pairs’ exist within the data base for niobium (Table 18).

Table 18: Reviewer derived site specific K_d for niobium at Simpevarp

Sample	Regolith concentration (mg kg ⁻¹ dw)	Soil pore water concentration (µg L ⁻¹)	K_d (L kg ⁻¹)	Soil type IN / OR
C	1.600	1.010	1584	IN
C same pore	1.900	1.010	1881	IN
D	1.700	0.141	12057	OR
E dup	1.700	0.096	17708	OR
E	1.400	0.115	12174	OR
H	1.400	0.115	12174	OR

Radium Data on “pore water/ solid phase of regolith”

In addition to data sheets containing analytical data for iodine, selenium and niobium, separate Excel data sheets were extracted from the Sicada data base containing data on ²²⁶Ra:

- *p_soil_pore_water_Ra.xls*
- *p_centrifugated_soil_Ra.xls*

The former data sheet contains 50 values for ²²⁶Ra in pore water while the latter contains 53 values for ²²⁶Ra in the solid phase in organic and inorganic soils. The reference given for these data is Sheppard *et al.* (2011) SKB R-11-24. From Table

2-1 (p. 11) in this reference it is possible to identify 48 ‘true sample pairs’ from which K_d values for ^{226}Ra can be calculated. Sheppard *et al.* (2011) summarise GM K_d s for this data set of 3.5, 3.4 and 1.5 m^3 / kg for clayey till, gyttja and peat, respectively. We calculate, from the sample pairs we identified, an overall GM of 3.56 m^3 / kg for all the sampling sites, which corresponds closely with the K_d s calculated by Sheppard *et al.* (2011).

Even though the data for ^{226}Ra have been collected for Forsmark only, this data set represents a statistically strong and defensible basis on which to estimate site specific K_d values for ^{226}Ra which provides SKB with a much better foundation for modelling this radionuclide than for the other elements we have examined.

Analysis of Sicada data on “filtered water / suspended matter”

Excel sheets extracted from the Sicada data base were as follows:

- *p_filtered_water.xls*
(separate sheets with the same name for Forsmark and Simpevarp)
- *p_suspended_matter.xls*
(separate sheets with the same name for Forsmark and Simpevarp)

The Activity Type (WC400 and WC401) and Activity IDs (13192089 - 13192094 and 13277137 - 13277142) indicated on both data sheets were first cross-checked against the entries in the *activity_comments.doc* and found to correspond to ‘Surface water sample - suspended material’ and ‘Surface water sampling - filtered water’, which is consistent with the types of data reported. As we requested, results are reported for iodine, niobium and selenium and are given in $\mu\text{g L}^{-1}$ for both filtered water and suspended matter.

Measurements of filtered water concentrations were carried out on samples collected 7th and 8th April 2008, measurements of suspended matter were carried out on samples collected on 7th April 2008 and 7th and 8th August 2008 (Table 19).

From a total of 24 analyses of filtered water and suspended matter, positive results for selenium and niobium are reported for all samples. Only one sample (SKB sample number 23003, indicated by * in Table 19) had a negative value for iodine (presumably indicating a value below detection limit), hence there are 23 positive data available for iodine.

Despite this apparently high availability of data, however, K_d values for suspended aquatic particulates can only be strictly calculated for paired samples collected in the same place at the same time. Insufficient information is available within the data sheets to judge whether filtered water and suspended matter samples were collected at the same locations. We assumed that they *had* been collected at the same locations and then checked to see how many pairs of sample were collected at the same time (ie. on the same day). Table 19 summarises our findings and indicates that at Forsmark there were no true sample pairs which could be used to calculate K_d s for suspended aquatic particulates. At Simpevarp there were 4 true sample pairs available, hence 4 K_d values can be calculated for iodine, selenium and niobium (i.e. 12 K_d values in total).

In conclusion, based strictly on ‘true sample pairs’, only 2 lake and 2 seawater K_d s can be calculated for I, Se and Nb, although analytical results are available for all samples except one (* 23003, limnic suspended matter, negative value for iodine on

08 Aug 2008, Forsmark). From the Sicada data sheets we have been provided with, only 4 K_d s are available for lake and marine water/suspended sediment.

Table 19: Summary of filtered water and suspended matter sample

Site	Date	Lake or Sea?	Filtered water	Suspended Sediment	Possible K_d
Forsmark	07 Apr 2008	Lake	0	1	0
Forsmark	07 Apr 2008	Sea	3	0	0
Forsmark	08 Apr 2008	Lake	3	0	0
Forsmark	07 Aug2008	Sea	0	2	0
Forsmark	08 Aug 2008	Lake	0	3	0 *
Simpevarp	15 Apr 2008	Lake	2	2	2
Simpevarp	15 Apr 2008	Sea	1	1	1
Simpevarp	16 Apr 2008	Lake	1	0	0
Simpevarp	16 Apr 2008	Sea	2	1	1
Simpevarp	16 Aug2008	Lake	0	1	0
Simpevarp	16 Aug 2008	Sea	0	1	0
TOTAL					4

Analysis of Sicada data on “filtered sediment / sediment pore water”

Analyses of filtered aquatic sediment (marine and limnic) and associated sediment pore waters are also available for the Forsmark site only, from which in situ K_d values can be calculated for submerged marine and lake sediments.

Excel sheets extracted from the SICADA data base were as follows:

- *p_filtered_sediment.xls* (Forsmark only)
- *p_sediment_pore_water.xls* (Forsmark only)

The Activity Type (WC500) and Activity IDs (13277223 - 13277229 and 13277284 - 13277286) indicated on both data sheets were first cross-checked against the entries in the *activity_comments.doc* and found to correspond to ‘Sediment sampling - pore water analysis’, which is consistent with the types of data reported. As we requested, results are reported for iodine, niobium and selenium and are given in $\mu\text{g L}^{-1}$ for filtered water and mg kg^{-1} dry solids for filtered sediment.

Measurements of pore water concentrations and filtered sediments were carried out on samples collected 8th, 9th and 10th April 2008 (Table 20). However, no sampling dates were provided for 4 samples of sediment pore water (SKB sample numbers 17250, 17251, 17252 and 17253).

From a total of 16 analyses of pore water and filtered sediment for which sampling dates were provided, positive results for iodine, selenium and niobium are reported. As for the filtered water and suspended matter suspended matter samples described in the previous section, we assumed that the pore water and filtered sediment samples had been collected at the same locations and then checked to see how many pairs of sample were collected on the same day. Table 20 summarises our findings and indicates that there were 6 true sample pairs available, hence six K_d values can be calculated for iodine, selenium and niobium (i.e. 18 K_d values in total). In

contrast to samples of filtered water and suspended sediment from the free water column, which are subject to dynamic change on a time scale of less than one day, we consider it reasonable to use sediment and pore water samples from consecutive days to calculate K_d s, even though these are not strictly ‘true sample pairs’. These are indicated in Table 20 with the † symbol. Use of these samples to calculate K_d s would increase the number of K_d values available from the Sicada data sheets to nine values.

As noted above, no sampling dates were given for samples 17250 – 17253 (four samples of porewater from marine sediment) and no data were given for iodine or niobium in these samples which had values for selenium only, so it is not clear how useful these values are.

The ecosystem type given for sample 16007 is Limnic but the sample description is ‘Filtered Sea Sediment’. This could be a typographic error, or it may indicate a degree of confusion in the classification of samples as ‘Limnic’ or ‘Marine’. Further possible confusion in the classification of filtered sediment samples is indicated by the descriptions of all samples in the *p_filtered_sediment.xls* data sheet as Regolith and Organic. Does this indicate that K_d values obtained from this data set are considered to be applicable to organic terrestrial regolith – i.e. soil?

Table 20: Summary of filtered sediment and pore water samples

Site	Date	Lake or Sea?	Pore water	Filtered Sediment	Possible K_d
Forsmark	08 Apr 2008	Lake	2	2	2
Forsmark	09 Apr 2008	Lake	4	3	3 †
Forsmark	10 Apr 2008	Lake / Sea? *	0	1	0
Forsmark	09 Apr 2008	Sea	0	1	0 †
Forsmark	10 Apr 2008	Sea	2	1	1 †
TOTAL					6

* Ecosystem type given as limnic but described as Filtered sea sediment.

Request to SKB: Please clarify whether K_d values obtained from filtered aquatic sediments are considered to be applicable to organic terrestrial regolith. Also, whether limnic and marine K_d s are considered to be interchangeable.

Conclusion

In summary, the following numbers of K_d values can be calculated based on SKB site data.

- Iodine: 3 (1 for inorganic soil, 2 for organic soil)
- Selenium: 13 (5 for inorganic soil, 8 for organic soil)
- Niobium: 7 (3 for inorganic soil, 4 for organic soil)
- Radium: 48 (20 for inorganic soil, 28 for organic soil)

The reference given in both data sheets (*p_soil_pore_water.xls* and *p_centrifugated_soil.xls*) is Sheppard et al. (2009) R-09-27, in which K_d values are reported, but not pore water or soil solid concentrations.

In Table 4-1 of R-09-27 K_d values are reported for 7 soils/sites, A to G. This table shows K_d s for iodine (native) for sites C, D and E only, but from the data sheets examined above K_d values can only be calculated for sites C and D. Furthermore, sites C and D are described in data sheet *p_centrifugated_soil.xls* as being of sub-types inorganic and organic, respectively, whereas in Table 4-1 of R-09-27 they are described as being 'sandy till' and 'clay gyttja'. Sandy till is certainly inorganic, but clay gyttja is only partly organic. Iodine K_d s for sites A, B, F and G are presented only as > or < estimates, which presumably reflects the missing values for this element in the Sicada data sheets.

For niobium, Table 4-1 of R-09-27 reports K_d values for niobium for sites C, D, E and G, which are consistent with the K_d s we have been able to calculate from the Sicada data sheets. Data for selenium within the Sicada sheets was sufficient to calculate K_d values for all sites, A to G, at Forsmark and Laxemar. Site H, which is identified in the Sicada data sheets and for which true soil/pore water data pairs exist for selenium and niobium, is not identified by Sheppard et al (2009).

Even though the data for ^{226}Ra have been collected for Forsmark only, this data set represents a statistically strong and defensible basis on which to estimate site specific K_d values for ^{226}Ra which provides SKB with a much better foundation for modelling this radionuclide than for the other elements we have examined.

4.3.2. Plant uptake

For the majority of the plant types considered in the SR-Site assessment and the four radionuclides being considered in this review, the concentration ratios used in the assessment were derived from literature data. The best estimate values have been recalculated as part of this review, and are shown in Table 21. Using the literature sources cited, the reviewers found that four of the best estimate values derived differed from those reported by SKB by more than 10%; these are indicated in the table by highlighting the value in a bold underlined font. Of those four values, only one (iodine CR for vegetables) is more than 15% different to the SKB reported value.

It is not clear why SKB disregarded data for uptake of iodine by cereal and vegetables as presented in IAEA (2010) for the best estimate value, despite those values being based upon 13 and 12 values, respectively, rather than the unspecified number of data points in Robens *et al.* (1988)³. Had the IAEA (2010) values been used instead this would have led to a significant reduction in the assumed concentration ratios (Table 22). The consequences of this on the calculated LDF for ^{129}I are considered further in Section 6.3, for which the consumption of vegetables is the dominant exposure pathway.

The concentration ratios used by SKB for pasture and berries are based upon the distributions derived for primary producers. For these, the site data used for I, Nb and Ra include grasses, herbs, shrubs and trees. The Se values are based solely on pasture, using the same values as the SR-97 and SAFE assessments (Karlsson and Bergström, 2002). There is some concern in using data pertaining to such a wide

³ Robens *et al.* (1988) contains data for both ^{129}I and ^{127}I . There are seven values for cereal grain reported for each isotope and eight values reported for leafy vegetables. It is not clear, though, how SKB have since taken those data and transformed them into the distributions used in the SR-97 and SAFE assessments, from which it is presumed the values were taken for the SR-Site assessment.

range of plant types, which exhibit varying behaviour, for all such plant types. That these plant types do not contribute significantly to the calculated doses (see Section 6) does not justify a choice of CR values which disregards the likely range observed between diverse plant groups which together make up the spectrum of potentially ingested vegetable matter.

Table 21: Derivation of plant concentration ratios from literature data only

Crop	Element	BE conc. ratio reported in literature source (see Table 11) kg dw soil kg dw ⁻¹ plant ^a	Carbon content assumed by SKB (Table 4-1 of Nordén et al. 2010) kgC kg ⁻¹ dw plant ^a	BE conc. ratio reported in Nordén et al. (2010) kg dw soil kgC ⁻¹ plant	BE conc. ratio calculated in this review kg dw soil kgC ⁻¹ plant
Primary prod.	Se	302E+01	0.51	4.4E+01	<u>3.9E+01</u>
Cereal	I	1.0E-01	0.39	2.6E-01	2.6E-01
	Nb	1.4E-02	0.45	3.1E-02	3.1E-02
	Ra	1.7E-02	0.45	3.8E-02	3.8E-02
	Se	2.0E+01	0.39	5.1E+01	5.1E+01
Root crops	I	1.0E-01	0.48	2.0E-01	2.1E-01
	Nb	4.0E-03	0.48	8.2E-03	8.3E-03
	Ra	1.1E-02	0.48	2.0E-02	<u>2.3E-02</u>
	Se	4.0E+00	0.1	3.9E+01	4.0E+01
Vegetables	I	3.0E-02	0.39	6.1E-01	<u>1.0E+00</u>
	Nb	1.7E-02	0.39	4.2E-02	4.4E-02
	Ra	9.1E-02	0.39	2.7E-01	<u>2.3E-01</u>
	Se	2.0E+00	0.03	6.7E+01	6.7E+01
Mushrooms	Ra	2.7E+00	0.46	5.9E+00	5.9E+00
	Se	2.0E+01	0.46	4.4E+01	4.3E+01

^a For the Se values, the literature source (Karlsson and Bergstrom, 2002) reported the concentrations on a fw basis for all except the primary producers, and so the carbon content is also presented on a fw basis where appropriate. Also, the iodine values for cereal and vegetables are on a fw basis.

Table 22: Derivation of select iodine plant concentration ratios from IAEA (2010) data

Crop	BE concentration ratio reported in IAEA (2010)	Carbon content assumed by SKB (Table 4-1 of Nordén et al. 2010)	BE concentration ratio reported in Nordén et al. (2010)	BE concentration ratio calculated in this review
	kg dw soil kg dw ⁻¹ plant	kgC kg ⁻¹ dw plant	kg dw soil kgC ⁻¹ plant	kg dw soil kgC ⁻¹ plant
Cereal	6.3E-04	0.45	2.6E-01	1.4E-03
Vegetables	6.5E-03	0.39	6.1E-01	1.7E-02

For iodine, site data is combined with site data from an unspecified source. There are no data in IAEA (2010), and the derivation of distributions from the data provided in Karlsson and Bergström (2002) (which cites Robens et al., 1988) or Avila et al. (2006a) does not yield the distribution given in Appendix D of Nordén et al. (2010).

Including, and beyond, the three elements focussed upon here, the general lack of mushroom specific data leads to either understorey plants or pasture CR values being used as a proxy. Note that although the iodine values in mushrooms are based on site-specific data, there is not a clear relationship between the value reported in Table 4-6 of Nordén et al. (2010) and Table 3-10 of Johansson et al. (2004), even after factoring in the conversion to Bq kg⁻¹ C in mushrooms / Bq kg⁻¹ dw soil, using the C content given in Table 4-1 of Nordén et al. (2010).

Appendix D of Nordén et al. (2010) lists the number of site specific plant CR values which were used to derive distributions for primary producers and mushrooms; only a selection of radionuclides is covered in that appendix as for many radionuclides there were no site data. According to Section 2.2 of Nordén et al. (2010), in deriving site specific CRs “*samples from different localities at both sites (Forsmark and Laxemar) were combined in order to generate a larger set of CRs. By using unpaired samples, additional variation caused by differences between sample sites may increase the GSD for the parameter value*”. There are two possible interpretations of this: (1) that all Forsmark plant measurements were combined with all Forsmark soil measurements, and the same for Laxemar; or (2) that the total number of plant measurements across both sites were combined with the total number of soil measurements across the two sites. On p. 32 of Nordén et al. (2010) it is stated that for mushrooms, bulk soil concentrations of radionuclides were used to derive the CRs, whilst for the primary producers it was all soil in the rooting zone. Using that description, an investigation of the Sicada data files received by the consultants (see Section 4.2) yield a substantially greater number of potential site-specific CR values than used by SKB (Table 23). It is therefore not clear how SKB generated their site-specific parameters.

Table 23: Number of site specific plant CR as derived by the reviewers and reported by SKB

Element	Forsmark		Simpevarp		Review method (1)	Review method (1)	No. reported in Nordén et al. (2010)
	No. plant measurements	No. org soil measurements	No. plant measurements	No. org soil measurements			

Primary producers ^a							
I	6	0	10	6	60	96	19
Nb	8	2	10	7	86	162	19
Ra	Not given	30	0	0	-	-	5
Mushrooms ^b							
I	31	9	0	0	279	279	9

^a Grasses, herbs, spruce shoots, *Vaccinium myrtillus*, *Fraxinus excelsior*, *Quercus robur*, *Alnus glutinosa*, *Picea abies*, *Juniperus communis*, *Sorbus aucuparia*

^b Fruiting bodies, mycelium

4.3.3. Transfer factors for terrestrial biota associated with human exposure calculations

With respect to the transfer factors for milk, the consultants found that, whilst the best estimate and GM data presented in Table 4-7 of Nordén et al. (2010) match the data given in Table 26 of IAEA (2010), the GSDs do not. Further reading of these two tables highlights the fact that the disagreement in GSD values between those used in SR-Site and those recommended in IAEA (2010) extends beyond the limited number of radionuclides considered here. Further, in some instances (Cd and Mo) the parameter values from the SAFE assessment, as reported in Karlsson and Bergström (2002), are used in preference to IAEA (2010) despite there being data for those elements in IAEA (2010).

As with the milk distributions, it was found that the best estimate and GM values used in the SR-Site assessment for the transfer of radionuclides to meat matched IAEA (2010), but not the GSD (see Table 4-8 in Nordén et al. (2010) and Table 30 in IAEA (2010)). The Se distribution used in SR-Site was correctly derived from the data presented in Karlsson and Bergström (2002) following the method given in Section 2.1 of Nordén et al. (2010). As with milk, further reading highlights the fact that the disagreement in GSD values between those used in SR-Site and those recommended in IAEA (2010) extends beyond the limited number of radionuclides considered here. Further, the Cd values in IAEA (2010) are disregarded, with those from the SR-Can assessment used instead.

Consideration is now given to the parameterisation of the uptake of radionuclides by wild herbivores. For Nb, site specific data were used, whereas for the other three radionuclides such data were lacking and so the kinetic allometric model described in Section 2.4 of Nordén et al. (2010) was used instead.

The kinetic allometric model of Nordén et al. (2010) is reproduced below for convenience.

$$CR_i = \frac{DMI \cdot fraUptake_i \cdot fraSoftTissues_i \cdot TbioI_i}{\ln(2) \cdot Weight} \cdot \left(1 - e^{-\ln(2) \frac{Tlife}{TbioI_i}} \right) \quad (1)$$

Here

- CR_i is the Concentration Ratio of the i^{th} element between the diet and soft tissues of the herbivore (Bq kg^{-1} fw per Bq kg^{-1} dw),
- DMI is the daily dry matter intake by the herbivore (kg dw d^{-1}),
- $fraUptake_i$ is the gut uptake fraction of the i^{th} radionuclide for herbivores (-),

- $fraSoftTissues_i$ is the fraction in soft tissues of total content of the i^{th} element in the herbivore (-),
- $Tbiol_i$ is the biological half time of the i^{th} element (d),
- $Weight$ is the body weight of the herbivore (kg fw),
- $Tlife$ is the life duration of the herbivore (d).

Three of these parameters are derived using, empirical, allometric relationships.

$$DMI = a1 \cdot Weight^{b1} \quad Tbiol_i = a2 \cdot Weight^{b2} \quad Tlife = a3 \cdot Weight^{b3} \quad (1)$$

Although the parameter values used for I and Ra are listed in Section 2.4 of Nordén et al. (2010), as there were no data for Se (either in Nordén et al., 2010, or the underlying report by Avila et al., 2006a) a modified model was used in which the biological half time of the element was disregarded.

$$CR_i = \frac{DMI \cdot fraUptake_i \cdot fraSoftTissues_i \cdot Tlife}{Weight} \quad (1)$$

The relevant parameters for the three radionuclides are given in below. The general data are given in Section 2.4 of Nordén et al. (2010), and the weight of the biota is given in Lofgren (2010). This, and reviewer-derived biota-specific values, are given in Table 24.

Table 24: Parameters used in the kinetic allometric model to derive herbivore CRs for I, Ra and Se

	Parameter	Units	Element specific value		
			I	Ra	Se
General	a1	kg d ⁻¹	6.60E-02	6.60E-02	6.60E-02
	b1	relative units	6.30E-01	6.30E-01	6.30E-01
	a2	d	1.70E+01	2.80E+02	-
	b2	relative units	1.30E-01	1.80E-01	-
	a3	d	3.70E+02	3.70E+02	3.70E+02
	b3	relative units	3.50E-01	3.50E-01	3.50E-01
	fraUptake _i	-	9.80E-01	2.00E-01	5.20E-01
	fraSoftTissue _i	-	1.00E+00	9.00E-02	1.00E+00
Roe deer	Weight	kg fw	2.13E+01	2.13E+01	2.13E+01
	DMI	kg dw ⁻¹	4.53E-01	4.53E-01	4.53E-01
	Tbiol _i	d	2.53E+01	4.86E+02	-
	Tlife	d	1.08E+03	1.08E+03	1.08E+03
	CR _i	(Bq kg ⁻¹ fw)/(Bq kg ⁻¹ dw)	7.61E-01	2.11E-01	1.19E+01
Moose	Weight	kg fw	2.79E+02	2.79E+02	2.79E+02
	DMI	kg dw ⁻¹	2.29E+00	2.29E+00	2.29E+00
	Tbiol _i	d	3.53E+01	7.72E+02	-
	Tlife	d	2.66E+03	2.66E+03	2.66E+03
	CR _i	(Bq kg ⁻¹ fw)/(Bq kg ⁻¹ dw)	4.11E-01	1.49E-01	1.13E+01

Note that the allometric model gives a concentration ratio in units of Bq kg⁻¹ fw per Bq kg⁻¹ dw, whereas in the SR-Site assessment the concentration ratios given in Table 4-10 of Nordén et al. (2010) are given in kgC kgC⁻¹.

For Nb, the derivation of the herbivore uptake should be much more straightforward, with the method as outlined in Section 4.3 of Nordén et al. (2010) being followed. Note that although the method given uses both mushrooms and vegetation consumption as a means of radionuclides entering the biota, Table 4-10 of Nordén et al. (2010) implies that only vegetation was assumed to be consumed for the Nb calculations. Whilst this may relate to the lack of site-specific mushroom measurements, further justification should be provided, given that a non-zero mushroom CR was used in other parts of the assessment.

Whilst some of the data used to derive a site-specific herbivore CR is clearly stated in the SR-Site reports, other parameters need to be derived from the site specific data. In Table 25 below, the concentrations of radionuclides in the biota are based on the geometric means of all the relevant biota data that the reviewers were able to calculate from the Sicada data provided as part of this review. Specifically, as Nordén et al. (2010) based some of the herbivore parameters on moose, roe deer and small rodents, the same has been done here. Entering the data below into the equation on p.40 of Nordén et al. (2010) does not yield the same result as presented in Table 4-10 of that report.

Table 25: Site specific data used to derive a herbivore CR for Nb

Parameter	Units	Value	Reference
[X] _{herbivore muscle}	mg kg ⁻¹ dw	0.001	Geometric mean of site data
[C] _{game muscle}	kgC kg ⁻¹ dw	0.44	Table 4-9 of Avila et al. (2010)
Y _{veg}	-	0.94	p41 of Avila et al. (2010)
[X] _{herbivore veg food}	mg kg ⁻¹ dw	0.004	Geometric mean of site data
[C] _{herbivore veg food}	kgC kg ⁻¹ dw	0.51	Table 4-9 of Avila et al. (2010)
Y _{mush}	-	0.06	p41 of Avila et al. (2010)
[X] _{mushrooms}	mg kg ⁻¹ dw	None available	
[C] _{mushrooms}	kgC kg ⁻¹ dw	0.46	Table 4-9 of Avila et al. (2010)

4.3.4. Concentration ratios used for aquatic biota

The number of biotic groups considered in the aquatic ecosystem is much greater than in previous assessments (freshwater and marine fish, freshwater invertebrates and marine plants), and is a reflection of the site descriptive modelling that has been undertaken since the SR-Can assessment. Further, the concentration ratios, and parameter distributions assumed, are based upon a combination of site measurements and recent literature.

By comparison, the SR-Can assessment values were based upon literature from 1972 (for the freshwater invertebrates and marine plants) and a combination of 1980s and 1990s literature for the fish (see Karlsson and Bergström, 2002, for further details).

Table 10-1 of SKB (2010) indicates that the consumption of aquatic biota dominates the exposure associated with ²³⁷Np, which is a key radionuclide in both the central corrosion and shear failure scenarios (SKB, 2010, 2011). Figure 13-5 of SKB (2011) indicates that ²³⁷Np may contribute 2% of the total exposure in the central corrosion case, whilst Figure S-11 of SKB (2011) indicates that ²³⁷Np contributes less than 1%

of the exposure in the shear failure scenario. Given this radionuclide does not form part of the focus of this element specific review and its minor role in terms of calculated dose, further consideration is not given in this review as to the parameterisation of the aquatic biota uptake of radionuclides.

4.4. Conclusion of review of derivation of element specific data

The primary focus of this review has been upon the derivation of the distribution coefficients (K_d) and the plant concentration ratios.

Regolith distribution coefficients

In summary, there appear to be both consistencies and inconsistencies between the analytical data as reported in the primary data base (Sicada) and the reporting of *in situ* K_d values for both Forsmark and Laxemar; see also Table 26.

Table 26: Summary of number of site specific K_d values

K_d type	Element	Number of site specific K_d values reported as used by SKB (Appendix D of Nordén et al., 2010)	Number of site specific K_d values determined by the reviewers
Inorganic soil	I	2	1
	Se	4	5
	Nb	2	3
	Ra	18	20
Organic soil	I	20	2
	Se	27	8
	Nb	20	4
	Ra	30	28
Limnic sediments	I	6	6
	Se	7	7
	Nb	7	7
	Ra	N/A	N/A
Marine sediments	I	5	3
	Se	5	3
	Nb	5	3
	Ra	N/A	N/A

Plant uptake

Whilst it is understood that SKB wished to calculate all concentrations of radionuclides in plants, and other biota, on a Bq kgC⁻¹ basis, this means that assumptions needed to be made as to the carbon content of crops and biota. It also means that it was not straightforward to compare the parameters values used against other parameter databases, such as IAEA (2010). Some errors have been found in the conversions SKB have applied to literature data to obtain concentration ratios in their chosen format.

There is also concern in the derivation of the concentration ratios used for the natural vegetation, where data pertaining to such a wide range of plant types, which exhibit varying behaviour, has been used to generate one distribution which is then used for all natural vegetation.

Terrestrial and aquatic animal uptake parameters

With respect to the parameterisation of radionuclide uptake into milk and meat, whilst the best estimate values are based upon the most recent literature compilations where possible (IAEA, 2010), there are numerous errors in the parameterisation of distributions used in any sensitivity or uncertainty calculations.

The wild herbivore transfers are based on a combination of kinetic-allometric model results and transfer rates derived from site data. However, the full information required to check the values is not present in the SR-Site reports, nor seemingly is the underlying data as provided in the Sicada database outputs supplied by SKB for this review. It is therefore not possible to conclude as to whether or not the values used in the SR-Site assessment are appropriate or not.

The number of types of aquatic biota considered in the SR-Site assessment has increased since SR-Can, in part as a result of the site investigations. The parameterisation of the uptake of radionuclides is based upon a combination of site data and recent literature compilations. This can be seen as an improvement upon the data used previously. However, as aquatic biota play a minor role in the calculated human exposures, no further consideration has been given to the use of site data and the derivation of parameter distributions used in the SR-Site assessment in this review.

5. Review of SKB's ¹⁴C modelling

In the preceding two sections consideration has been given to the data used to represent the dynamics of trace elements, and radionuclides, in the biosphere, and the human exposures associated with those radionuclides. As essential elements, carbon and hydrogen are modelled separately from the other elements. As ¹⁴C has been demonstrated by SKB to be a potential cause of high human exposure in the shear failure scenario (Figure S-11 of SKB, 2011), consideration has been given in this review to the ¹⁴C model used in the biosphere aspect of the SR-Site assessment.

5.1. SKB's presentation

In the SR-Site assessment a specific activity model was used. This is a completely different conceptual model to that used in the preceding SR-97 and SR-Can assessments, which was based on the concentration ratio approach used for trace elements.

5.1.1. Conceptual model

Appendix A of Avila et al. (2010) provides details of the modelling of transfers between ecosystem compartments. Figure A-1 from that report is reproduced here, with additional highlighting of transfers that are somehow special to ¹⁴C (Figure 20). With respect to human exposure the key outputs of this model are the ¹⁴C specific activities in the terrestrial and aquatic biota, as these are then assumed to be maintained throughout the food chain to humans. The transfers of ¹⁴C to the biota are given by transfers 26 and 30 (see p109 of Avila et al. 2010). However, these transfers are implemented as annual transfer rates (y^{-1}).

It is not until reading the implementation of the model in Ecolego (p112-157 of Avila et al. 2010) that the manner in which ¹⁴C specific activities in the biota is detailed mathematically. According to the expressions on p136-139, the ¹⁴C specific activities ($Bq\ kgC^{-1}$) are equal to either `conc_Aqu_PRIMARY_PRODUCER` or `conc_Ter_PRIMARY_PRODUCER` depending on whether it is aquatic or terrestrial biota; the use of these concentrations is determined by the model switch `switcherC` (equal to one for ¹⁴C, and zero otherwise). These concentrations are determined using the following equations.

$$conc_Aqu_PRIMARY_PRODUCER = \frac{Aqu_PRIMARY_PRODUCER}{Aqu_biom_pp \cdot Aqu_area_obj} \quad (4)$$

$$conc_Ter_PRIMARY_PRODUCER = \frac{Ter_PRIMARY_PRODUCER}{Ter_biom_pp \cdot Ter_area_obj} \quad (5)$$

The amount of ¹⁴C (Bq) in the two primary producer compartments is determined by solving differential equations, using the transfers shown in Figure 20. In the specific activity equations, both the areas (`ter_area_obj`, `aqu_area_obj`) are object specific time-dependent values, as is the aquatic primary producer biomass (`Aqu_biom_pp`). The terrestrial primary producer biomass is based upon that of a wetland (p346 of Löfgren 2010).

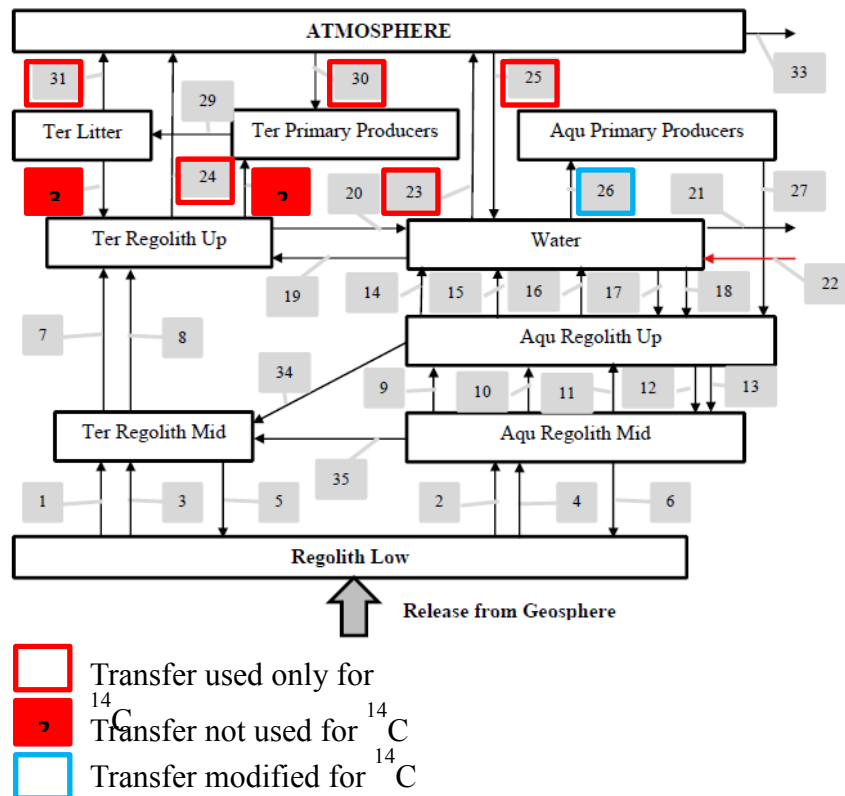


Figure 20: SKB ecosystem model with ^{14}C specific transfers highlighted

5.1.2. Data

As it is a completely different conceptual model it is not possible to directly compare transfer parameterisations between SR-Site and previous assessments. However, the adult ingestion and inhalation dose coefficients used are identical to those used in the SR-Can assessment. Nordén et al. (2010) gives EU (1996) as the source for these values.

Within the SR-Site documentation, Nordén et al. (2010) references Avila et al. (2010) for details of the specific activity model. According to Avila et al. (2010), detailed information about the carbon content of tissues in the various biota can be found in the ecosystem specific reports (Andersson, 2010; Aquilonius, 2010; Löfgren, 2010). In this review consideration has therefore been given separately to the parameterisation of the three ecosystem types.

Terrestrial ecosystem

The main entry point of ^{14}C into the terrestrial food chain is fixation of carbon from air by primary producers. Therefore, the atmosphere was included as a compartment in the radionuclide model for assessment of ^{14}C . The parameters used in the ^{14}C biosphere assessment are listed in Table 27; the parameter values and their justification are given in Löfgren (2010).

Table 27: Parameters used in SR-Site for ¹⁴C modelling in the terrestrial ecosystem

Parameter	Description	Units	Type ^a
Ter_area_obj	Area of the terrestrial ecosystem in the biosphere object	m ²	OTS
conc_C_atmos	Concentration of C in the atmosphere	kg m ⁻³	G
frac_C_atmos	Fraction of decomposed C leaving the wetland and being released to the atmosphere as CO ₂	-	G
Ter_biom_pp	Biomass of terrestrial primary producers	kgC m ⁻²	G
Ter_conc_C_regoUp	Concentration of DIC in the upper terrestrial regolith (peat)	kgC m ⁻²	G
Ter_degass_C	Degassing rate of DIC in the terrestrial ecosystem	kgC m ⁻² y ⁻¹	G
Ter_decomp	Decomposition rate	y ⁻¹	G
vel_wind	Wind velocity	m s ⁻¹	G
Ter_z_roughness	Zero displacement height of vegetation	m	G
Agri_z_roughness	Zero displacement height of vegetation	m	G
Ter_z_mixlay	The height of the mixing layer for forested wetland vegetation	m	G
Agri_z_mixlay	The height of the mixing layer for agricultural land	m	G
H_veg_pp	Height of vegetation in forested wetland	m	G
H_veg_agri	Height of vegetation in agricultural land	m	G

^a OTS – Object specific time series. OSS – Object specific parameter. G – site generic parameter.

Although a number of the parameters are stated as being ‘site specific’ in Appendix B of Avila et al. (2010), the reality is that, with the exception of the terrestrial area of the object, a single value was used for all the biosphere objects. It is also only the terrestrial area of the object which is assumed to be time dependent.

Further, in the ¹⁴C assessment limited use has been made of site specific data for the model parameterisation. Most of the parameter values come either from the ¹⁴C model developed previously by Avila and Pröhl (2008), or in the case of conc_C_atmos, are based on global measurements reported in the literature.

Parameters used to describe gas-exchange between surface waters and the atmosphere was determined from site data and site modelling (Andersson 2010; Aquilonius 2010). Crop specific biomass data are reported in Löfgren (2010). Whereas for most plant types a single value of primary production is given, for cereals values are given for both the edible portion and total cereal. However, despite the crop specific information contained within the SR-Site documentation, when the ¹⁴C specific activity in the terrestrial biota is calculated it is only the biomass of primary producers (i.e. natural vegetation) that is used, irrespective of the actual crop under consideration.

According to Avila et al. (2010), parameters for wind velocities and height of the mixing layer were derived from site data, whereas the values for the zero displacement height were taken from literature (Nordén et al. 2010). However, the zero displacement height is not given in that reference and is instead given in Avila et al. (2010). The wind velocity data are given in Table 13-8 of Löfgren (2010), noting that the Sicada database ID is Sicada_09_054_windspeed. These values are

based on measurements from a local meteorological station, at Högmasten, taken over a 26 month period. However, it is not clear at what height this wind speed has been measured; the Avila and Pröhl (2008) model uses a wind speed at 10 m.

Limnic and marine ecosystems

Unlike in the model developed by Avila and Pröhl (2008), the ^{14}C model used in the SR-Site assessment is the same for the limnic and marine ecosystems. The parameters used are listed Table 28. In contrast with the terrestrial ecosystem many of the parameters are biosphere object specific, and most of those are also time dependent.

Table 28: Parameters used in SR-Site ^{14}C limnic and marine ecosystem models (adapted from Appendix B of Avila et al., 2010)

Parameter	Description	Units	Type ^a	Underlying report
Aqu_area_obj	Water area in lake basin	m ²	OTS	TR-10-05
area_subcatch	Area of the sub-catchment	m ²	OSS	TR-10-05
area_wshed	Watershed area	m ²	OTS	TR-10-05
Aqu_biom_pp_macro	Biomass of macroflora and macrofauna	kg C m ⁻²	OTS	TR-10-02 TR-10-03
Aqu_biom_pp_plank	Biomass of pelagic biota	kg C m ⁻²	OTS	TR-10-02 TR-10-03
Aqu_biom_pp_ubent	Biomass of microphytobenthos and benthic bacteria	kg C m ⁻²	OTS	TR-10-02 TR-10-03
Aqu_prod_pp_macro	Net productivity of benthic community	y ⁻¹	OTS	TR-10-02 TR-10-03
Aqu_prod_pp_plank	Net productivity of pelagic community	y ⁻¹	OTS	TR-10-02 TR-10-03
Aqu_prod_pp_ubent	Net productivity of microbenthic community	y ⁻¹	OTS	TR-10-02 TR-10-03
Aqu_degass_C	C degassing rate. Release of C from lake water surface to atmosphere	kg C m ⁻² y ⁻¹	OTS	TR-10-02 TR-10-03
gasUptake_C	Uptake of C from atmosphere to water body (mainly CO ₂).	kg C m ⁻² y ⁻¹	OTS	TR-10-02 TR-10-03
Lake_conc_DIC	Concentration of DIC in water	kg C m ⁻³	G	TR-10-02
Sea_conc_DIC				TR-10-03
Lake_conc_PM	Concentration of particulate matter in water	kg dw m ⁻³	G	TR-10-02
Sea_conc_PM				TR-10-03

^a OTS – Object specific time series. OSS – Object specific parameter. G – site generic parameter.

5.2. Motivation of the assessment

Although the SR-Site assessment the potential impacts of ^{14}C entering the biosphere is based on the specific activity approach, as outlined in Avila and Pröhl (2008)⁴, the citation of the 2008 report is not a declaration that that exact model has been used for the SR-Site assessment. Assumptions relating to the sources of ^{14}C to the atmosphere and water, from which biota are assumed to take up ^{14}C in either terrestrial or aquatic ecosystems differ from those of the 2008 model. One of the many differences is that in SR-Site losses of ^{14}C from a water body to the atmosphere as a result of degassing, and the uptake of ^{14}C from the atmosphere to the water body, are included. These transfers are both object and time dependent, as their formulation depends upon factors such as primary production in the water body (see p.403-405 of Andersson et al. 2010). Further differences are discussed in the consultants' assessment below.

When using a specific activity approach it is assumed that the ratio of radioactive to stable isotope in the environmental media is equal to that of the biota of interest; the equation for ^{14}C is given below.

$$^{14}\text{C}_{biota} = \text{stable}\text{C}_{biota} \cdot \left(\frac{^{14}\text{C}_{biotaenvironment}}{\text{stable}\text{C}_{biotaenvironment}} \right) \quad (6)$$

In the SR-Site assessment the ^{14}C concentrations in the biota are determined by dividing the inventory of ^{14}C (Bq) estimated to be in that biota at any given time by that of the stable C content of the biota at that time. Without presentation of the $^{14}\text{C}/\text{stable}\text{C}$ ratio in the relevant environmental media it is not immediately possible to say whether or not a truly specific activity model has been utilised in this assessment; the equations as presented in the SR-Site documentation (specifically Avila et al. 2010) seem, on face value, to be little different from those used for modelling the uptake of trace radionuclides using a concentration ratio approach.

Further, according to Table 4-1 of Avila et al. (2010) the peak LDF value for ^{14}C was calculated for object 118, at the time 2650 CE. As this is the value that was taken forward and used in the SR-Site assessment it is pertinent to (a) be able to reproduce this value, and (b) be confident that this value is appropriate compared with others models.

5.3. The Consultants' assessment

Figure 21 shows the primary SR-Site documentation used in the review of the ^{14}C assessment. In addition, data from the SICADA database was used for time series dependent parameters, such as the terrestrial and aquatic areas of objects.

⁴ The ^{14}C specific activity model contained within Avila and Pröhl (2008) was developed for the SFR 1 SAR-08 and KBS-3H safety assessments.

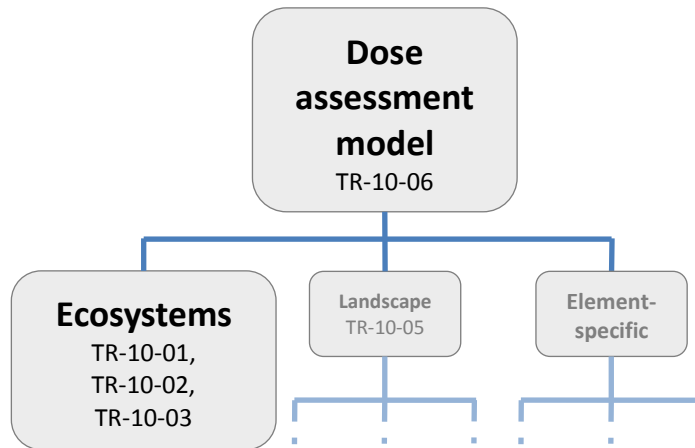


Figure 21: SR-Site documents used in the review of the ^{14}C assessment

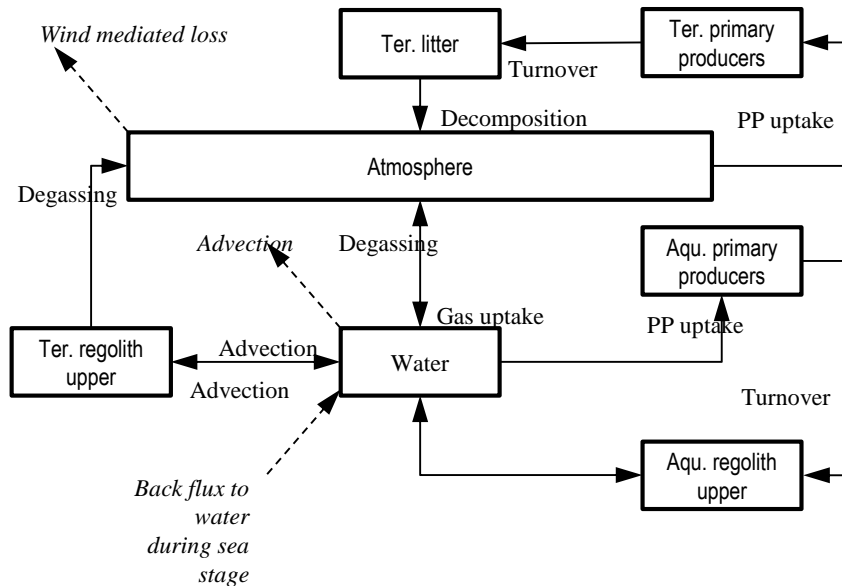


Figure 22: SR-Site ^{14}C model with a focus on transfers directly affecting atmosphere, water and both terrestrial and aquatic primary producers

5.3.1. Conceptual model

Figure 20 demonstrated SKB's presentation of the ^{14}C ecosystem model. In Figure 22 below, the details of the transfers are given; this partial reproduction of the earlier figure focuses on those compartments directly connected to atmosphere, water, terrestrial and aquatic primary producers.

The following additional processes are present in the aquatic aspect of the SR-Site as compared to the Avila and Pröhl (2008) model.

- Recycling of matter from the primary producers via sediment.
- Recycling of ^{14}C in the water back to the sediment via advection and sedimentation.
- A two-way exchange of ^{14}C between the water and the atmosphere.

- The possibility of ^{14}C to enter the water body in runoff from the land after flooding events.

In the terrestrial aspect of the ecosystem, the atmosphere has multiple sources of ^{14}C , as compared to the singular source assumed in Avila and Pröhl (2008). These sources are the release of ^{14}C as a consequence of litter decomposition and also degassing from water bodies within the same biosphere object. The atmosphere also has the additional loss mechanism of gas uptake by the water body.

If a truly specific activity model has been used (e.g. Avila and Pröhl, 2008; Sheppard et al., 2006) then the $^{14}\text{C}/^{12}\text{C}$ ratio in the atmosphere should be the same as that of the terrestrial primary producers, and the $^{14}\text{C}/^{12}\text{C}$ ratio in the water should be the same as that of the aquatic primary producers. As the mathematical model is not formulated directly in such a manner, the application of an implementation of the SR-Site model in Section 5.3.3 is a test as to whether this concept holds.

5.3.2. Data

As noted in Section 5.1.2, the specific activity of ^{14}C in the terrestrial biota is calculated in such a way that only the biomass of the primary producers is used, rather than any of the other plant types. If a larger plant biomass were assumed it would lead to a decrease in the calculated specific activity, and vice versa. The question is then whether or not the primary producer biomass is an appropriate choice.

It is only for the primary producers that a biomass (kgC m^{-2}) is given in the SR-Site documentation; for all other plant types only a production rate ($\text{kgC m}^{-2} \text{y}^{-1}$) is reported (see Löfgren, 2010). For primary producers an annual production rate (y^{-1}) is given, meaning that it is possible to derive annual production rates for the other plant types that would yield the same mean biomass as the primary producers (Table 29). From this analysis it is clear that the annual production rate for the other crops would need to be substantially lower for the other plant types if they were to have as high a biomass as the primary producers.

Table 29: Derivation of annual production rates (y^{-1}) of plant types that would give the same biomass (kgC m^{-2}) as primary producers (5.99 kgC m^{-2})

Plant type	Production rate ($\text{kgC m}^{-2} \text{y}^{-1}$)	Annual production rate that would yield the same biomass as primary producers (y^{-1})
<i>Primary producers</i>	4.79E-01	8.00E-02
Berries	1.27E-04	2.12E-05
Mushrooms	1.22E-04	2.04E-05
Cereal	1.68E-01	2.80E-02
Root vegetables	1.27E-01	2.12E-02
Vegetables	1.35E-01	2.25E-02
Fodder	2.00E-01	3.34E-02

5.3.3. Derivation of peak LDF value (biosphere object 118)

The SR-Site landscape model has been previously implemented in Ecolego (Xu, 2012), based on the description in Appendix A of Avila et al. (2010), and was used in the initial phase review of SR-Site (Klos and Wörman, 2013a). This implementation of the SR-Site biosphere model has been used here to verify SKB's results using the information available in the SR-Site reports, and associated Excel files. In addition, the ¹⁴C LDF has also been calculated for this object using the Avila and Pröhl (2008) conceptual model.

Landscape evolution of biosphere object 118

According to Table 10-2 of Aquilonius (2010), this object begins transitioning between a marine basin and a lake basin at 2531 CE (threshold_start), becomes regarded as a lake basin at 2848 CE (Isolation year), gains a terrestrial component at 2900 CE, and is fully isolated from the sea at 3059 CE (threshold_stop). Agriculture is assumed to commence at this location at 3205 CE (threshold_agri; see Table 7-13 of Lindborg 2010). Throughout the simulation period this object maintains a non-zero aquatic area.

In addition to the generic data listed in the preceding sections, various site specific data are required for the calculations, as defined in Avila and Pröhl (2008).

- Area of the aquatic and terrestrial aspects of the biosphere object
- Average depth of the aquatic part of the biosphere object

Dietary composition of biosphere object 118

From the start of the simulation, until after the peak LDF was calculated in the SR-Site assessment this object is a mostly aquatic object. This means that there is no external radiation contribution to the ¹⁴C exposure. As the water body is considered to be (partly) saline drinking water is assumed to come from a well drilled into the newly formed land. Although the water body is considered as saline in terms of water consumption, it is considered to comprise both freshwater and marine components in terms of biota production.

In particular, there is a scaling factor *threshold_sea_lake*, defined by the following equation.

$$threshold_sea_lake = \frac{threshold_stop - time}{threshold_stop - threshold_start} \quad (7)$$

This is used throughout the aquatic exposure model to provide a linear scaling of the aquatic body from being marine to freshwater as the landscape evolves (see Appendix A of Avila et al., 2010). Given the information presented above, this has a value of 0.775 at 2650 CE. The reviewers' interpretation of this is that at 2650 CE, SKB appear to estimate that 77.5% of the aquatic part of the biosphere object will be marine and 22.5% will be freshwater. This scaling parameter is used to determine the production of edible fish and crayfish, using the following equations.

$$prod_edib_crayfish = prod_edib_cray_Lake \cdot (1 - threshold_sea_lake) \quad (8)$$

$$\begin{aligned}
 prod_edib_fish = & \left[\begin{array}{l} prod_edib_fish_Lake \\ \cdot (1 - threshold_sea_lake) \end{array} \right] \\
 & + \left[\begin{array}{l} prod_edib_fish_Sea \\ \cdot threshold_sea_lake \end{array} \right]
 \end{aligned}
 \tag{9}$$

Using the production data for these biota given in Andersson (2010) and Aquilonius (2010), the human diet at 2650 CE has been determined by the consultants to comprise 66% fish, 13% crayfish, and 24% natural terrestrial food stuffs (berries, mushrooms and game). Whilst such information is of interest for the majority of radionuclides, the consultants considers it more informative for the aquatic exposure to know what proportion of the human diet is coming from the freshwater and marine sources, as these are the two water bodies for which a ¹⁴C specific activity is calculated at each time and which are then used in Avila and Pröhl (2008) to estimate human exposures from ingestion. Based upon the information provided in the SR-Site documentation, at 2650 CE it is estimated that 51% of the diet will come from freshwater sources (fish and crayfish) and 24% will come from the sea (fish).

Verification of SKB's ¹⁴C LDF calculations for biosphere object 118

In order to verify SKB's ¹⁴C LDF value used in the SR-Site assessment, here the LDF for biosphere object 118 has been independently calculated, following the same mathematical model. Whether their conceptual model is implemented as a specific activity model or not is evaluated by considering the calculated ¹⁴C specific activities in the two biotic compartments, and also the specific activity in the water body and atmosphere, all as time series. For both ecosystems the abiotic and biotic components should be equivalent to each other.

Figure 23 shows the calculated ¹⁴C specific activities in the aquatic and terrestrial ecosystems over the simulation period, in the Ecolego implementation of the SR-Site biosphere model. These indicate a high degree of agreement between the two pairs of specific activities (an r² of more than 0.99 in each ecosystem), giving confidence that the SR-Site ¹⁴C biosphere model is truly a specific activity model despite not being clearly formulated as such. The calculated peak ¹⁴C specific activities in the aquatic and terrestrial ecosystems occur at 2650 and 2715 CE respectively. However, the calculated peak ¹⁴C LDF is at 2569 CE, 81 years earlier than that reported by SKB, although the peak LDF (5.44E-12 Sv y⁻¹) agrees with the SKB value to 2 sf.

In the SR-Site model, the peak in the aquatic ecosystem relates to ¹⁴C contaminated material entering the water body as a result of runoff from the newly formed terrestrial ecosystem during the transition between ecosystems. For uncertainty analysis, SKB state that the transition from open sea water to an isolated lake might reasonably commence either 200 years earlier or later than their reference assumption, allowing for a 1 m greater or slower land rise. Altering only the time at which this transition is assumed to begin, from 2531 to 2331 CE, gives a calculated peak ¹⁴C of 6.00E-12 Sv y⁻¹, occurring at 2380 CE.

As an independent review, the LDF calculated using the SR-Site is compared here against what would have been reported using the Avila and Pröhl (2008) model. This has been achieved by incorporating the Avila and Pröhl equations for a constant release into the Ecolego implementation of the SR-Site model, so that the time series of volumes, areas and diet were congruent.

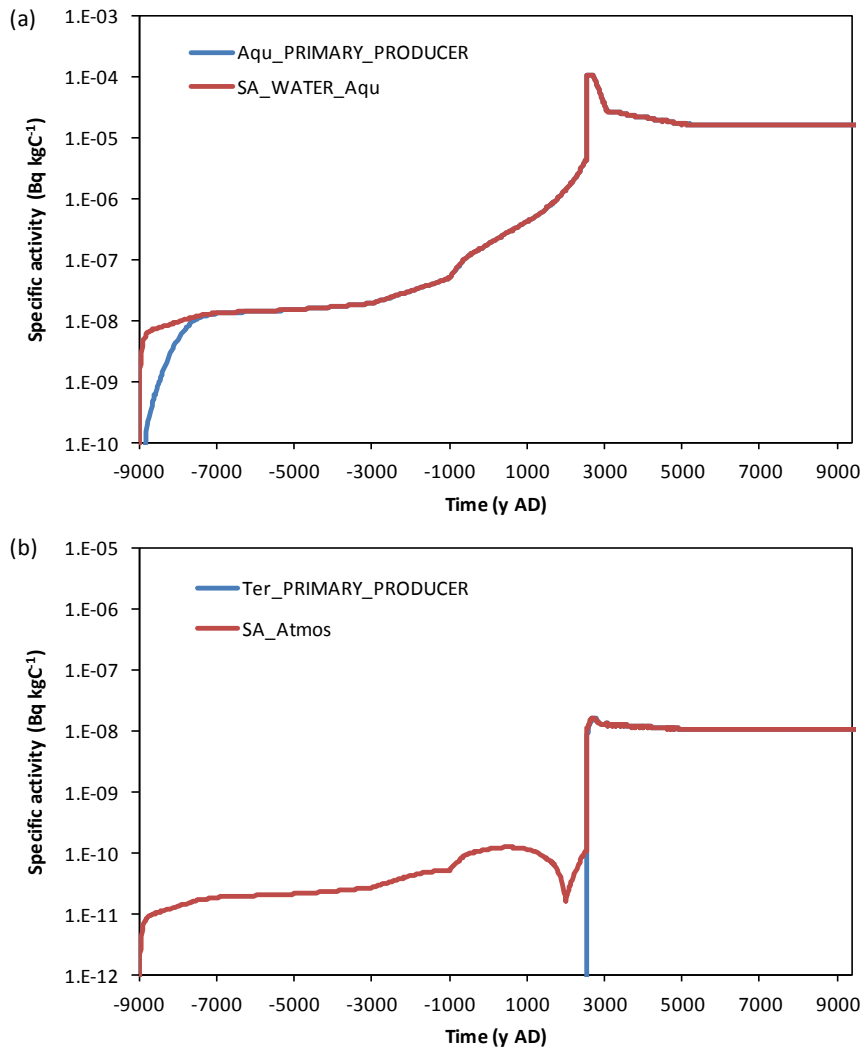


Figure 23: Calculated ^{14}C specific activity in biosphere object 118. (a) Aquatic primary producers and the water body in which they live; (b) Terrestrial primary producers and the atmosphere.

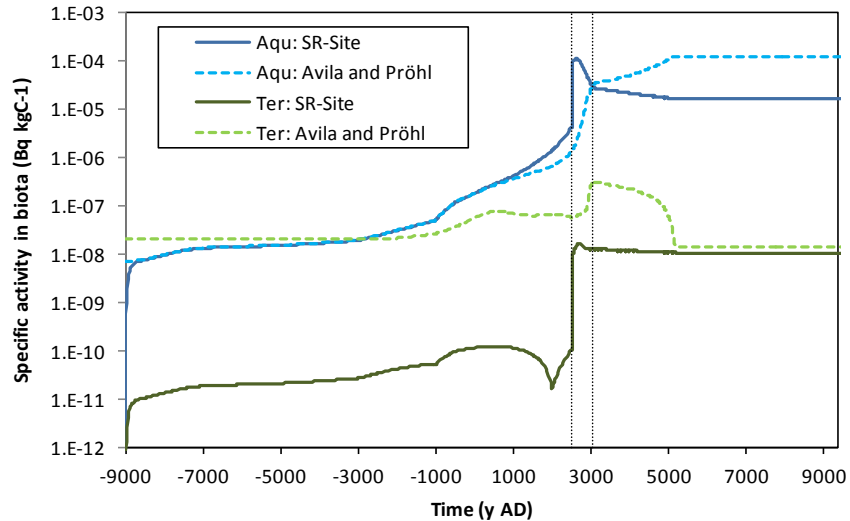


Figure 24: Comparison of SR-Site and Avila and Pröhl (2008) model derived specific activity of ^{14}C in the biota of the two ecosystem

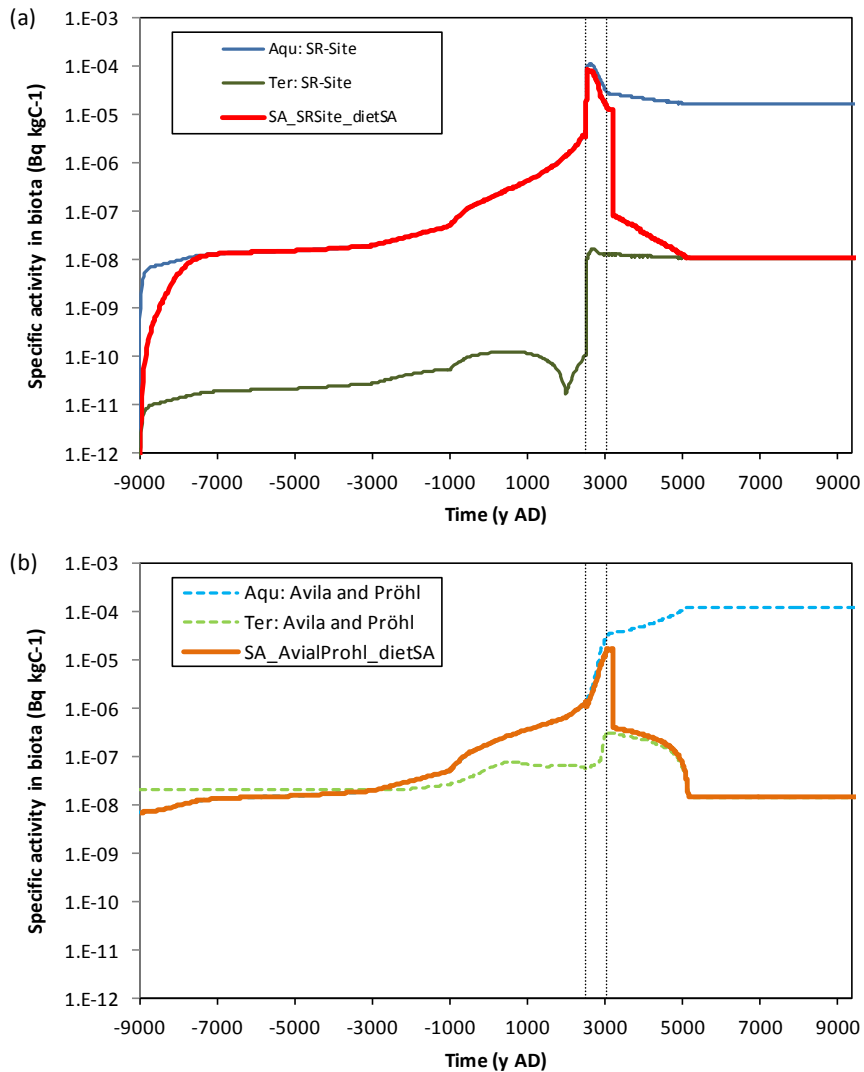


Figure 25: The specific activity in the aquatic (blue) and terrestrial (green) biota for each model, and the effect of dietary composition on the specific activity of the total diet (red/orange). (a) SR-Site model; (b) Avila and Pröhl (2008) model.

Figure 24 shows that a direct implementation of the simpler model developed for SKB previously cannot capture the influx of ^{14}C during the transition phase. Whilst a release of ^{14}C from sediments that become soil the atmosphere is represented, the movement of ^{14}C from the land to the water is not. Whilst the simpler model may have higher specific activities in each of the ecosystems as compared to the SR-Site model at certain times, these times do not correspond to times when the human diet comprises food primarily from that ecosystem (Figure 25). It is for this reason that the peak calculated ^{14}C LDF using the Avila and Pröhl model is only 20% of that calculated using the SKB model ($1.08\text{E-}12 \text{ Sv y}^{-1}$); the peak is also calculated to occur later, at 3100 CE.

5.4. Conclusion of review of ^{14}C modelling

Based on the analyses presented above, it is considered that the model used by SKB in SR-Site for the assessment of potential impacts to humans from ^{14}C is a specific activity model. Such a model offers a better representation of ^{14}C dynamics than a traditional concentration model, as used in the previous HLW/SF assessments. Further, it provides a more conservative estimate of the potential impacts than the simpler model developed for other SKB assessments, SFR 1 SAR-08 and KBS-3H. It also demonstrates that SKB's ^{14}C biosphere assessment model approach is congruent with other organisations, such as ÉdF and guidelines used in the Canadian nuclear industry (CSA, 2008; Sheppard et al., 2006).

The peak LDF for ^{14}C is associated with the transition period in the landscape evolution. In the SR-Site model the peak LDF occurs early in this transition period, when there is a flux of radionuclides from the newly formed land into the water body as a result of flooding.

6. Review of SKB's interpretation of human exposure routes

The preceding section focussed upon the data used to support the assessment of radionuclide migration within the biosphere and uptake into plants and animals. In this section, consideration is given as to how the radionuclide concentrations in environmental media and biota translate into the landscape dose factors (LDFs) as defined in Avila et al. (2010). Specifically, consideration is given here to human exposure assumptions.

The focus of the other aspects of the element specific data review has been upon four radionuclides (^{79}Se , ^{94}Nb , ^{129}I and ^{226}Ra), which are also the focus of the review here. Exposure calculations relating to ^{14}C were already considered in the preceding section.

6.1. SKB's presentation

In the SR-Site assessment, SKB present the total exposure rates of humans, with the food ingestion rate based on an adult male, spending 100% of their time outside to maximise the potential inhalation exposure. The radionuclide specific dose coefficients associated with human exposure are given in Section 6.1.2 of Nordén et al. (2010).

Although the method used for defining the human diet is described in Section 3.2.3 of Avila et al. (2010), and the equations are given in Appendix A of the same report, the actual time series diet data for each biosphere object are neither presented in the reports, nor is any reference made to Sicada. The implication of this is that the dietary data used is calculated solely within the implementation of the LDF model in Pandora. Without access to the software and the code used to implement the mathematical model it is therefore not possible to audit the numerical values of dietary consumption used.

Further details of the underlying human exposure assumptions, together with the radionuclide specific data relating to ^{79}Se , ^{94}Nb , ^{129}I and ^{226}Ra , and results for those radionuclides as presented in the SR-Site assessment are summarised below.

6.1.1. Total exposure rates and dietary composition

The total exposure rates (food and water ingestion, inhalation) are based upon the values used in the SR-Can assessment (see Table 6-9 of Nordén et al. 2010). It is also assumed that humans spend 100% of their time outside, thereby maximising their potential external and inhalation exposures.

As noted in Section 3.2.3 of Avila et al. (2010), no assumptions have been made regarding food preferences of future individuals. Instead, in the calculation of food ingestion doses it is assumed that the human diet reflects the production capacity of different foods in the biosphere objects. That report goes on to state the following further assumptions about the future human diet.

“Further, it is assumed that future human inhabitants will be self-sustaining and will utilize all available food sources in proportion to their production. The production capacity of human food in a biosphere object is directly determined by the size of the contaminated object, (i.e. the size of the sea basin or the size of the wetland and the surface water), and the sustainable yield of natural food stuffs and agricultural products, which in turn may vary with climatic conditions. Assuming that food production is the limiting factor for humans living in the biosphere object, the number of individuals that can be sustained in a biosphere object is thus proportional to the area of the object. However, the size of the population that can be sustained also depends on land use, since the productivity per unit area of crop is two to three orders of magnitude larger than the productivity of natural food stuffs in a wetland.

All types of food sources from both aquatic and terrestrial parts of a biosphere object are considered in the dose calculations. It is assumed that wetlands will at least partly be converted to agricultural land when this is possible. Thus, when the object is submerged the human diet consists of sea food. When the object has been isolated from the sea, the diet consists of natural food stuffs from the lake/stream and from the wetland. When agriculture is possible, the diet will be a combination of natural food stuffs and agricultural produce. The contribution of each food type to the human diet is assumed to be proportional to the production of that food type in the object. When agriculture is possible, it is deemed equally likely that the wetland is used for production of natural food stuffs, cereals, root crops, vegetables or fodder for beef and dairy production. [...] It is important to note that the assumption of self-sustained future inhabitants of the area does not imply that this is a “stone-age”-like culture. It only sets the constraint that the population is obtaining all its food locally from available resources.”

The implication of the second paragraph is that when agriculture is possible that the land use is split such that 20% of the terrestrial land area is given over to each of the broad plant types: natural food stuffs, cereals, root crops, vegetables and fodder. This is confirmed by the equations given on p.140-154 in Appendix A of Avila et al. (2010), which further clarifies that game and livestock are each assumed to effectively occupy 20% of the terrestrial area once agriculture is possible.

Ingestion dose coefficients for both food and water are determined using different equations depending on whether the climate is in a permafrost period or not. The contributions from terrestrial foodstuffs are dependent upon the size of the terrestrial area (ter_area_obj) and whether or not agriculture is present ($time_GE_threshold_agriculture = 1$), whereas the aquatic foodstuff production rates are reliant upon there being sufficient depth of water available in the object ($depth_max \geq z_min_prod_edib_fish_Lake$ and $depth_aver \geq z_min_prod_edib_crayfish_Lake$). This means that the diet associated with each biosphere object is distinct from any other object, and that for each object the diet evolves over time.

Although this description of the how the human diet is determined is given the numerical values used are not reported in any of the SR-Site documentation.

6.1.2. Data relating to the peak LDF values for ⁷⁹Se, ⁹⁴Nb, ¹²⁹I and ²²⁶Ra used in the SR-Site assessment

Table 4-1 of Avila et al. (2010) details the peak LDF values which were calculated to support the SR-Site assessment, together with the contributions of exposure pathways (external, inhalation, ingestion of water and ingestion of food), the biosphere object ID of where the peak value was determined for a unit flux of the radionuclide (1 Bq y⁻¹) and the number of people supported by the biosphere object at that time. By combining that information with the time series data relating to the aquatic and terrestrial object area (aqu_area_obj and ter_area_obj, obtained from Parameters_TS_all_basins.xlsx) it is possible to ascertain the nature of the ecosystem to which these peak LDFs relate.

The peak LDF calculated by Avila et al. (2010) occurred in biosphere object 121_03 for three out of the four radionuclides of concern in this review, but at differing times, with the ⁹⁴Nb peak occurring in object 124 (Table 30). For each of the radionuclides considered in this review, the peak LDF was determined by SKB to have occurred when the object was fully terrestrial and had the potential to be used for agriculture.

Table 10-1 of SKB (2010) provides further details as to the contributing pathways for three of the radionuclides. For ⁷⁹Se the key human exposure pathways are the ingestion of vegetables and cereal, and for ¹²⁹I it is the ingestion of vegetables and milk which contribute most to dose, whilst for ²²⁶Ra it is the ingestion of vegetables and water. Table 4-1 of Avila et al. (2010) states that 98% of the peak LDF associated with ⁹⁴Nb is expected to come from external exposure.

Whilst ⁹⁴Nb is expected to dominate the potential mean annual effective dose for the period 10,000 to 60,000 CE, the other three radionuclides are then shown to dominate the potential mean annual effective dose for the shear failure scenario after 60,000 CE, with ²²⁶Ra as the most influential (Figure S-11 of SKB, 2011).

6.2. Motivation of the assessment

For all radionuclides except ^{108m}Ag, ⁹⁴Nb and ^{166m}Ho it is the ingestion of water and food which contribute more than 91% of the exposure (see Table 4-1 of Avila et al. 2010). It is therefore relevant to consider the dietary assumptions relating to humans, and dose coefficients for ingestion and inhalation. In particular, it is pertinent to understand what specific foodstuffs are assumed by SKB to contribute to the human diet at the time of calculated peak exposure from a radionuclide. This then feeds back to the underlying assumptions relating to the uptake of the radionuclides into those foodstuffs.

6.3. The Consultants' assessment

Figure 26 shows the primary SR-Site documentation used in the review of the human exposure assessment. In addition, data from the SICADA database was used for time series dependent parameters, such as the terrestrial and aquatic areas of objects.

Table 30: Data relating to the peak LDFs for ⁷⁹Se, ⁹⁴Nb, ¹²⁹I and ²²⁶Ra

Parameter name	Unit	Radionuclide				Note(s)
		⁷⁹ Se	⁹⁴ Nb	¹²⁹ I	²²⁶ Ra	
Peak LDF	(Sv y ⁻¹)/ (Bq y ⁻¹)	1.2E-9	4E-12	6.5E-10	3.8E-12	a
Time of peak LDF	CE	4750	9400	4050	9400	a
Biosphere object for peak LDF	-	121_03	124	121_03	121_03	a
Sum of contribution from external exposure and inhalation	%	0	98	0	0	a
Percentage exposure from ingestion of water	%	0	0.2	0.1	54.3	a
Percentage exposure from ingestion of food	%	100	1.8	99.9	45.7	a
ter_area_obj at time of peak LDF	m ²	81876	83390	81876	81876	b
Time_threshold_agriculture	CE	3870	2229	3870	3870	c
Aqu_area_obj at time of peak LDF	m ²	0.0001	210	0.0001	0.0001	d
depth_max at time of peak LDF		0.0001	0.38	0.0001	0.0001	d
z_min_prod_edib_fish_Lake	kgC m ⁻² y ⁻¹	1	1	1	1	e
depth_aver at time of peak LDF		0.0001	0.19	0.0001	0.0001	d
z_min_prod_edib_crayfish_Lake	m	2	2	2	2	f

a Table 4-1 of Avila et al. (2010)

b Values given in Parameters_TS_all_basins.xlsx for time points 3499, 3500 and 3600 CE only for object 121_03, and the last time point for object 124 is 2600 CE.

c Parameters_SS.xlsx

d A nominal value, as given in Parameters_TS_all_basins.xlsx for the time 3600 CE for 121_03. Value for object 124 is for 2600 CE.

e Units given as on p 406 of Andersson (2010), but text refers to m, which is more sensible. The discussion of this parameter in that report makes it clear that fish would not be expected to be present in the biosphere object 121_03.

f Andersson (2010)

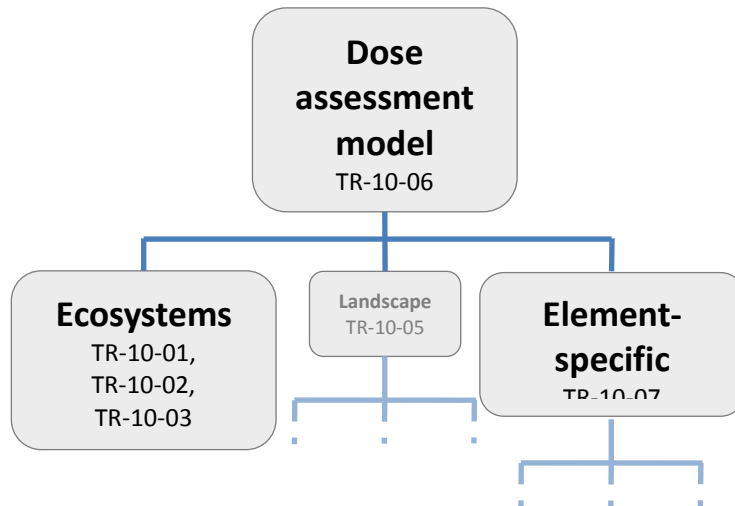


Figure 26: SR-Site documents used in the review of the human exposure assessment

6.3.1. Dietary composition

As has been noted above, the biosphere object under consideration (121_03) was fully terrestrial, and used partially for agriculture at the time that the peak LDF values were calculated by SKB. As the area of the object did not change during that time, the productivity of the various food stuffs, and thus human diet composition, can be readily calculated using the equations given in Appendix A of Avila et al. (2010). Production data per m² is given for each of the food stuffs in Section 13.3.5 of Löfgren (2010), and is reproduced in Table 5-3 of Avila et al. (2010). This data is reproduced here, and has been used to derive total production rates for 121_03 by the consultants using the equations in Avila et al. (2010); see Table 31.

Table 31: Human diet composition in Object 121_03 following the onset of agriculture

Crop	Production of edible crop * kgC m ⁻² y ⁻¹	Production of food stuff in the biosphere object kgC y ⁻¹	Contribution to diet %
Vegetables	1.35E-1	2.21E+3	35
Tubers	1.27E-1	2.08E+3	33
Cereal	1.14E-1	1.87E+3	30
Milk	3.00E-2	9.83E+1	< 1.57
Meat	1.00E-3	3.28E0	< 0.053
Berries	1.27E-4	2.08E0	< 0.034
Mushroom	1.22E-4	2.00E0	< 0.032
Game	8.26E-6	1.35E-1	< 0.003

* With the exception of milk and meat, the production rates were taken from Löfgren (2010). These values are also repeated in Table 5-3 of Avila et al. (2010), which is where the values for meat and milk were taken from.

The consultants note that the percentage contributions to diet derived here should be equally valid for any other fully terrestrial biosphere objects, with agriculture, where any water body is of insufficient depth to permit either fish or crayfish to live.

In Löfgren (2010) production rates for meat and milk are given in units of kgC food kgC⁻¹ fodder; the mean values are 6E-3 and 1.48E-1 for meat and milk respectively. It is noted in Löfgren (2010) that these values need to be multiplied by the production rate of fodder (prod_fodder, mean value 2E-1 kgC m⁻² y⁻¹) to obtain values for use in the assessment. Löfgren (2010) go on to highlight that

“...this was not done in the radionuclide modelling (Avila et al. 2010) and the estimate above was instead used directly, meaning that the actual meat production per unit area of suitable land was underestimated by a factor 5”.

The same is noted for the milk. However, it is the correctly scaled production rates, to 1 significant figure, which were presented in Table 5-3 of Avila et al. (2010). It is therefore not clear as to whether there was an underestimation of the meat and milk production used in the calculation of the LDF values, or whether the statements made in Löfgren (2010) are incorrect.

6.3.2. Timing of the peaks

As noted above, the peak LDF values calculated for all these radionuclides occur after the site is fully terrestrial, and the biosphere object is used for agriculture. Appendix B of Avila et al. (2010) lists the various parameters which have been used in the model. Tracking the object specific time series parameters relating to the terrestrial ecosystem back to the Excel data files (Parameters_TS_all_basins.xlsx), the last data points for all the terrestrial parameters in 121_03 are given at 3600 CE, which corresponds to when the mire is assumed to stop growing. At this last time point for the landscape modelling of 121_03 there is an aquatic water body of nominal size assumed to be present (1E-8 m³, based on the data presented in Table 2 above). However, the peak times for the LDFs reported by SKB are 4750, 9400, 4050 and 9400 CE for ⁷⁹Se, ⁹⁴Nb, ¹²⁹I and ²²⁶Ra respectively.

SKB's approach to the modelling of human dose in agricultural ecosystems in the SR-Site assessment has been previously discussed in detail in Klos and Wörman (2013a). They note that the SR-Site landscape model, following the theoretical time at which agriculture will become possible in that object, takes the radionuclide concentrations accumulated in the upper regolith as the initial conditions from which to derive an estimate of the agricultural soil radionuclide concentration over a 50 year period following conversion. This is then used to determine the human exposure dose. Klos and Wörman further observed that *“it might be anticipated that the highest consequences would arise after the longest accumulation time, or that a steady-state concentrations would be established in the wetland phase”*. However, this is not the case for either ⁷⁹Se or ¹²⁹I; the reasons for this relate to the landscape modelling, and are discussed elsewhere in this report.

6.3.3. Radionuclide specific LDF

Given the high contributions of vegetables, tubers and cereals to the human diet in biosphere object 121_03, based upon the assumptions above, it is not surprising that these were found by SKB to be among the highest pathways of exposure to humans. In this section, consideration is given to sensitivities around the LDFs associated with the four trace radionuclides.

The primary exposure pathway for ^{94}Nb is external radiation (98%). Given this, and that the plant CRs derived by the reviewers are in close agreement with those reported by SKB, consideration need not be given to the parameterisation of the food contamination for this radionuclide. The external exposure calculations are based upon standard methodologies, and are considered conservative in as much as the person spends 100% of their time in a location to receive such an exposure.

For ^{79}Se and ^{129}I it is the consumption of food only which gave rise to the dominant contribution to exposure (over 99%) in the SR-Site assessment. For ^{129}I , milk is a highly contributing pathway also. With respect to ^{79}Se , the reviewer derived plant CRs were in broad agreement with those reported by SKB (Table 21), and so there is little concern with the LDF reported by SKB given the assumptions made. However, for ^{129}I the consumption of vegetables is one of the key exposure pathways (see Table 10-1 of SKB, 2010). In Section 4.3.2, the reviewers found that if the IAEA (2010) CR data had been used instead of the Robens et al. (1988) data the vegetable CR value would have been only 3% of the one given in Nordén et al. (2010). This would be expected to lead to a substantial reduction in the derived LDF value used in the assessment.

For ^{226}Ra , the peak LDF value was calculated at the end of the simulation period that SKB used (9400 CE). Figures 3-6 and 3-7 of Avila et al. (2010) indicate that the highest calculated soil concentration was in the agricultural soil rather than the mire, and that the highest calculated ^{226}Ra concentrations in food sources were for mushrooms, vegetables and game. However, combining the data presented in Figure 3-7 of Avila et al. (2010) with the dietary contributions presented in Table 3 above, it is vegetables which for the results presented by SKB would contribute at least 80% of the exposure associated with food consumption, with up to 10% coming from each of tubers and cereals for a fully terrestrial biosphere object with agriculture. Although no site specific data was available for the transfers of ^{226}Ra into these crops, the parameters used by SKB are based directly upon the most recent international compendium of biosphere data (IAEA 2010), converted from kg dw plant kg^{-1} dw soil to kgC plant to kg^{-1} dw soil. Whilst the cereal value seems to have been correctly converted, based on the data presented in Table 17 of IAEA (2010) and Tables 4-1 and 4-3 of Avila et al. (2010), the same is not true for vegetables and tubers (see Table 21 above, in Section 4.3.2). If the reviewer derived plant CRs were used instead, the estimated exposure from food consumption would be reduced.

According to Table 4-1 of Avila et al. (2010) food consumption contributes 45.7% of the total exposure from ^{226}Ra , with the remainder coming from the ingestion of water (see also Table 30 above). Using the well capacity given in Löfgren (2010), $82,502 \text{ m}^3 \text{ y}^{-1}$, and assuming a release of 1 Bq y^{-1} of ^{226}Ra into the well, a dose from ingestion water of $2.04\text{E-}12 \text{ Sv y}^{-1}$ has been calculated by the reviewers. This would then contribute 63.5 % of the exposure, not 54.3 % as reported by Avila et al. (2010).

6.4. Conclusion of review of SKB's interpretation of human exposure routes

Assumptions in the landscape modelling, relating to the migration and accumulation of radionuclides in the soil, mean that for almost all the radionuclides considered in the SR-Site assessment the peak LDF is associated with an agricultural ecosystem.

For the radionuclides focussed upon in this review, the combination of dietary composition and plant CRs means that the consumption of vegetables dominates the exposure for ^{79}Se , ^{129}I and ^{226}Ra . However, the SR-Site CR value used for ^{129}I is substantially higher than the reviewer derived value, meaning that for the SR-Site assessment the LDF associated with this radionuclide could justifiably be reduced. Taking the SKB methodology as described in Avila et al. (2010), and the parameter values reported elsewhere in the SR-Site documentation, there is no cause for concern that the LDF associated with these key radionuclides have been underreported.

7. The Consultants' overall assessment

7.1. SKB's interpretation of hydrological modelling

Water movement is the prime mover in the landscape. The review of the hydrology in the SR-Site dose assessment modelling has concentrated on i). the understanding of the near surface hydrology in the Forsmark landscape (Bosson et al., 2010), ii). how this is used to set the basis for the hydrological drivers of the radionuclide transport model via six key model parameters (Löfgren 2010) and iii) the implementation of the hydrological parameters in the dose assessment model (Avila et al., 2010).

Key findings are:

- The hydrology in the dose assessment model is substantially different to that represented by the “average object” that is employed by Bosson et al. (2010) to summarise and represent the hydrology of basins in the future landscape.
- A significant discrepancy is the translation from Mike-She balance to Radionuclide model. Many of the interactions shown in the hydrology of the “average object” are not reproduced in the radionuclide transport model and there is no justification or discussion in either Löfgren (2010) or Avila et al. (2010) to support the change in structure of the hydrology.
- The “average object”, on which the hydrology of each of the basins in the dose assessment modelling is based, is neither representative of the range of lake-mire objects to be expected in the future Forsmark landscape nor is it representative of other key object classes, most notably the stream object (from which the highest LDFs are obtained in SR-Site) and the hydrological model of agricultural land.
- The hydrology as modelled is suitable only for a snapshot (at 5000 CE for an aggregate of six lakes currently in existence in the present-day terrestrial biosphere) of lake-mire objects during the evolution of the Forsmark site.

There are some outstanding Requests For Information that are being communicated to SKB. It is anticipated that responses to these will be investigated in a further application of the dose assessment model discussed below.

Consequently, it is hard to state with confidence that the hydrological representations in the dose assessment model are fit for purpose. The impact on the uncertainty in the calculated LDFs is therefore unknown. An investigation using GEMA-Site would be a suitable way of addressing the issues since it offers a high degree of flexibility.

7.2. Independent landscape modelling

The objective of the development of an alternative dose assessment model was to allow the possibility of carrying out an independent numerical review of the LDFs calculated in SR-Site. The model – GEMA-Site – encompasses a high degree of site specific detail while retaining a highly flexible structure for implementing alternate realisations of hydrology within an evolving basin. It can therefore be seen as being

intermediate in complexity between the relatively simple Reference Biosphere modelling approach (IAEA, 2003) and that employed by SKB (Avila et al., 2010).

Using a simple interpretation of the hydrology within a representative basin (ie, generic in the context of the future Forsmark landscape) calculated LDFs are similar to those presented by SKB in SR-Site.

The LDFs employed in SR-Site are maximum doses over the entire future landscape and therefore there is an element of the values effectively “selecting” the most radiologically sensitive locations and times in the future landscape. In the results from GEMA-Site discussed here there has been no optimisation to give higher-end LDF values.

Application of GEMA-Site to determine the potential uncertainty in LDF values is therefore recommended.

7.3. Derivation of nuclide specific data

The primary focus of this review has been upon the derivation of the distribution coefficients (Kd) and the plant concentration ratios.

7.3.1. Distribution coefficients

In general there appear to be both consistencies and inconsistencies between the analytical data as reported in the primary data base (SICADA) and the reporting of in situ Kd values for both Forsmark and Laxemar. The reviewers have been unable to achieve the same number of paired samples from the site specific data as claimed by SKB in Appendix D of Nordén et al. (2010). The exception to this is the ²²⁶Ra regolith Kds. Even though the data for ²²⁶Ra have been collected for Forsmark only, this data set represents a statistically strong and defensible basis on which to estimate site specific Kd values for ²²⁶Ra which provides SKB with a much better basis for modelling this radionuclide than for the other elements we have examined.

7.3.2. Plant uptake

Whilst it is understood that SKB wished to calculate all concentrations of radionuclides in plants, and other biota, on a Bq kgC⁻¹ basis, this means that assumptions needed to be made as to the carbon content of crops and biota. It also means that it was not straightforward to compare the parameters values used against other parameter databases, such as IAEA (2010). Some errors have been found in the conversions SKB have applied to literature data to obtain concentration ratios in their chosen format.

There is also concern in the derivation of the concentration ratios used for the natural vegetation, where data pertaining to such a wide range of plant types, which exhibit varying behaviour, has been used to generate one distribution which is then used for all natural vegetation.

7.3.3. Terrestrial and aquatic animal uptake parameters

With respect to the meat and milk transfer factors, there are clear discrepancies between the GSD values given in the SR-Site documentation (Nordén et al., 2010) and the underlying literature source (primarily IAEA, 2010). When distributions were derived from the SR-Can values (Karlsson and Bergström, 2002), again there are discrepancies. Whilst according to Nordén et al. (2010) this will not affect the calculation of the LDFs, which are based on deterministic calculations only, such disregard for the correct transcription of values from one document to another does not help to instil confidence in the values used in the assessment.

The wild herbivore transfer factors are difficult to interpret and verify. It is therefore not possible to conclude as to whether or not the values used in the SR-Site assessment are appropriate or not.

For the aquatic biota, the concentration ratios used as based on much more recent literature compilations than previous assessments, and have been supplemented with some site data. However, as aquatic biota play a minor role in the calculated human exposures, no further consideration has been given to the use of site data and the derivation of parameter distributions used in the SR-Site assessment in this review.

7.4. ^{14}C modelling and assessment

Based on the analyses presented in Section 5.3 of this report, it considered that the model used by SKB in SR-Site for the assessment of potential impacts to humans from ^{14}C is a specific activity model. Such a model offers a better representation of ^{14}C dynamics than a traditional concentration model, as used in the previous SKB HLW/SF assessments. Further, it provides a more conservative estimate of the potential impacts than the simpler model developed for other SKB assessments, SFR 1 SAR-08 and KBS-3H.

It also demonstrates that SKB's ^{14}C biosphere assessment model approach is congruent with other organisations, such as ÉDf and guidelines used in the Canadian nuclear industry (CSA, 2008; Sheppard et al., 2006).

7.5. Human exposure

The vast majority of the peak LDF values as determined by SKB are associated with an ecosystem that, at the time of the peak LDFs, is fully terrestrial with agriculture possible, and also with no freshwater body (object 121_03). This means that the dietary composition is dominated by the consumption of three crops: vegetables, tubers and cereal. It is therefore not surprising that SKB found these food sources to dominate the exposure.

8. References

- Andersson K, Tostenfeldt B, Allard B, 1982. Sorption behaviour of long-lived radionuclides in igneous rocks. In: Environmental migration of long-lived radionuclides. Symposium Knoxville, TN, USA, 21-31 July 1981. ed. IAEA, Vienna. pp 111–131.
- Andersson E. (ed.), 2010. The limnic ecosystems at Forsmark and Laxemar-Simpevarp. SR-Site Biosphere. SKB TR-10-02, Svensk Kärnbränslehantering AB.
- Aquilonius K (ed.), 2010. The marine ecosystems at Forsmark and Laxemar-Simpevarp. SR-Site Biosphere. TR-10-03, Svensk Kärnbränslehantering AB.
- Avila R., 2006a. Model of the long-term transfer of radionuclides in forests. SKB TR-06-08, Svensk Kärnbränslehantering AB.
- Avila R., 2006b. The ecosystem models used for dose assessments in SR-Can. SKB R-06-81, Svensk Kärnbränslehantering AB.
- Avila R., Ekström P.-A., Åstrand P.-G., 2010. Landscape dose conversion factors used in the safety assessment SR-Site. SKB TR-10-06, Svensk Kärnbränslehantering AB.
- Beresford N.A., Brown J., Copplestone D., Garnier-Laplace J., Howard B., Larsson C.M., Oughton D., Pröhl G., Zinger I. (eds), 2007. D-ERICA: An integrated approach to the assessment and management of environmental risk from ionising radiation. Description of purpose, methodology and application. EC contract number FI6R-CT-2004-508847, European Commission, Brussels.
- Bergström U., Andersson K., Røjder B., 1984. Variability of dose predictions for cesium-137 and radium-226 using the PRISM model. Studsvik (NW-84/656).
- Bergström U., Nordlinder S., 1990. Individual radiation doses from unit releases of long lived radionuclides. SKB TR 90-09, Svensk Kärnbränslehantering AB.
- Bergström, U., Nordlinder, S., 1991. Individual doses from radionuclides released to the Baltic coast. SKB TR 91-41, Svensk Kärnbränslehantering AB.
- Bosson E., Sassner M., Sabel U., Gustafsson L.-G., 2010. Modelling of present and future hydrology and solute transport at Forsmark. SR-Site Biosphere. SKB R-10-02, Svensk Kärnbränslehantering AB.
- Coughtrey P.J., Jackson D., Thorne M.C., 1985. Radionuclide distribution and transport in terrestrial and aquatic ecosystems. Associated Nuclear Services, Epsom, UK (EUR-8115-VI).
- Davis PA, Zach R, Stephens ME, Amiro BD, Bird GA, Reid JAK, Sheppard MI, Sheppard SC, Stephenson M, 1993. The disposal of Canada's Nuclear Fuel Waste: The Biosphere Model, BIOTRAC, for Postclosure Assessment. AECL Research, Whiteshell Laboratories, Pinawa, Manitoba (AECL 10720, COG-93-10).
- Egan., M., Little, R, Walke, R. 2012. Review of Landscape Models used in SR-Site. SSM Technical Note, Report number 2012:46. ISSN: 2000-0456.
- Engdahl A., Hannu S., Ternsell A., 2006. Chemical characterisation of deposits and biota. Oskarshamn site investigation. SKB-P-06-20, Svensk Kärnbränslehantering AB.

Engdahl A., Rådén R., Borgiel M., Omberg L.-G., 2008. Oskarshamn and Forsmark site investigation. Chemical composition of suspended material, sediment and pore water in lakes and sea bays. SKB P-08-81, Svensk Kärnbränslehantering AB.

EU, 1996. Council Directive 96/92/EURATOM of 13 May 1996 laying down basic safety standards for the protection of the health of workers and the general public against the dangers arising from ionizing radiation. Luxembourg: European Commission.

Deitermann W.I., Hauschild J., Robens-Palavinskas E., Aumann D.C., 1989. Soil-to-vegetation transfer of natural I-127, and of I-129 from global fallout, as revealed by field measurements on permanent pastures. *Journal of environmental radioactivity*, Vol. 10, pp. 79–88.

Grolander S., Roos P., 2009. Forsmark site investigation. Analysis of radioactive isotopes in near surface groundwater, surface water, biota and soil. SKB P-09-66, Svensk Kärnbränslehantering AB.

Hannu S., Karlsson S., 2006. Forsmark site investigation. Chemical characterisation of deposits and biota. SKB P-06-220, Svensk Kärnbränslehantering AB.

IAEA., 1994. Handbook of parameter values for the prediction of radionuclide transfer in temperate environments (Produced in collaboration with the International Union of Radioecologists). International Atomic Energy Agency, Vienna, Austria. (Technical Reports Series No. 364).

IAEA 2003 Reference biospheres for solid radioactive waste disposal Report of BIOMASS Theme 1 of the BIOSphere Modelling and ASSESSment (BIOMASS) Programme IAEA-BIOMASS-6 (Vienna: International Atomic Energy Agency Safety)

IAEA., 2004. Sediment distribution coefficients and concentration factors for biota in the marine environment. IAEA Technical Reports Series 422, International Atomic Energy Agency, Vienna.

IAEA., 2010. Handbook of parameter values for the prediction of radionuclide transfer to humans in terrestrial and freshwater environments. IAEA Technical Reports Series 472, International Atomic Energy Agency, Vienna.

Johanson K.J., Nikolova I., Taylor A.F.S., Vinichuk M.M., 2004. Uptake of elements by fungi in the Forsmark area. SKB TR-04-26, Svensk Kärnbränslehantering AB.

Karlsson S., Bergström U., 2002. Element specific parameter values used in the biospheric models of the safety assessments SR97 and SAFE. SKB R-02-28, Svensk Kärnbränslehantering AB.

Klos, RA, Shaw, GG, Xu, S, Nordén, M, and Wörman, A (2011). Potential for high transient doses due to accumulation and chemical zonation of long-lived radionuclides across the geosphere-biosphere interface. *Radioprotection*. 46(6), p453 – p459

Klos, RA., L. Limer, G. Shaw and A. Wörman (2012) Initial review phase – Dose Assessment Methodology SSM Technical Note, Report number 2012:59. ISSN: 2000-0456.

Klos, RA., Wörman A., 2013a. Technical note: Initial review phase – Further review of select elements in SKB's Dose Assessment Methodology. Swedish Radiation Safety Authority (SSM2011-592, SSM 2011-4544, 3030007-4033).

- Klos, RA and Wörman, A., 2013b. Uncertainties in doses from agricultural ecosystems following conversion from wetlands. Accepted for presentation at the 2013 International High-Level Radioactive Waste Management Conference, Albuquerque, New Mexico USA, April-May 2013.
- Klos, RA, Limer, L, Shaw, G, Pérez-Sánchez, D, & Xu, S, 2013. Advanced spatio-temporal modelling in long-term radiological assessment models – radionuclides in the soil column, *J. Radiol. Prot.* **34** (2014) 31-50. <http://stacks.iop.org/0952-4746/34/31>
- Klos, RA, 2014. Model description and test: GEMA-Site 1.0. SSM Report in preparation.
- Lindborg T (ed.), 2010. Landscape Forsmark – data, methodology and results for SR-Site. SKB TR-10-05, Svensk Kärnbränslehantering AB.
- Löfgren A. (ed), 2010. The terrestrial ecosystems at Forsmark and Laxemar-Simpevarp. SR-Site Biosphere. SKB TR-10-01, Svensk Kärnbränslehantering AB.
- McKinley IG, Scholtis A, 1992. Compilation and comparison of radionuclide sorption databases used in recent performance assessments. In: Radionuclide sorption from the safety evaluation perspective, OECD, Paris, pp. 21–55.
- Nordén S., Avila R., de la Cruz I., Stenberg K., Grolander S., 2010. Element-specific and constant parameters used for dose calculations in SR-Site. SKB TR-10-07, Svensk Kärnbränslehantering AB.
- Robens E., Hauschild J., Aumann D.C., 1988. Iodine-129 in the environment of a Nuclear Fuel Reprocessing Plant: III Soil To Plant Concentration Factors for Iodine-129 and Iodine-127 and their Transfer Factors to milk, egg and pork. *Journal of Environmental Radioactivity.* 8 (1), 37–52.
- Roos P., Engdahl A., Karlsson S., 2007. Oskarshamn and Forsmark site investigations. Analysis of radioisotopes in environmental samples. SKB P-07-32, Svensk Kärnbränslehantering AB.
- Sheppard SC, Ciffroy P, Siclet F, Damois C, Sheppard MI, Stephenson M. 2006. Conceptual approaches for the development of dynamic specific activity models of ¹⁴C transfer from surface water to humans. *Journal of Environmental Radioactivity* 87, 32-51.
- Sheppard S., Long J., Sanipelli B., Sohlenius G., 2009. Solid/liquid partitioning coefficients (K_d) for selected soils and sediments at Forsmark and Laxemar-Simpevarp. SKB R-09-27, Svensk Kärnbränslehantering AB.
- SKB, 2010. Biosphere analyses for the safety assessment SR-Site – synthesis and summary of results. SKB TR-10-09, Svensk Kärnbränslehantering AB.
- SKB, 2011. Long-term safety for the final repository for spent nuclear fuel at Forsmark: Main report of the SR-Site project. SKB TR-11-01, Svensk Kärnbränslehantering AB.
- Thompson SE, Burton CA, Quinn DJ, Ng C, 1972. Concentration factors of chemical elements in edible aquatic organisms. (UCRL-50564, Rev 1).
- Tröjbom M., Söderbäck B., 2006a. Chemical characteristics of surface systems in the Simpevarp area. Visualisation and statistical evaluation of data from surface water, precipitation, shallow groundwater, and regolith. SKB R-06-18, Svensk Kärnbränslehantering AB.
- Tröjbom M., Söderbäck B., 2006b. Chemical characteristics of surface systems in the Forsmark area. Visualisation and statistical evaluation of data from shallow

groundwater, precipitation, and regolith. SKB R-06-19, Svensk Kärnbränslehantering AB.

Tröjbom M., Söderbäck B., Johansson P.-O., 2007. Hydrochemistry in surface water and shallow groundwater. Site descriptive modelling, SDM-Site Forsmark. SKB R-07-55, Svensk Kärnbränslehantering AB.

Tröjbom M., Nordén S., 2010. Chemistry data from surface ecosystems in Forsmark and Laxemar- Simpevarp. Site-specific data used for estimation of CR and Kd values in SR-Site. SKB R-10-28, Svensk Kärnbränslehantering AB.

US EPA, 1999. Understanding variation in partition coefficient, Kd, values. Volume I: The Kd model, methods of measurements, and application of chemical reaction codes. EPA 402-R-99-004A, U.S. Environmental Protection Agency.

Xu S, Wörman A, Dverstorp B, Klos R, Shaw G, Marklund L, 2008. SSI's independent consequence calculations in support of the regulatory review of the SR-Can safety assessment. SSI Report 2008:08, Statens strålskyddsinstitut (Swedish Radiation Protection Institute).

Xu, S, 2012. Private communication. Ecolego implementation of the SR-Site landscape model from the description in Appendix A of Avila et al. (2010).

Xu S., Dverstorp, B & Nordén, M, 2013. Independent modelling in SSM's licensing review, Int. High-Level Radioactive Waste Management Conf. (Albuquerque, NM, April–May) , American Nuclear Society.

Walke, R, 2013. Modelling Comparison of Simple Reference Biosphere Models with LDF Models, Quintessa Limited report to Strålsäkerhetsmyndigheten (SSM), SSM, Stockholm, Sweden.

Wielgolaski FE, Bliss LC, Svoboda J, Doyle G, 1981. Primary production of tundra. In: Bliss LC, Heal OW, Moore JJ (eds). Tundra ecosystems: a comparative analysis. Cambridge: Cambridge University Press, pp 813.

Coverage of SKB reports

Table A1.1: Summary of reports reviewed

Reviewed report	Reviewed sections	Comments
R-10-02	All	Main document describing underlying hydrological understanding
TR-10-01	Section 13	Derivation of parameters for use in the dose assessment modelling in TR-10-06
TR-10-02	Parts	Supporting the description of the hydrology of lake/mire systems and how these are translated into the dose assessment modelling in TR-10-06
TR-10-03	Parts	
TR-10-05	Parts	
TR-10-06	Appendix A, Appendix B	Use of model description to define how hydrological data were used.
TR-10-07	All sections.	Focus given to five radionuclides: ^{14}C , ^{79}Se , ^{94}Nb , ^{129}I and ^{226}Ra .
R-10-08		
R-10-28		

Interpretation of MIKE-SHE

Generally, in wet climate we can assume that the groundwater surface follows the topography and, therefore, all landscape topography acts as boundary condition to the flow in all points in the groundwater domain. Figure x shows the vertical velocity distribution at ground surface based on the assumption that the groundwater surface follows the topography and the spectral method proposed by Wörman et al. (2006). The result of this approach is a highly variable distribution of velocity values on the top surface and a corresponding hierarchical system of flow cells in the subsurface (3D) domain. The modelling approach presented in R-10-02 (Bosson et al., 2010) uses a combination of constant infiltration for most of the domain and head boundary conditions in limited locations where there are surface water objects in the landscape. The area proportion of head boundary condition is relatively limited by the representation of streams and the lakes, which should give a high influence of the constant infiltration boundary condition on the flow analysis. On p62 of Bosson et al. (2010) it is said

“The top boundary condition is expressed in terms of the precipitation and potential evapotranspiration (PET). The precipitation and PET are assumed to be uniformly distributed over the model area, and are given as time series.”

Consequently, the assumed infiltration velocities contradicts the infiltration distribution associated with the constant head condition applied e.g. in SKB report on regional groundwater modelling (R-09-19) as well as a number of other hydrogeological studies (Tóth, 1963; Smith and Chapman, 1983; Wörman et al., 2006; Jiang et al., 2013). Since, the approach also recognizes limited head boundary conditions there will be variable discharge (and possible recharge) within these wet objects and, therefore, also a certain hierarchical system of flow cells in the subsurface. On p. 37 of Bosson et al. (2010) it is stated that the SDM-Site, MIKE-SHE model area is 37 km². In the same figure there are 14 different wet landscape objects with coverage that seems to be about 10-20%. Thus, it seems like the area that from a modelling point of view allows for a variable flow velocity at the surface is rather limited and this should have implications for the way that the model is behaving at large scale.

In conclusion, the use of a combined infiltration and head boundary condition is physically sound, but the lack of knowledge (data) of the spatial distribution in the infiltration boundary condition and the assumption that it is constant over a large portion of the domain introduces uncertainty in the flow analysis. SKB has not motivated this approach and not investigated the relative errors propagated to the parameterization of the Pandora model and the dose assessment. An analysis of the relative error associated with using a constant head boundary condition following the topography shows that this approach leads to slightly larger infiltration rates than limited by the precipitation, so a suggested correction is to smooth the top boundary condition so that the actual infiltration is met (Marklund and Wörman, 2011).

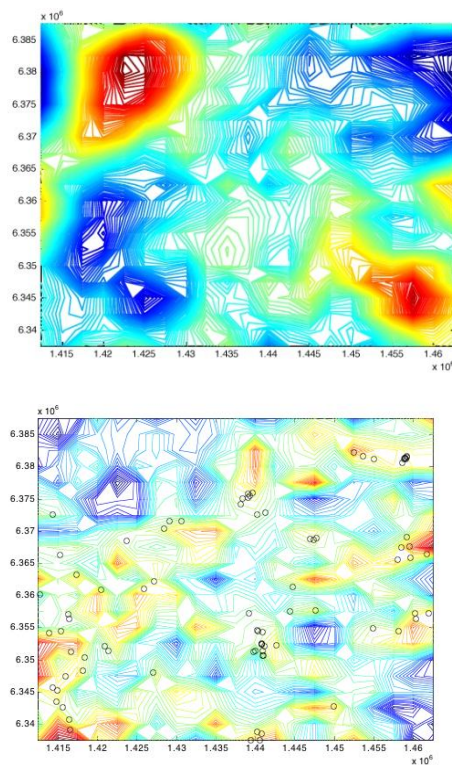


Figure 27: Topography (right-hand side) and vertical velocity distribution at ground surface (left-hand side). The solution to the vertical velocity distribution was derived based on the method by Wörman et al. (2006) and a head boundary condition following the topography. Dots represent discharge points for trace particles released in a uniform grid at 500 m depth.

References

- Jiang, X.-W., L. Wan, and X.-S. Wang (2013), Recent advances in the hydraulics and geochemistry of the theory of regional groundwater flow, paper presented at International Symposium on Regional Groundwater Flow: Theory, Applications and Future Development, China Geological Survey, Xi'an, China.
- Marklund, L., and A. Wörman (2011), The use of spectral analysis-based exact solutions to characterize topography-controlled groundwater flow, *Hydrogeology Journal*, 19(8), 1531-1543.
- Smith, L., and D. S. Chapman (1983). On the thermal effects of groundwater flow: 1. Regional scale systems, *Journal of Geophysical Research: Solid Earth*, 88(B1), 593-608.
- Tóth, J. (1963), A theoretical analysis of groundwater flow in small drainage basins, *Journal of Geophysical Research*, 68(16), 4795-4812.
- Wörman, A., A. I. Packman, L. Marklund, J. W. Harvey, Stone, S. H., 2006. Exact three-dimensional spectral solution to surface-groundwater interactions with arbitrary surface topography, *Geophysical Research Letters*, 33(7), L07402.

Constant hydrological parameters in the radionuclide transport model

This appendix contains the details of the review of the constant hydrological parameters used in the radionuclide transport model.

1. Water flux from the till (adv_low_mid);
2. Water flux from the postglacial/glacial deposits to the peat layer ($Ter_adv_mid_up_norm$);
3. Water flux to and from lake sediments normalized by the flux from the mire ($Aqu_adv_mid_up_norm$);
4. Runoff;
5. Fraction of the water flux that goes to the mire ($fract_mire$); and
6. Water flux describing the lake flooding ($Flooding_coef$).

1. Water flux from the till ($adv_low_mid = v_{Low}^{Mid}$)

P342 of Löfgren (2010) states:

This parameter represents the total advective flux from the regoLow (till) to the Ter_regoMid and Aqu_regoMid (which are the postglacial and the glacial deposits) (m/y). This was estimated by summing the net fluxes from Ter_regoLow and Aqu_regoLow in Figure 13-2. $(60-17) + (9-8) = 44 \text{ mm/y} = 0,044 \text{ m/y}$ (Table 13-6).

This velocity is therefore based on the net vertical flow in the combined lower regolith (aquatic and terrestrial):

$$\begin{aligned}
 v_{Low}^{Mid} &= \left(\begin{array}{c} \text{outflow from} \\ \text{lower regolith} \end{array} \right) - \left(\begin{array}{c} \text{Inflow to} \\ \text{lower regolith} \end{array} \right) \\
 &= \left(\begin{array}{cc} v_{terLow} + v_{aquLow} \\ v_{terMid} \quad v_{aquMid} \end{array} \right) - \left(\begin{array}{cc} v_{terMid} + v_{aquMid} \\ v_{terLow} \quad v_{aquLow} \end{array} \right) \\
 &= 60 + 9 - 17 - 8 = 44
 \end{aligned}$$

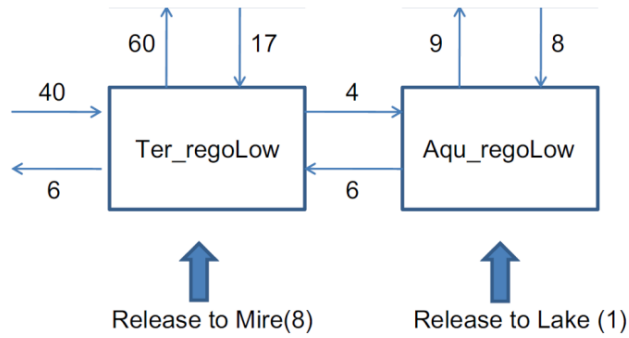


Figure 28: adv_low_mid

However the key importance of this flux is the origin. Fluxes between the terrestrial and aquatic Low compartments need not be included in the balance for the combined lower regolith, so, it can be seen that this 44 mm a^{-1} originates in the sub-catchment **and** the bedrock. Balance on the combined lower regolith gives

$$\begin{aligned}
 v_{Low}^{Mid} &= \left(\begin{array}{c} \text{External inflow to} \\ \text{lower regolith} \end{array} \right) - \left(\begin{array}{c} \text{Downstream loss} \\ \text{from lower regolith} \end{array} \right) \\
 &= \left(\begin{array}{c} v_{subCatch} \\ v_{terLow} \end{array} + v_{geo}^{terLow} + v_{geo}^{aquLow} \right) - \left(\begin{array}{c} v_{terLow} \\ \text{Downstream} \end{array} \right) \\
 &= 40 + 10 - 6 = 44
 \end{aligned}$$

The 10 mm a^{-1} here comes from the mass balance scheme in Figure 8 (rather than the 9 mm a^{-1} implied in Figure 4) and the entire lower regolith compartment is in balance. The flux represented by v_{Low}^{Mid} can be seen to be part of the near-surface

hydrology circulation sketched in Figure 7 and we can therefore interpret the normalised fluxes in Table 2 as an expression of this circulation at different depths in the regolith.

2. Water flux from the postglacial/glacial deposits to the peat layer

$$(Ter_adv_mid_up_norm = f_{terMid}^{terUp})$$

P342 of Löfgren (2010) states:

This parameter represents the advective flux in the terrestrial object from the regoMid to the regoUp normalized by the net lateral advective fluxes from the mire. This flux was obtained as follows: The flux from the regoMid was set to $(239+492+17) = 748 \text{ mm/y}$ (see Figure 13-2). The flux from other compartments to the regoMid was set to $(436 + 10) = 446 \text{ mm/y}$ (see Figure 13-2). The normalized net flux was accordingly $(748-446)/(972+17) = 0.31$ (Table 13-6).

Using Fig 8-5's values to parameterise this implies:

$$\begin{aligned}
f_{\text{terMid}}^{\text{terUp}} &= \frac{\text{net flux through terMid}}{\text{total water flux in basin}} \\
&= \frac{\sum_{j \neq \text{terMid}} v_{\text{terMid } j} - \sum_{i \neq \text{terMid}} v_{i \text{ terMid}}}{\text{total water flux out of basin}} \\
&= \frac{\left(\begin{matrix} v_{\text{terMid}} \\ \text{terWater} \end{matrix} + v_{\text{terMid}} + \begin{matrix} v_{\text{terMid}} \\ \text{terLow} \end{matrix} \right) - \left(\begin{matrix} v_{\text{terWater}} \\ \text{terMid} \end{matrix} + v_{\text{aquMid}} \right)}{v_{\text{terWater}}^{\text{Loss}} + v_{\text{terMid}}^{\text{Loss}} + v_{\text{Low}}^{\text{Loss}}} \\
&= \frac{(239 + 492 + 17) - (436 + 10)}{972 + 17 + 6} \\
&= 0.30536
\end{aligned}$$

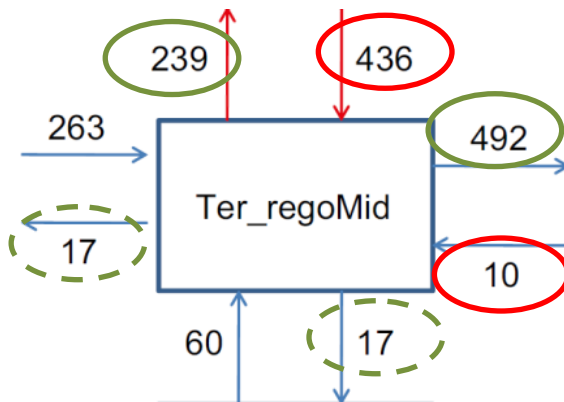


Figure 29: Ter_adv_mid_up_norm

In this expression the greyed entries are part of the mass balance scheme but have been neglected (without comment) by SKB. They are included here for completeness. Note: we are now working with the advective *velocities*⁵ to represent advective *fluxes*. There is an area factor that is not stated directly but which can be inferred from the analysis (see below).

The derived numerical value corresponds to the value in Figure 4. NB there is some ambiguity in deciding if $v_{\text{terMid}}^{\text{Low}}$ or $v_{\text{terMid}}^{\text{Loss}}$ is meant here. They both have the same numerical value (17 mm a⁻¹). The problem is that SKB are not clear as to the physical basis for this derivation and the documentation is weak.

Looking at the advective velocities for the terMid compartment it is not at all clear why those indicated in the inset figure are used and the 263 and 60 mm a⁻¹ inputs are not involved.

It is not possible to account for all fluxes through terMid in the same way that it is for the fluxes through the lower regolith. The utility of this normalised flux is to scale the upward flows through terMid relative to the overall sub-catchment. This is a useful idea but it is not clear that it has been achieved correctly or consistently.

⁵ The indices for the velocities here can be taken from the column (source) and first row (destination) of the matrix in Figure 8.

Part of the problem is that the combined fluxes through the compartment are subsumed into a single upward flow.

3. Water flux to and from lake sediments normalized by the flux from the mire ($Aqu_adv_mid_up_norm = f_{aquMid}^{aquUp}$)

P344 of Löfgren (2010) states:

*This parameter represents the advective flux in the aquatic object between the regoMid and the regoUp and between the regoUp and the water normalized by the net lateral advective fluxes from the mire. This flux was obtained by adding all fluxes to and from the lake sediment and normalizing by the fluxes out from the mire (sub-catchment area *runoff). Total flux to the lake sediment is set to $(145 + 492) / (972 + 17) = 637 / (989) = 0.64$ and total flux from the lake sediment is set to $(627 + 10) / (972 + 17) = 637 / (989) = 0.64$ (Table 13-6).*

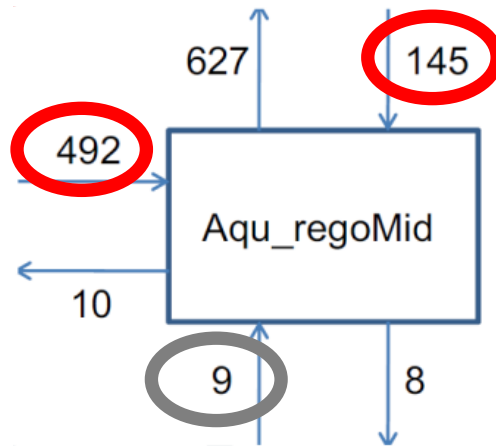


Figure 30: $Aqu_adv_mid_up_norm$

Interpreted in a clearer way, this is

$$f_{aquMid}^{aquUp} = \frac{v_{aquWater}^{aquMid} + v_{terMid}^{aquMid} + v_{aquLow}^{aquMid}}{v_{terWater}^{downstream} + v_{terMid}^{downstream} + v_{terLow}^{downstream}}$$

$$\equiv \frac{145 + 492 + 9}{972 + 17 + 6} \approx \frac{145 + 492}{972 + 17}$$

This “flux” is there for a measure of the fraction of the total discharge from the object; the denominator is the total loss downstream from the basin. The numerator is total velocity (surrogate for flux) entering the aquatic mid-regolith. It is also numerically equivalent to the total flux of water entering the basin (object + sub-catchment) from all sources (including the bedrock).

This normalised flux can therefore be better stated as the fraction of the total water entering the system that passes through the aquatic mid-regolith. It represents a mass balance on the mid-regolith compartment of the “average object”.

Comment: *In applying mass balance considerations SKB need to better identify sources and sinks for each compartment. If the relative sizes of the fluxes can be*

calculated for the basins and (dose model) objects in the basins, it would be better in future assessments to use the fluxes directly rather than to invent these normalised fluxes. In any case the normalised fluxes are not well justified.

The problem is that the complex set of fluxes for the *terMid* and *aquMid* compartments are replaced by a single parameter derived in a seemingly arbitrary way from the fluxes in the “average object” calculated from MIKE-SHE. The approach is a simplification too far and there is no documented justification.

4. Runoff = $(P - E)$

For future modelling convenience, the balance between precipitation and evapotranspiration is used in the SSM models. This allows variations and different climate conditions to be modelled. SKB prefer to use the term *runoff* for the same quantity.

P345 of Löfgren (2010) states:

The runoff parameter represents the total mean annual runoff for the SDM-site model area in MIKE SHE. Of the total mean annual runoff of 0.186 m, 0.144 m is runoff from surface streams and 0.042 m is direct runoff from the surface to the sea. The runoff was estimated by calculating a water balance based on three years of simulation. The calculation was based on the final MIKE SHE SDMSite model /Bosson et al. 2008/. Minimum, maximum and the standard deviation for runoff were taken from long time regional measurements at Vattholma (SMHI station 50110). The statistics was based on a time series of monthly mean discharge from 1,917 to 2,000. The long time series was also compared to results from the MIKE SHE model of the Forsmark area describing the hydrological conditions at different time periods (2000AD, 5000AD and 10000AD). The model results are similar to the long term data set from Vattholma. Hydrological data from the Vattholma station are described in /Larsson-McCann et al. 2002b/. (Mean=0.186, SD= 0.08, min= 0.07, max= 0.45 m y⁻¹).

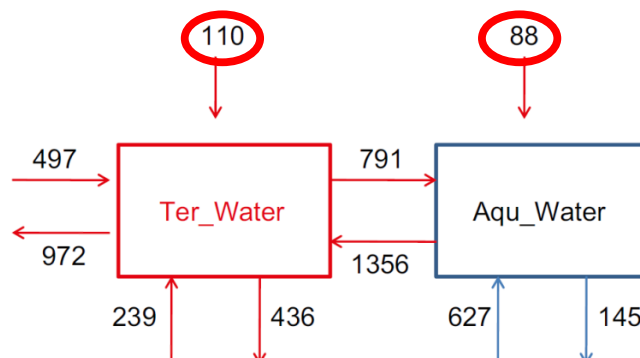


Figure 31: Runoff

Rather than the figures derived from the MIKE-SHE calculations (combined 198 mm a⁻¹) there are reasons to use the lower values. Why there should be a discrepancy is not pursued here.

5. Fraction of the water flux that goes to the mire ($fract_mire = f_{mire}$)

P342 of Löfgren (2010) states:

This parameter represents the fraction of the advective flux from the regoLow that goes to the mire. The fraction of the total flux from the regolith low that goes to the mire was estimated as: $(60-17) / 44 = 0.98$ (see Figure 13-2, Table 13-6).

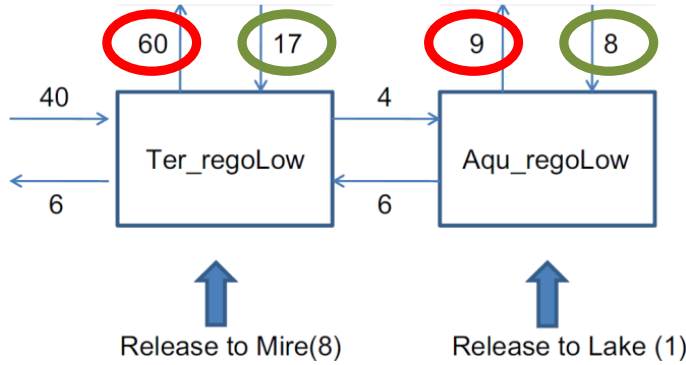


Figure 32: *fract_mire*

Mass balance for this parameter is calculated on the basis of balance at the lower regolith:

$$\begin{aligned}
 f_{mire} &= \frac{\text{net flux from Low to terMid}}{\text{total upward flux from Low}} \\
 &= \frac{60 - 17}{60 - 17 + 9 - 8} = \frac{43}{44} \\
 &= 0.9772
 \end{aligned}$$

This is one which would be expected to vary in time – as used in the radionuclide transport model, *fract_mire* = 1 when there is no water in the object. This can be investigated by the requested data for the six objects as a function of time.

6. Water flux describing the lake flooding (*Flooding_coef* = f_{flood})

P344 of Löfgren (2010) states:

*This coefficient describes the part of the gross annual lateral flux of water entering the biosphere object that also is transported from the lake to the mire (Figure 13-2c). In the model the flux from the mire to the lake is represented by $\text{runoff} \cdot \text{area_catchment} \cdot (1 + \text{Flooding coefficient})$ (see Figure 13-2c). The MIKE-SHE results suggest that the flux leaving the biosphere object is represented by $(972 + 17)$ (Figure 13-2a and b), which is synonymous to $\text{runoff} \cdot \text{area_catchment}$. The MIKE-SHE results also suggest that the flux from the mire to the lake is $(791 + 492 + 972 + 17)$. Accordingly, this gives the expression $\text{runoff} \cdot \text{area_catchment} \cdot (1 + \text{Flooding coefficient}) = 791 + 492 + 972 + 17$. By assuming that $\text{runoff} \cdot \text{area_catchment}$ is equal to $(972 + 17)$ and rearranging the expression, *flooding_coef* is equal to $(791 + 492 + 972 + 17) / (972 + 17) - 1 = 1.3$ (Table 13-6).*

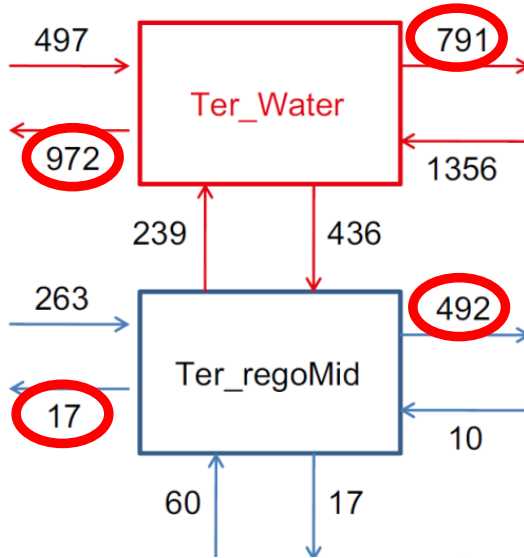


Figure 33: Flooding_coef

As written in Table 2, the flooding coefficient is related to the total flux in the sub-catchment.

The flooding coefficient is determined on the basis of the fluxes out of the mid and water compartments of the terrestrial system. Essentially what their assumption means is that the whole of the flow **out of terMid and terWater** corresponds to the flooding amount superimposed on the non-flooding amount. With this interpretation we get

$$1 + f_{flood} = \frac{\text{total flux out of terrestrial system}}{\text{total input to basin}}$$

From which

$$\begin{aligned}
 1 + f_{flood} &= \frac{v_{terWater} + v_{terMid} + v_{terWater} + v_{terMid}}{v_{terWater} + v_{terMid}} \\
 &= \frac{791 + 492 + 972 + 17}{972 + 17} = \frac{2272}{989} \approx 2.3
 \end{aligned}$$

Comparison of element specific parameters used in SR-Site assessment with previous SKB assessments

This appendix contains comparisons of the best estimate parameter values used in the SR-Site assessment with those used in previous SKB assessments, specifically SR-97 and SR-Can.

Distribution coefficients (K_d)

The K_d values used in the preceding SR-97 and SR-Can assessments are documented in Karlsson and Bergström (2002) and Avila (2006a); the latter report contains the forest data used in SR-Can. These data are reproduced here in Table 32, and the best estimate values used in SR-Site are compared against those from the previous assessments by computing the ratio of the values in Figure 34.

Table 32: Distribution coefficients used in previous assessments (K_d, m³ kg⁻¹ dw)

Element	Media	Best estimate	Distribution	Low	High	Reference
Se	Soil	1E-2	LT	1E-3	1E-1	Coughtrey et al. (1985)
	Organic soil	2E0	LT	2E-1	2E+1	IAEA (1994)
	Suspended matter in lakes	5E0	LT	1E0	1E+1	Coughtrey et al. (1985)
	Suspended matter in brackish water	5E0	LT	1E0	1E+1	Coughtrey et al. (1985)
I	Soil	3E-1	LT	1E-1	1E0	Bergström et al. (1983)
	Organic soil	3E-2	LT	3E-3	3E-1	IAEA (1994)
	Suspended matter in lakes	3E-1	LT	1E-1	1.E0	Coughtrey et al. (1985)
	Suspended matter in brackish water	3E-1	LT	1E-1	1E0	Coughtrey et al. (1985)
Ra	Soil	5E-1	LT	1E-2	1E0	Bergström et al. (1984)
	Organic soil	2E0	LT	2E-1	2E+1	IAEA (1994)
	Suspended matter in lakes	1E+1	LT	1.E0	1E+2	Bergström et al. (1984)
	Suspended matter in brackish water	1E+1	LT	1E0	1E+2	Bergström et al. (1984)

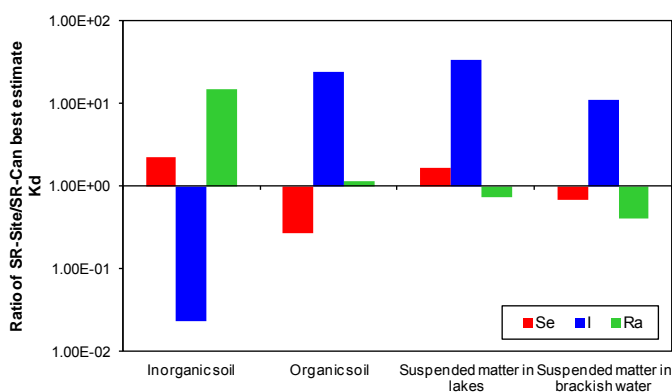


Figure 34: Ratio of SR-Site/previous assessment K_d values

Plant uptake concentration ratios (CR)

The root uptake parameters used in previous assessments are documented in Karlsson and Bergström (2002), and are reproduced here in Table 33.

Table 33: Root uptake transfers used in previous assessments (CR, [Bq kg⁻¹]/[Bq kg⁻¹ dry or wet weight soil])

Element	Plant type	Best estimate	Distribution	Low	High	Reference
Se	Pasturage ^a	1E0	LT	4E-1	3E0	Estimated from Coughtrey et al. (1985) ^c
	Cereals ^b	2E-1	LT	2E-2	1E0	Estimated from Coughtrey et al. (1985) ^c
	Root crops ^b	6E-2	LT	1E-2	3E-1	Estimated from Coughtrey et al. (1985) ^c
	Vegetables ^b	3E-1	LT	3E-2	3E0	Estimated from Coughtrey et al. (1985) ^c
I	Pasturage ^a	6E-1	LT	6E-2	6E0	Deitermann et al. (1989)
	Cereals ^b	1E-1	LT	1E-2	1E0	Robens et al. (1988)
	Root crops ^b	1E-2	LT	1E-3	1E0	Robens et al. (1988)
	Vegetables ^b	3E-2	LT	3E-3	3E-1	Robens et al. (1988)
Ra	Pasturage ^a	8E-2	LT	2E-2	4E-1	IAEA (1994) ^d
	Cereals ^b	1E-3	LT	2E-4	5E-3	IAEA (1994) ^d
	Root crops ^b	4E-3	LT	4E-4	2E-2	IAEA (1994) ^d
	Vegetables ^b	5E-3	LT	3E-4	1E-1	IAEA (1994) ^d

^a Dry weight

^b Wet weight

^c In Coughtrey et al. (1985) a range of $\sim 2 \rightarrow 66$ is presented for “pasturage herbage”. A best estimate of 20 has been used and this value has been converted into wet weight for cereals, root crops and vegetables (assuming water contents of 10, 80 and 90%, respectively).

^d The ranges used in SR 97 (low ten times lower than best estimate, maximum ten times higher than best estimate) has been changed to those presented in IAEA (1994). The values used for cereals, root crops and vegetables in SR 97 (0.07, 0.002 and 0.05 respectively) were referred to IAEA (1994) but did not match those given so they were corrected and the values presented here is those used in the SAFE study. The values for cereals, root crops and vegetables were converted to be valid for wet weight (10% water in cereals, 80% in root crops and 90% in vegetables).

¹⁴C assessment

In the SR-97 and SR-Can assessments, ¹⁴C dynamics were modelled using a concentration ratio approach. In those assessments it was assumed that plants could only be contaminated via root uptake for all the elements. Further, it was assumed that plants would not take up any carbon via their roots, meaning that plants were not a ¹⁴C exposure pathway for humans either directly or indirectly, via animal consumption of plants. This means that the highest exposures of humans to ¹⁴C came from the aquatic ecosystems, with well water consumption dominating in their well model and consumption of fish dominating in lake, running water and coastal models. The following data, reproduced from Karlsson and Bergström (2002), were used in the SR-97 and SR-Can assessments (Table 34); the justifications for those parameter values can be found in Karlsson and Bergström (2002).

Table 34: Parameters used for ¹⁴C modelling in previous assessments

Parameter	Media	Best estimate	Distribution	Low	High	Reference
K_d ($m^3 kg^{-1} dw$)	Soil	1E-3	LT	4E-4	1E-2	Best estimate from Andersson et al. (1982)
	Organic soil	7E-2	LT	7E-3	7E-1	Davis et al. (1993)
	Suspended matter in lakes	1E-3	LT	1E-4	1E-2	Bergström and Nordlinder (1990)
	Suspended matter in brackish water	1E-3	LT	1E-4	1E-2	Estimated from McKinley and Scholtis (1992)
Uptake in biota ($L kg^{-1} fw$)	Freshwater fish	5E+4	LT	5E+3	5.1E+4	IAEA (1994)
	Baltic fish	2E+3	T	1.8E+3	3E+3	Derived from data in Hesböl et al. (1990)
	Freshwater invertebrates	9E+3	LT	9E+2	1E+4	Thompson et al. (1972)
	Marine water plants	2E+3	LT	2E+2	1E+4	Thompson et al. (1972)
Metabolism	Milk ($d L^{-1}$)	1E-2	LT	5E-3	2E-2	
	Meat ($d kg^{-1}$)	3E-2	LT	1.5E-2	6E-2	
Translocation ($m^2 kg fw$)	All crops	1E-1	T	1.E-2	3E-1	Estimated
Adult dose coefficients ($Sv Bq^{-1}$)	Ingestion	5.8E-10				
	Inhalation	5.8E-9				



2014:35

The Swedish Radiation Safety Authority has a comprehensive responsibility to ensure that society is safe from the effects of radiation. The Authority works to achieve radiation safety in a number of areas: nuclear power, medical care as well as commercial products and services. The Authority also works to achieve protection from natural radiation and to increase the level of radiation safety internationally.

The Swedish Radiation Safety Authority works proactively and preventively to protect people and the environment from the harmful effects of radiation, now and in the future. The Authority issues regulations and supervises compliance, while also supporting research, providing training and information, and issuing advice. Often, activities involving radiation require licences issued by the Authority. The Swedish Radiation Safety Authority maintains emergency preparedness around the clock with the aim of limiting the aftermath of radiation accidents and the unintentional spreading of radioactive substances. The Authority participates in international co-operation in order to promote radiation safety and finances projects aiming to raise the level of radiation safety in certain Eastern European countries.

The Authority reports to the Ministry of the Environment and has around 315 employees with competencies in the fields of engineering, natural and behavioural sciences, law, economics and communications. We have received quality, environmental and working environment certification.

Strålsäkerhetsmyndigheten
Swedish Radiation Safety Authority

SE-171 16 Stockholm
Solna strandväg 96

Tel: +46 8 799 40 00
Fax: +46 8 799 40 10

E-mail: registrator@ssm.se
Web: stralsakerhetsmyndigheten.se